(2)

NAVAL POSTGRADUATE SCHOOL
Monterey, California

THESIS

A STUDY OF THE AIRWAKE AERODYNAMICS
OVER THE FLIGHT DECK OF AN AOR MODEL SHIP

by

Mark M. Rhoades

September 1990

Thesis Advisor: J. Val Healey

Approved for public release; distribution is unlimited.

Unclassified
SECURITY CLASSIFICATION OF THIS PAGE

REPORT DOCUMENTATION PAGE

Form Approved OMB No 0704-0188

1a REPORT SECURITY CLASSIFICATION UNCLASSIFIED	1b RESTRICTIVE MARKINGS
2a SECURITY CLASSIFICATION AUTHORITY	3 DISTRIBUTION/AVAILABILITY OF REPORT Approved for public release; distribution unlimited
2b DECLASSIFICATION/DOWNGRADING SCHEDULE	
4 PERFORMING ORGANIZATION REPORT NUMBER(S)	5 MONITORING ORGANIZATION REPORT NUMBER(S)
6a NAME OF PERFORMING ORGANIZATION Naval Postgraduate School 6b OFFICE SYMBOL (If applicable) AA/He	7a NAME OF MONITORING ORGANIZATION Naval Postgraduate School
6c ADDRESS (City, State, and ZIP Code) Monterey, CA 93943-5000	7b ADDRESS (City, State, and ZIP Code) Monterey, CA 93943-5000
8a NAME OF FUNDING/SPONSORING ORGANIZATION 8b OFFICE SYMBOL (If applicable)	9 PROCUREMENT INSTRUMENT IDENTIFICATION NUMBER
8c ADDRESS (City, State, and ZIP Code)	10 SOURCE OF FUNDING NUMBERS PROGRAM ELEMENT NO / PROJECT NO / TASK NO / WORK UNIT ACCESSION NO.

11 TITLE (Include Security Classification)
A STUDY OF THE AIRWAKE AERODYNAMICS OVER THE FLIGHT DECK OF AN AOR MODEL SHIP

12 PERSONAL AUTHOR(S)
Rhoades, Mark M.

13a TYPE OF REPORT	13b TIME COVERED	14 DATE OF REPORT (Year, Month, Day)	15 PAGE COUNT
Master's Thesis	FROM _____ TO _____	1990, September	103

16 SUPPLEMENTARY NOTATION The views expressed in this thesis are those of the author and do not reflect the official policy or position of the Department of Defense or the United States Government

17 COSATI CODES			18 SUBJECT TERMS (Continue on reverse if necessary and identify by block number)
FIELD	GROUP	SUB-GROUP	Flow Visualization, Simulated Atmospheric Boundary Layer, Helium Bubble Flow Visualization, Smoke Visualization, AOR Class ship

19 ABSTRACT (Continue on reverse if necessary and identify by block number)

This study investigated the airwake of an AOR Class model ship to provide basic flow pattern and velocity information to aid in solving the elusive problem of blade strikes experienced by H-46 helicopters when they engage or disengage rotors aboard AOR ships. This investigation used the NPS flow visualization tunnel modified to simulate the atmospheric boundary layer. A detailed visualization was completed of the airflow near the flight deck area of a four-foot model in a stationary mode, utilizing helium bubbles smoke, photographic and video equipment. The results show that the airwake is usually made up of two regions, one that is relatively smooth and one that is extremely turbulent. The dividing line is a shear layer that is created from the air flowing around the port face of the hangar. Another feature found both in the flow visualization as well as the velocity measurements, was the presence of a significant upward component of flow over the port edge of the flight deck. It was found that this flow had nearly the same speed as the velocity at the ship's anemometer position (continued on reverse)

20 DISTRIBUTION/AVAILABILITY OF ABSTRACT	21 ABSTRACT SECURITY CLASSIFICATION
☒ UNCLASSIFIED/UNLIMITED ☐ SAME AS RPT ☐ DTIC USERS	Unclassified
22a NAME OF RESPONSIBLE INDIVIDUAL J. Val Healey	22b TELEPHONE (Include Area Code) (408) 646-2804 22c OFFICE SYMBOL AA/HE

DD Form 1473, JUN 86 Previous editions are obsolete.
S/N 0102-LF-014-6603

SECURITY CLASSIFICATION OF THIS PAGE
Unclassified

but was inclined at an angle of between 15° and 25°. This upward flow, combined with highly variable recirculations over the flight deck could be a significant contributing factor in the occurrence of blade strikes. In addition, some attempts were made to eliminate some of the more unruly flow patterns by using curved deflectors. These attempts had some success but will require further study.

Approved for public release; distribution is unlimited.

A Study of the Airwake Aerodynamics
over the Flight Deck of an AOR Model Ship

by

Mark M. Rhoades
Lieutenant, United States Navy
B.S., University of Michigan, 1983

Submitted in partial fulfillment
of the requirements for the degree of

MASTER OF SCIENCE IN AERONAUTICAL ENGINEERING

from the

NAVAL POSTGRADUATE SCHOOL
September 1990

Author: Mark M. Rhoades
Mark M. Rhoades

Approved by: J. V. Healey
J. Val Healey, Thesis Advisor

L. V. Schmidt
L. V. Schmidt, Second Reader

E. R. Wood
E. R. Wood, Chairman
Department of Aeronautics and Astronautics

ABSTRACT

This study investigated the airwake of an AOR Class model ship to provide basic flow pattern and velocity information to aid in solving the elusive problem of blade strikes experienced by H-46 helicopters when they engage or disengage rotors aboard AOR ships. This investigation used the NPS flow visualization tunnel modified to simulate the atmospheric boundary layer. A detailed visualization was completed of the airflow near the flight deck area of a four-foot model in a stationary mode, utilizing helium bubbles, smoke, photographic and video equipment. The results show that the airwake is usually made up of two regions, one that is relatively smooth and one that is extremely turbulent. The dividing line is a shear layer that is created from the air flowing around the port face of the hangar. Another feature found both in the flow visualization, as well as the velocity measurements, was the presence of a significant upward component of flow over the port edge of the flight deck. It was found that this flow had nearly the same speed as the velocity measured at the ship's anemometer position but was inclined at an angle of between 15° and 25°. This upward flow, combined with the highly variable recirculations over the flight deck could be a significant contributing factor in the occurrence of blade strikes. In addition, some attempts were made to eliminate some of the more unruly flow patterns by using curved deflectors. These attempts had some success but will require further study.

TABLE OF CONTENTS

LIST OF TABLES

LIST OF FIGURES

ACKNOWLEDGEMENTS

My appreciation is extended to Professor J. Val Healey for his guidance, assistance and patience. I wish also to thank Mr. Al McGuire, Mr. John Moulton, Mr. Ron Ramaker, Mr. Jack King and Mr. Patrick Hickey for their technical and material support of this project. Their quick response to all requests was always very appreciated. Many thanks are also needed to go to Mr. Tony Cricelli, whose extra hours of support for the computer was irreplaceable. Appreciation is also extended to the people who work in the photolab. Their good work is readily evident in this paper.

I also want to express my greatest appreciation to my wife, Toni, and my new son, Christian, for their patience and understanding in this long, laborious undertaking.

I. INTRODUCTION

A. SHIPBOARD OPERATIONS

One of the most important aspects of the Navy's mission is to provide the country's first line of defense, which often requires long-distance travel to the point of deployment. To accomplish this, the logistic support of the "Mobile Logistic Support Force" (MLSF) ships [Ref. 1] is needed. This group of ships consists of the following ship classes: AE, AO, AOR, AFS and AOE. These ships travel with the fleet, carrying most of the needed supplies for that particular fleet's deployment. During this deployment, the supply ship will replenish the warships with the necessary fuel and material goods. There are two basic methods used to accomplish these resupply operations; connected replenishment (CONREP) and vertical replenishment (VERTREP) [Ref. 1].

CONREP is accomplished by maneuvering the two ships so that they are side by side, approximately 80 to 200 feet apart. The goods are transferred via a trolley type system over high tension cables that are connected to both ships. This method is used when the supply ship refuels other ships, or for transferring heavier loads than can be transferred by VERTREP.

The second method of replenishment is VERTREP, which is accomplished by placing the material goods into a cargo net. Then, by using a sling that is attached to this net, the goods are carried underneath a helicopter from the supply ship to the receiving ship. NWP-14 Rev. D states that, "this method permits increased flexibility and

considerable latitude in replenishment, particularly regarding time and location of the underway replenishment (UNREP) operation. The specific advantages to using VERTREP instead of CONREP are:

1. Reduction in overall time required to replenish the supported forces or units
2. Reduction or elimination of time that screening ships are required to be off station
3. Reduction in personnel involved
4. Capability of replenishing units in a dispersed formation
5. Capability of replenishing units engaged in tasks which make it impossible for them to come alongside
6. Capability of replenishing units in heavy weather conditions when alongside steaming is hazardous or impossible
7. Capability of replenishing units on station in shallow water or at anchor."

In summary, long fleet deployments required for national security need many helicopter operations to accomplish efficient logistic support. An essential element of the VERTREP operation is the H-46 helicopter.

B. THE PURPOSE OF THIS STUDY

The H-46 helicopter is the principal helicopter used for VERTREP. Using a tandem rotor configuration, the H-46 is much more tolerant of varying wind directions over the ship decks than tail rotor helicopters. However, the H-46 is not without problems, one of the most prominent of which is its tendency to have blade strikes under varying conditions, particularly in the presence of port-side winds on AOR class ships.

A blade strike occurs when a rotor blade impacts the fuselage of the helicopter while the rotor is turning. Blade strikes typically occur in the low rotor rpm regime (less that 20% of normal rotor rpm), which is encountered during rotor engagement and disengagement. The best method to avoid blade strikes is to operate within the safe wind envelopes that are determined by the Naval Air Test Center (NATC).

The process of establishing the safe envelopes is called "dynamic interface testing," and is accomplished by testing the various flight operations of the desired type of helicopter, on and around the desired ship. This testing determines what wind speed and direction combinations allow safe operation of the helicopter. As one can guess, this process is long, laborious, and expensive, and frequently aborted or curtailed because of calm weather. In addition, it is only valid for the particular ship-helicopter combination tested.

One type of ship-helicopter combination that has proven to be more elusive in yielding a consistently safe envelope is the AOR-1 class ship and the H-46 helicopter. Past operations allowed the use of the wind envelope shown in Figure 1 for rotor engagement and disengagement, which is the most permissive envelope. All angles are referenced such that the helicopter's nose always points in the 000° direction and angles are measured clockwise. Dynamic interface tests by NATC, as well as past experience by operational squadrons, have shown that this envelope does not guarantee safe rotor engagements/disengagements for H-46 helicopters aboard AOR ships. To combat this problem, some helicopter squadrons have started using the wind envelope determined for operations on aircraft carriers [Ref. 2]. This has no scientific basis since the flows

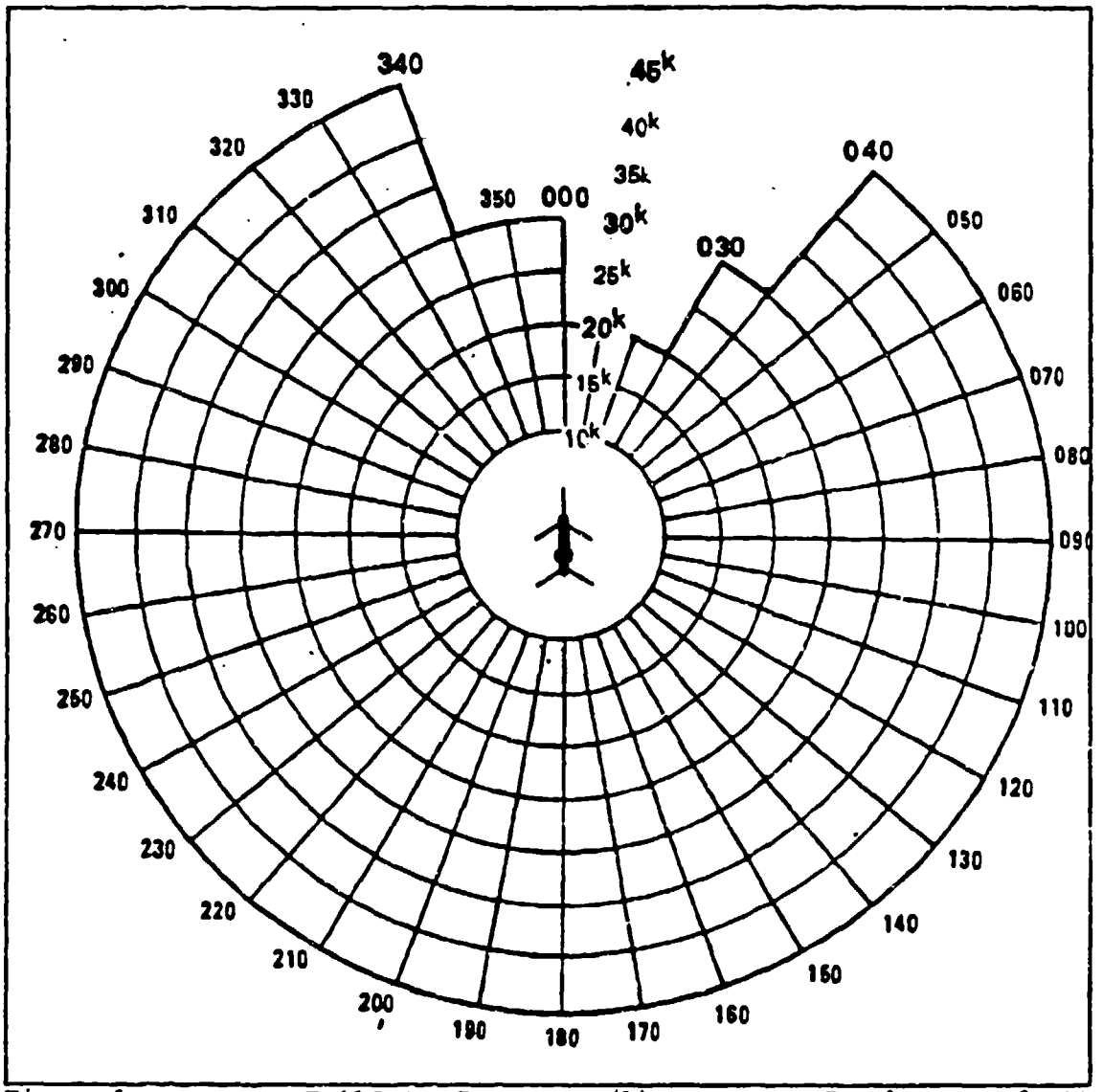

Figure 1. H-46 Rotor Engagement/Disengagement Envelope. [Ref. 1]

are radically different, but has shown some success in those squadron's histories by reducing the frequency of the occurrence of blade strikes. This envelope is more restrictive in that it requires the wind speeds from the 250° through 030°, relative to the helicopter's nose, be only 20 knots or less. Despite this additional restriction, blade strikes still have occurred.

All underway replenishment (UNREP) operations require very careful planning and execution. On the supply ship, the required items must be brought out of storage and placed on deck in the same order as they will be transferred. Items that must be transferred to the first receiving ship should be readily accessible, being at the head of the line, so to speak, and not behind the other items that will be transferred later in the UNREP operation. Due to the limited deck space available, careful and orderly packing is required. A blade strike can cause a serious interruption in that UNREP operation, hampering the fleet schedule and leading to the possible loss of material goods, especially food items.

In addition, damage to the helicopter from a blade strike can be very expensive as is evidenced by one particular blade strike that cost $491,911 to repair the helicopter to operational status [Ref. 3].

Because of these factors and for the safety of the crew, dynamic interface testing has continued on this particular ship-helicopter combination. However, at the present time testing is very expensive, e.g. one set of tests, off the southern Californian coast, cost approximately $45,000. Unfortunately, the environmental conditions were too limited to permit the desired range of wind speeds and directions to be obtained, consequently, very little data were acquired. [Ref. 4]

Continuing investigation is required to determine the cause of the blade strike problem. Unfortunately, as shown above, the environment of the open ocean is a poor laboratory, and is not cooperative enough to allow thorough, uniform dynamic interface testing. This study attempts to circumvent the lack of control inherent in nature by using

a wind tunnel that is specially set up to simulate the atmospheric boundary layer. This wind tunnel provides the uniform conditions necessary to thoroughly determine the flow patterns around the flight deck area. It is hoped that, from studying these flow patterns, some of the contributing factors of the blade strike problem can be determined.

A few quantitative measurements were made to investigate the flow velocity at the location of the model ship's anemometer and several locations over the flight deck. These were taken in an attempt to establish a database for comparison with other data obtained in the real world at some future time, and to determine the relative magnitudes of the velocity statistics on the deck and in the free stream flow.

Although this study will primarily benefit the H-46 community, it also has a broader scope in that it identifies some of the poor aerodynamic features of the AOR class ship, such as the large hangar with square corners and the high flight deck. These poor features, discussed in detail later in the Results and Conclusion chapters, should be avoided in future ship designs.

II. BACKGROUND

A. BLUFF BODY AERODYNAMICS

Understanding bluff body aerodynamics is the first step to understanding the three-dimensional airflow experienced by the ship, the helicopter deck, and subsequently the helicopter rotor. Unfortunately, bluff body aerodynamics is a lengthy subject so the following will cover only the highlights of the subject. Detailed discussions are available in the references cited below.

By definition, a bluff body is one that has, for given flow conditions, a massive separated region in its wake [Ref. 5]. It becomes apparent that Navy ships can be considered three-dimensional bluff bodies after first observing the design of a typical navy ship, the DD-963, and then observing a schematic of a flow visualization representation over a DD-963 model [Ref. 14], see Figure 2. To aid in understanding the complexity of the flow around a bluff body, one can look at a study by Hunt, Abell, Peterka, and Woo [Ref. 6]. This study established the presence of an inverted U-shaped vortex on the downwind side of the body whose ends remained in contact with the ground, as shown in Figure 3. In addition, it was established that turbulence causes the reattachment point to be highly unstable, and alters the flow field around the body by producing increased mixing near the separated shear layers [Ref. 5]. Trying to relate this flow to actual airflow over ships is an extremely difficult task. One cannot find many studies on the subject and even those that do exist have serious flaws. This researcher's study along

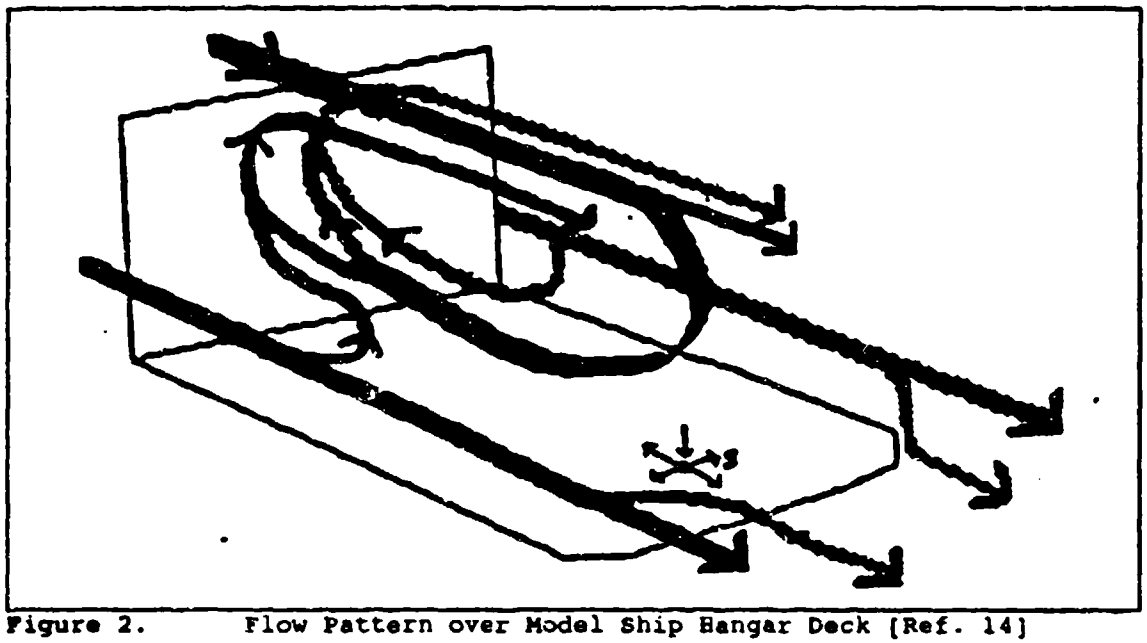

Figure 2. Flow Pattern over Model Ship Hangar Deck [Ref. 14]

with other studies currently being done at the Naval Postgraduate School will, hopefully, improve that situation. For now, one must look to studies of somewhat similar objects.

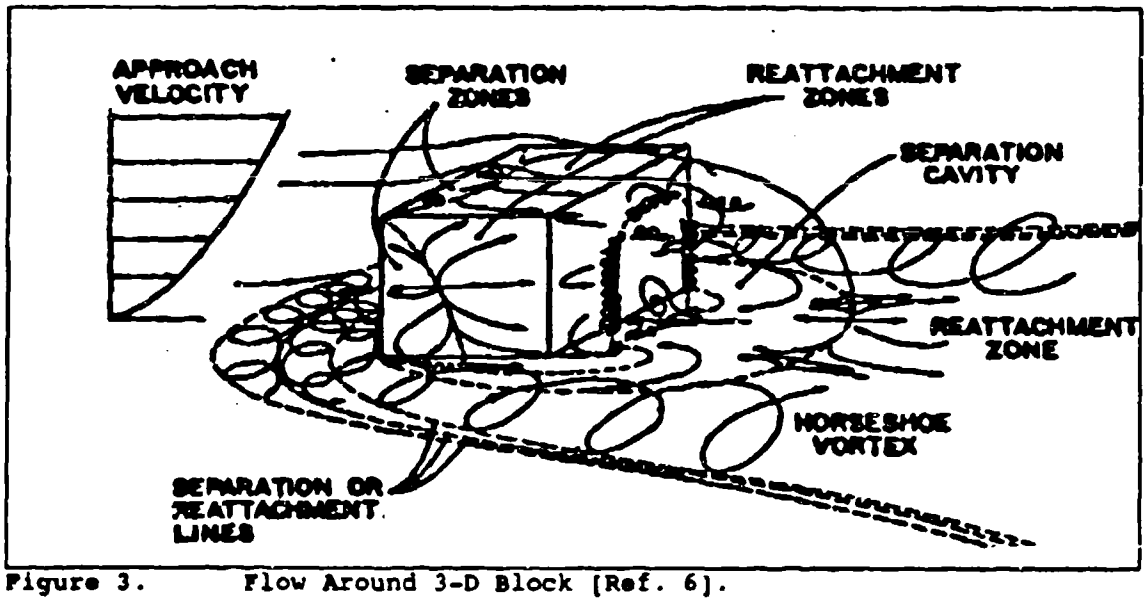

Figure 3. Flow Around 3-D Block [Ref. 6].

One such area, where much time and effort have been devoted, is in the area of wind flow around buildings [Ref. 7].

Recent investigations in the flow around buildings have advanced the understanding of physical flow processes occurring in the near and far wake regions. But, according to Sinha and Gupta [Ref. 8], there is still a high level of misunderstanding on how the winds actually flow around the building despite the many studies done in this area. They believe that these misconceptions are probably caused by "conceptual extensions of two-dimensional flow". Studies which have been conducted in boundary layer wind tunnels [Ref. 8-10 in Ref. 7] show that three-dimensional objects have fundamental differences in flow patterns relative to those of two-dimensional objects.

Figure 4 provides an illustration of the flow patterns around a square building; this shape is more or less typical of modern shipboard helicopter hangars. The figure shows

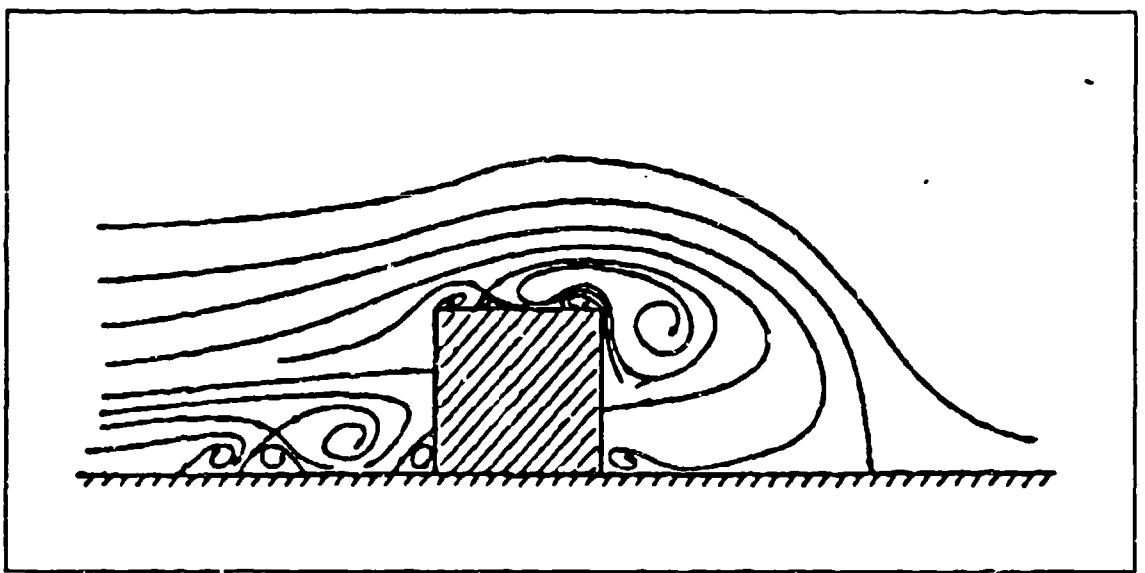

Figure 4. Flow Over a Square Building with the Flow Moving from Left to Right. [Ref. 7]

that the approaching flow is divided by a streamline which stagnates on the side of the building. This phenomenon is dependent to the first order, on building height-to-width ratio, building height-to-boundary-layer-height ratio and upstream surface roughness [Ref. 7]. The lower part of this flow strikes the building, flows downward and rolls up into a vortex. It then wraps around the building into the horseshoe shape, like that which is shown in Figure 3. This horseshoe vortex can be identified in the flow for quite some distance downstream. The wind that impinges above the stagnation region, which occurs somewhere near the top of the building's face depending on building height-to-width ratio [Ref. 7], flows out toward the front edges of the object. As the flow reaches the edges it separates and may or may not reattach to the surface of the obstacle before reaching the leeward edge. This reattachment depends on many factors such as building-length-to width ratio, height-to-length ratio and upstream roughness.

A separation cavity covers the rear face of the object, whose length is defined by the distance from the building to the centerline reattachment point downwind of the body, and is normalized by the building height. It can vary from two to six building heights [Ref. 11 in Ref. 7]. As a result of this variation, the reattachment "point" is more accurately called a reattachment zone. There is an equivalent zone on a ship's flight deck. The airflow on many ships would not correspond to the flow just discussed. However, the airstream tends to divide and flow around the ship, like that shown in the figure, so the previously discussed flow is not completely unrealistic.

To get a clear picture of this separation cavity is quite difficult, due to the high level of turbulence inside this region. Bearing in mind that the size of the cavity changes with

ship yaw angle and, to some degree, with pitching and rolling of the ship, it is little wonder that creating an accurate rotor engage/disengage envelope has been both difficult and unsuccessful.

B. FLOW VISUALIZATION

Flow visualization has been used many times throughout history. It is generally used to get an overall, or global picture of what is happening in a particular flow field. This information is usually used to determine specific areas of interest for further study or quantitative measurement.

To visualize a flow field one must contaminate the flow with something that is easily visible, preferably non-toxic and capable of accurately following the flow [Ref. 9]. There are many particles that meet two out of three of these criteria but very few that have all three. Some examples of particles that have been used are smoke, helium bubbles, dust particles, and steam. Of these particles, some have better characteristics than the others depending on each flow visualization situation. Particle selection is usually based on:

1. the nature of the flow -- whether it is steady or turbulent
2. the area of interest -- far from the surface, near to the surface, or on the surface
3. the recording method to be used – visual, video camera, still photography.

The two main areas of interest for this study were "far from the surface" and "near to the surface." These terms are relative in nature, for example in this study "far from

the surface" was more than 25 mm from the ship model's surface, usually the flight deck's surface, and "near the surface" was less than 25 mm from the surface; 25 mm corresponds to 4.15 m (13.5') on the real AOR.

To visualize these two areas required two different types of particles; smoke and helium bubbles. Smoke was used to visualize the "near the body" flow because it was easily injectable to the areas of interest. Smoke traces out streak lines. A streak line is, by definition, the locus of all fluid particles that have passed through prescribed fixed point during a specified interval of time [Ref. 9].

The primary disadvantage to using smoke was that, in turbulent flows such as used in this study, the smoke streak lines dispersed quickly into an amorphous cloud. This was the main reason that smoke was used only to visualize the "near to the surface" flows, where the smoke streak lines still maintained their integrity. Because of the dispersion, it was not possible to obtain clear photographs. Due to the problems with using photography, illustrations, derived mainly from video recordings, have been used to show the smoke streakline patterns.

The other technique used was that of helium bubble flow visualization. Helium bubbles are soap/glycerine bubbles filled with helium gas, which can be made neutrally buoyant when passed through a centrifugal filter. These bubbles also trace out streak lines when they are introduced into the flow. By studying these lines one can find the average flow paths around the model; numerous examples appear in the results section, later in this paper.

Helium bubbles can be used in wind tunnels that have moderate turbulence [Ref. 9], whereas many other types of particles cannot. However, the biggest disadvantage of using helium bubbles was that the bubbles only reflect about five percent of the incident light [Ref. 9], so careful selection and placement of light sources was required.

C. MODELING THE ATMOSPHERIC BOUNDARY LAYER

There are many sources of information on the atmospheric boundary layer. A good discussion on how this type of boundary layer can be characterized, as it occurs over the ocean, is available in Healey's, *The Prospects for Simulating the Helicopter/Ship Interface*. Some information from that report is given below to provide the reader with a small, but important amount of background on some aspects of an atmospheric boundary layer.

An atmospheric boundary layer cannot be simulated in an ordinary wind tunnel because these boundary layers have velocity profiles that vary with height, and turbulence intensities that depend upon mean windspeed and surface roughness. This is drastically different from the usual low turbulence intensity and near uniform velocity profiles found in normal wind tunnels. There are several different parameters that are important in describing and modeling an atmospheric boundary layer. These parameters, according to Healey, are:

1. The windspeed averaged over a period of time. This is called the mean speed.
2. The standard deviation σ of the longitudinal (along wind) windspeed fluctuations about the mean which, when divided by the mean speed, yields the parameter turbulence intensity.

3. The longitudinal length scale of the turbulence, which is a measure of the mean length of the most energetic eddies in the turbulence.

4. The spectrum function of the turbulence, which indicates how the energy is distributed among the frequencies present in the turbulence.

A ship's airwake is a function of wind speed, ship speed and angle between the wind and ship heading. These speeds are used to find the wind/ship speed ratio. [Ref. 10]

One needs to know the wind/ship speed ratio because relative wind speeds do not provide enough information to characterize the flow over a ship's flight deck. This is because one cannot determine the correct amount of turbulence intensity in the flow based only on the relative wind speed value. Most helicopter envelopes are written in terms of relative wind over a flight deck because this relative wind is easily measured, however the accuracy of ship's anemometers are subject to question. A ship's relative wind is made up from the true wind velocity and the artificial wind velocity, of uncertain value, created by the ship's movement through the atmosphere. The true wind velocity over the ocean carries with it an amount of turbulence intensity. Empirical relationships are available from the Engineering Sciences Data Unit, for neutral winds, which can be used to estimate the amount of turbulence intensity [Ref. 11]. However, the artificial wind created by the ship's movement does not have any turbulence intensity associated with it. Therefore a 40-knot relative wind created by 10 knots of true wind and 30 knots of artificial wind will contain a much lower turbulence intensity than a 40-knot true wind blowing over a stationary ship deck. This study simulates a stationary ship, thus

assuming the worst case scenario which is a flow containing the maximum turbulence intensity.

Exact duplication of every aspect of an atmospheric boundary layer in a wind tunnel environment is not possible. However, there exists a method of modelling the wind profile which has led to very satisfactory results. [Ref. 12] This method uses the power law:

$$\frac{u}{u_{Ref}} = \left(\frac{z}{z_{Ref}}\right)^n$$

This equation relates windspeed and elevation, where u is the along-wind speed at a specified elevation, z. The values of u_{Ref} and z_{Ref} are said to be the wind speed and elevation at the reference point. The exponent, n, is a constant and should be the same in both the real and modelled flows. In this study, z_{Ref} is the height at the top of the boundary layer (788 mm) and the u_{Ref} is the velocity at that height. The n value was determined to be 0.11 during the most recent calibration. A plot of the mean velocity profiles, for different points across the test section, is shown in Figure 5.

Modelling the atmospheric flow around a ship is simplified because ship's are sharp-edged bluff bodies and the flow patterns around such bodies essentially do not change as long the Reynolds number is maintained above approximately 10,000 [Ref. 10]. The minimum Reynolds number value was 26,000 for this study, which allowed the viscous-to-inertial simulation of the ship's airwake to be achieved using wind velocities that were greater than 1.2 m/sec.

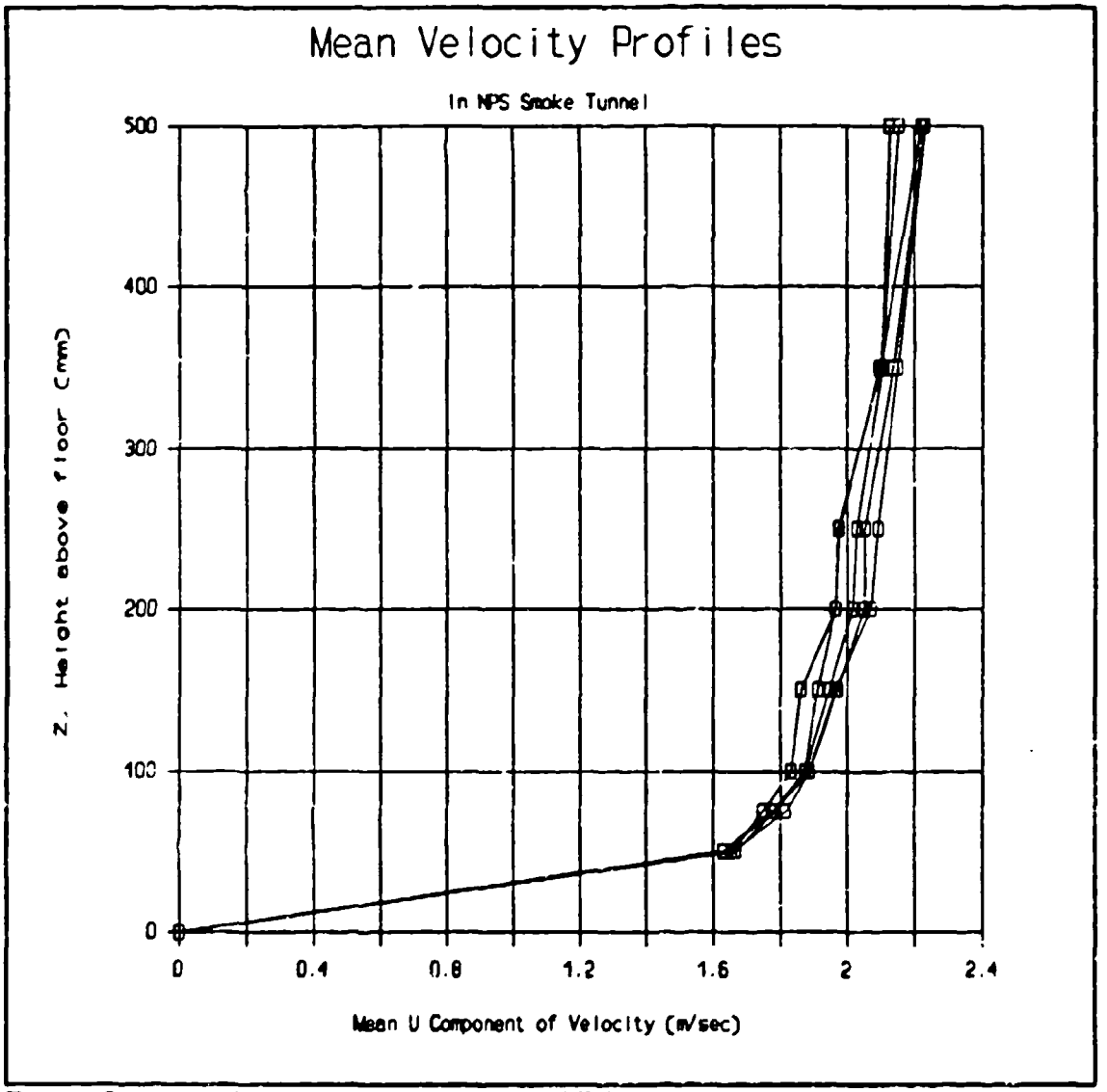

Figure 5. Mean Velocity Profiles in NPS Smoke Tunnel.

Analysis of the data from the clean tunnel indicate that the longitudinal length scale and spectrum function scale from the model to full size quite well. [Ref. 13]

III. EXPERIMENTAL APPARATUS

A. WIND TUNNEL

This study used the Naval Postgraduate School's flow visualization wind tunnel which had been modified to simulate the atmospheric boundary layer for ship airwake studies.

The tunnel is an open-circuit one, with air entering an inlet that measured 4.5 m X 4.5 m (15' X 15'). As the air entered the tunnel, it passed through a 7.5 cm (3") honeycomb. A 9:1 ratio square contraction cone directed the flow into test section that was 1.5 m X 1.5 m (5' X 5'), and 6.7 m (22') long, see Figure 6. The flow was then exhausted into the atmosphere through a fan, which used variable pitch blades to control the speed of the flow.

An observation booth was located on the side of the tunnel. A glass window, 1.6 m X 1.1 m (5.2' X 3.5'), provided the primary viewing area from the observation room and a second one, 0.4 m X 1.23 m (1.33' X 4'), was installed in the tunnel's roof. A third window, 1.5 m X 0.6 m (5' X 2'), installed on the opposite wall from the main window, allowed for horizontal illumination when necessary. The main viewing window had sufficient area for most of the photography, with the top window used for illumination and some vertical photography. A circular turntable was located on the floor of the tunnel which supported the ship model at the waterline. The ship model, turntable,

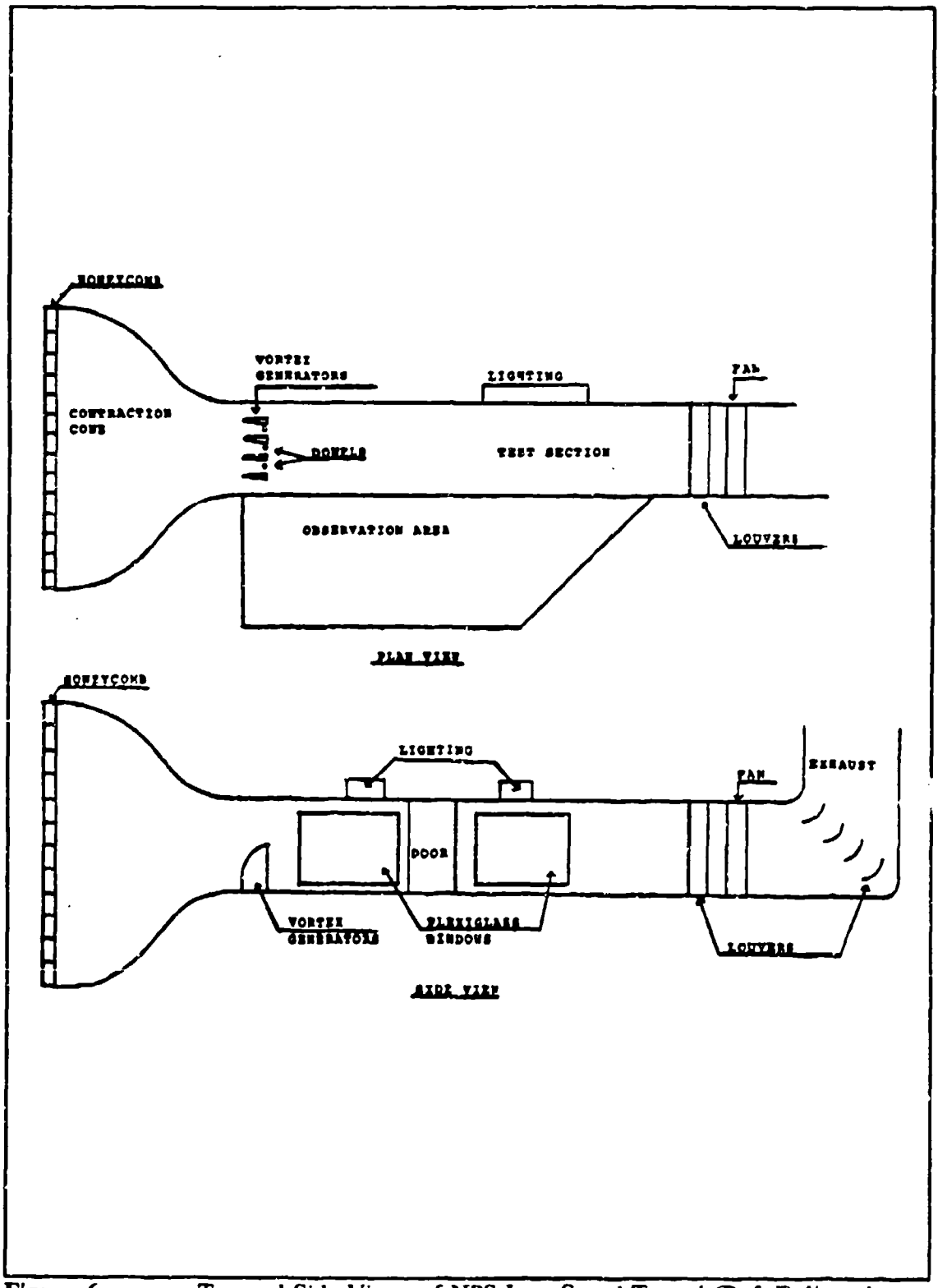

Figure 6. Top and Side Views of NPS Low Speed Tunnel (Ref. Bolinger)

and the interior of the wind tunnel test section were all painted a flat black to maintain low light reflectivity.

The wind tunnel flow simulated the neutral atmospheric boundary layer that occurs in strong winds over the ocean. The boundary layer extended from the floor up to 750 mm (30") vertically. As discussed earlier in this paper, there are several methods to create sheared turbulent boundary layers. In this case, the Counihan method was used: four vortex generators that were the shape of a quarter ellipse, when viewed from the side, generated the shear and the turbulence. See Figure 6. These vortex generators were 0.75 m (2.5') high, 0.375 m (1.25') in the direction of the flow and 75 mm (3") maximum thickness at the base of the trailing edge. They were constructed of aluminum and styrofoam. From a top view, the vortex generators appeared wedge-shaped. The same was true when looking from the test section toward the rear of the vortex generators. Tapered rods were placed between the vortex generators to create more uniform mean velocity profile across the width of the tunnel with an appropriate vertical profile.

To calibrate the tunnel, velocity and turbulence intensity measurements were made using a hot-wire anemometry system; the results are shown in Table 1 and Table 2.

B. MODEL

A four-foot model was constructed out of wood by "Memorabilia" in the Philippines. The "area of interest", i.e. the rear half of the model, was painted a flat black. It was made to scale with the use of excerpts from AOR blueprints provided by

TABLE 1. TEST SECTION VELOCITY DATA (m/sec)

		Z - Height from floor in millimeters							
		50	75	100	150	200	250	350	500
Y Distance from far wall in NPS Smoke Tunnel V_o = 2.83 m/sec	450	1.63	1.78	1.87	1.91	1.96	1.98	2.10	2.22
	600	1.66	1.75	1.83	1.86	1.97	1.97	2.10	2.15
	750	1.67	1.78	1.88	1.95	2.02	2.03	2.11	2.13
	900	1.65	1.82	1.89	1.96	2.07	2.09	2.15	2.23
	1050	1.67	1.78	1.89	1.97	2.05	2.05	2.14	2.23
	ave.	1.67	1.78	1.87	1.93	2.01	2.02	2.12	2.19
	V/V_o	0.59	0.63	0.66	0.68	0.71	0.71	0.75	0.77
	σ	.016	.025	.023	.045	.048	.050	.023	.048

TABLE 2. TEST SECTION TURBULENCE INTENSITY DATA (%)

		Z - Height from floor in millimeters							
		50	75	100	150	200	250	350	500
Y Distance from far wall in NPS Smoke Tunnel	450	12.6	9.80	8.60	7.20	6.60	6.40	6.10	4.50
	600	13.1	10.5	8.40	8.00	7.10	6.90	6.20	5.70
	750	12.0	9.20	8.20	6.90	6.50	6.00	5.10	4.70
	900	12.8	9.40	8.40	6.60	5.90	5.50	4.70	3.80
	1050	12.3	10.1	8.60	7.00	6.30	6.00	5.30	4.40
	ave.	12.5	9.80	8.44	7.14	6.48	6.16	5.48	4.62
	σ	0.43	0.52	0.17	0.53	0.44	0.52	0.65	0.69

Puget Sound Naval Shipyard. The resulting scale was 1:164.75. Table 3 summarizes the dimensions of the AOR ship model and the real AOR ship.

As stated earlier, a circular turntable was made to support the model. It was made of 3/4" plywood with a hole the shape of the model's horizontal cross section. This hole was sized so that the ship was supported and rested at its normal waterline as shown in Figure 7, which is an excerpt from *Jane's Fighting Ships.*

TABLE 3. SHIP/MODEL DIMENSIONS

	Model	Ship
Length	4'(1.2 m)	659'(202.8 m)
Beam	7"(17.8 cm)	96'(29.5 m)
Flight deck height above the waterline	2.94"(7.46 cm)	40.3'(12.4 m)

In addition, a 47 mm diameter hoop was constructed of 0.79 mm (1/32") diameter wire. This hoop was supported from the center using wire, of the same diameter, by a "T" structure, such that vertical wire was perpendicular to the hoop's plane. Figure 8

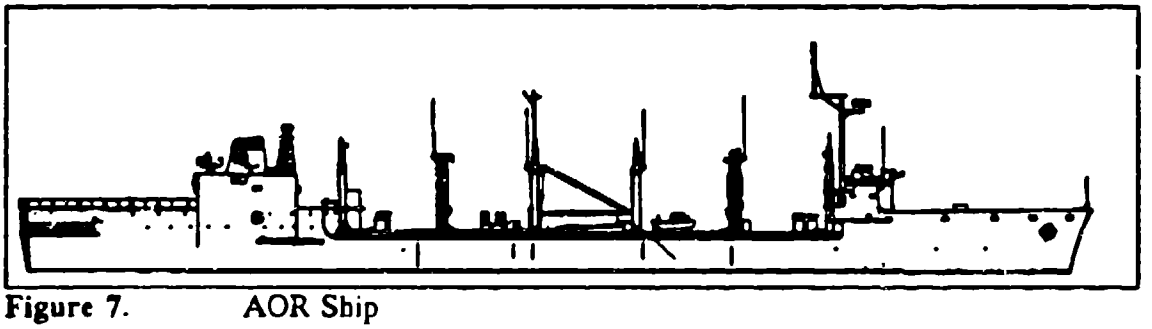

Figure 7. AOR Ship

Figure 8. Illustration of Wire Hoop used to Represent Locus of the Rear Rotor Tip of an H-46.

shows the wire hoop installed in the model's flight deck. The vertical wire was placed in a small hole in the deck so that the hoop was supported at 30.16 mm (1 3/16") above the flight deck's surface, which when increased to full scale corresponds with 5.13 m height of the rear rotor.

C. HELIUM BUBBLE GENERATION

Helium bubbles were generated by a bubble generator made by Sage Action, Inc. A second bubble generator was constructed at the Naval Postgraduate School, by Aeronautical department technicians, as a backup in case the first generator failed. A

schematic of the two systems can be seen in Figure 9, which is an excerpt from Ref. 14.

The helium bubble generator used compressed air, helium gas, and a small amount of soap film solution. This solution, a proprietary mixture of soap, glycerine, and possibly other additives, was also purchased from Sage Action. The bubble control console used three valves to control the flow rates of the three components: air, helium and soap film solution. Each component was delivered to a bubble generating head by

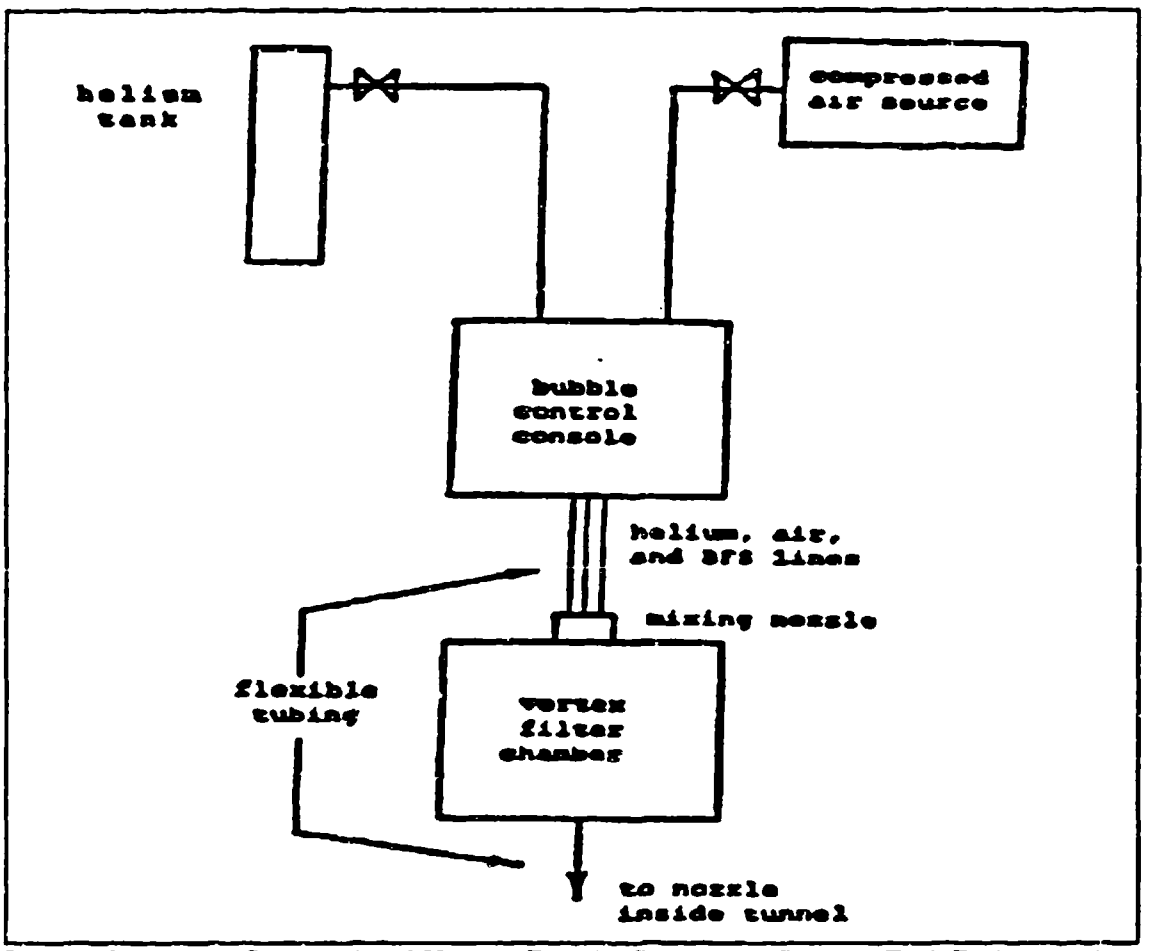

Figure 9. Schematic of Helium Bubble Generation System (Ref. Biskaduros)

a flexible tubing. Inside the head, the soap film encapsulated an amount of helium and was forced out of the head by the compressed air. The bubbles were then injected into a vortex filter chamber. The filter was a plexiglass cylinder, with dimensions of 38.1 cm (15") high by 17.78 cm (7") in radius, that used the injected air to form a vortex inside the cylinder. This caused the heavier bubbles to hit the outer wall and burst or fall to the bottom of the filter. The lighter bubbles gathered at the top of the filter or were centrifuged inward where they collapsed on a tube located in the center of the cylinder, and which extended down to about the middle of the cylinder. The neutrally buoyant bubbles remained swirling in the middle of the filter and eventually were forced out through this center tube. The bubbles then traveled through a 11 mm (7/16") flexible tubing to a piece of bent metal tubing that had a 9.5 mm (3/8") diameter, which was used to conduct the bubbles into the flow just ahead of the model inside the wind tunnel.

D. SMOKE GENERATION

A theater fog machine manufactured by Rosco Corporation was used to generate smoke. The machine used their proprietary "fog juice." Due to previous difficulties in earlier thesis work involving flow visualization using the same system [Ref. 15], the output of the fog machine was ducted into a plastic drum 1 m (40") high and about 0.5 m (20") in diameter. This allowed the vapor to collect and cool. A small, variable speed, in-line blower was attached to the drum to draw the cooled vapor along 3.175 mm (1/8") diameter plastic tubes into the areas to be studied.

E. LIGHTING

Several light sources were used in various combinations. Xenon arc lamps procured from Sage Action, Inc. and Oriel Corporation were primarily used. There were two 150 watt lamps and two 300 watt lamps, all of which had attached collimation optics. These lamps had an optimum color temperature range of 5000° - 6000° Kelvin and provided a very white light. The arc lamp power supplies permitted variations in the current to provide variable light intensity.

F. STILL PHOTOGRAPHY

A Hasselblad 2000 FCW medium format camera with Tessar 110 mm f2, and 150 mm f2.8 lenses was used for still photography. Accessories used with the camera were a Bogen tripod, Polaroid film pack and an A12, 120 size film pack.

G. VIDEO

Video equipment used was a Panasonic WV-1850, 800 line closed-circuit camera using 25 mm or 50 mm f1.4 automatic iris lenses, a Panasonic WV-5470, 850 line monitor, and a Mitsubishi HS-423UR, 440 line super-VHS video cassette recorder.

H. COMPUTER SUPPORT

A Compaq Deskpro 386/25 microcomputer, equipped with a 80387 coprocessor, was the primary computer used during this study. For permanent storage, the computer had a 300 M-byte hard disk, a 1.2 M-byte 5-1/4" minidisk drive and a 1.44 M-byte 3-1/2" microdisk drive. The computer also had 16 M-bytes of random access memory and a

VGA monitor capable of displaying 800 X 600 pixels. The disk operating system used was Compaq Microsoft-DOS version 3.31. Data acquisition was achieved through a Metrabyte DAS16/16F analog-to-digital board installed inside the computer.

I. HOT WIRE ANEMOMETER

A hot wire anemometer was used to initially calibrate the wind tunnel. This ensured that the proper velocity profiles did exist and that the turbulence intensity, and other velocity statistics, were as desired. Below is the list of equipment associated with the hot wire anemometry system:

1. Dantec 55R91 Hot Wire Probe
2. Dantec 55C01 CTA Units and 56C17 Bridges and Signal Conditioners
3. Metrabyte DASH-16 Analog-to-Digital Converter (12-bit word)
4. Compaq Deskpro 386/25 Micro Computer
5. Metrabyte "Streamer" Software Package
6. Dantec "acqWIRE" Software Package
7. Three 20 m coaxial cables.

A triple-wire probe was used, which could determine the pertinent velocity statistics within acceptable levels, so long as the instantaneous velocity vector remained within 20° of the probe axis [Ref. 16]. The probe was held in position using a simple, heavy lab stand. The characteristics of the hot wire probe are summarized in Table 4.

TABLE 4. HOT WIRE PARAMETERS

Diameter	8.89 microns
Active Length	1.25 mm
Ambient Temperature Resistance (20 C)	0.6 ohms(all wires)
Temperature Coefficient of Resistance	0.42%
Maximum Temperature	300 C
Minimum Velocity	0.2 m/s
Frequency	300 kHz
Material	Platinum Plated Tungsten

The hot wire anemometer was made up of three channels, one for each coordinate axis. Each channel consisted of the following:

1. a sensor wire on the triple-wire probe
2. a 20 m coaxial cable which connected the probe to the bridge circuit
3. a constant temperature anemometer unit
4. a bridge circuit
5. a signal conditioner.

A single frame, with a built-in power supply, housed the last three listed items for all three channels. All of the above equipment was purchased from the DANTEC Corporation and assembled into the complete hot wire anemometry system at the Naval Postgraduate School by Professor J. V. Healey.

The hot wire anemometer used three fine wires or films, as part of the probe, which were heated electrically and placed in the flow stream. An incorporated feedback control circuit varied the voltage across each sensor wire so that the temperature of these wires or films remained nearly constant. Then, via the calibration process, the voltage across each wire could be related to the velocity of the flow stream passing over the wire. For a more detailed discussion of hot wire anemometers the reader is referred to Goldstein's, *Fluid Mechanics Measurements* [Ref. 9]. The raw voltage signal was then passed through the signal conditioner, which incorporated an adjustable low pass filter set at 1 kHz and the amplifier set at five. This amplification was done to improve the resolution of the system, and brought the voltages from around 1.5 V to about 7.5 V.

After conditioning, the signal was sent to the Metrabyte Dash16 Analog-to-Digital converter. This unit was set to the unipolar position such that it converted the voltages (0 through 10 volts) to digital values (0 through 4096). These values were written onto the computer's hard disk in binary form using the Metrabyte "Streamer" program. Following the recording of the digital information, the Dantec "acqWIRE" software package was used to process the data to determine the values of the velocity components as well as many other important flow parameters.

IV. EXPERIMENTAL PROCEDURE

The main area of the ship superstructure which was of interest was the flight deck area of the AOR, particularly the aft port corner of the flight deck. This area was selected because the highest frequency of blade strikes occurred when the helicopter's rear rotor was located in this region.

The relative angular measure used was measured clockwise from the ship's head, therefore straight ahead of the ship was the 000° relative position and directly behind the ship was the 180° relative position. This measurement system is consistent with the relative angular measurements used in the fleet.

The ship's position was varied through the following yaw angles: 0°, 30°, 50°, 70°, 90°, and 110°, all measured clockwise from the tunnel centerline to the ship's longitudinal axis. This simulated winds varying from 000° to the 250° relative directions, which were of particular interest because they coincided with most of the blade strikes on AOR ships. No pitch or roll effects were examined in this study because of Johns' findings, reported in his thesis study completed in 1988, in which he states:

> As the observations progressed through many combinations of pitch and roll in the static mode, it became apparent that there was no significant differences detectable on the helium bubble photographs or video.

A. HELIUM BUBBLES

Capturing a three dimensional flow field on a two dimensional photograph appeared difficult and it was. It required many long and laborious hours of set-up and trial-and-

error to correctly match the lighting, camera position, exposure time and lens settings to obtain a good clear picture. As stated earlier in this paper, helium bubbles reflect only about five percent of the incident light. Therefore, they had to be illuminated with as much light as possible. If, however, the ship model was illuminated with the high intensity light, the photographs of the bubbles became totally washed out due to excessive glare from the model's surface. The method that was found to work best was to illuminate the air surrounding the ship model with high intensity collimated lights, with the beams of light being very close but not touching the model, and to use a lower intensity light to illuminate the entire ship area. This caused the helium bubbles to show up as bright streaks and the softer light allowed the outline of the ship to be visible. Unfortunately, each ship yaw position required a unique lighting configuration to obtain optimal results. When helium bubbles were used to visualize turbulent flows, the bubbles scattered and tended to avoid the regions of highest interest, such as recirculation zones. There were two methods employed to overcome this problem. One was to lengthen the exposure times; this allowed more bubble traces to be captured on the photograph thus increasing the probability that some bubbles would enter the region of interest. The second method was to inject the bubbles as closely to the area of interest as possible, but not so close as to significantly disturb the flow field.

The helium bubbles were introduced into the flow using a 9.5 mm (3/8") copper tube bent around 90° in a smooth bend. This allowed the helium bubbles smooth entry into the flow and maximized the concentrations where desired. The tube was placed in the flow through a number of holes that spanned the tunnel floor horizontally and were

about 1 m upstream of the center of the test section. Only one hole was used at any one time, with the others being sealed. During the 0° yaw position the bubble input tube was placed in the forward superstructure of the model. This did not appreciably affect the flow and allowed for maximum concentration of bubbles in the area of interest.

Care had to be taken to ensure that the camera was exposed to as little direct reflection of the light beams as possible. This was done, when possible, by photographing from an aspect that was just ahead of the plane of the rear hangar face. When photography from the rear of the model was required, the lights were placed slightly below the level of the flight deck and slightly ahead of the plane of the rear face of the hangar. This allowed the hangar face and the flight deck to be in the shadow, while the air just above the flight deck was brightly illuminated. The lighting configuration utilized for each model yaw position is shown in Appendix A.

The Hasselblad camera was used for all of the still photography. The first step in the process was to take pictures with Polaroid monochrome (3000 ASA) film to determine the proper exposure settings. The second step was to take pictures with Kodak TMAX 400 monochrome film using the previously determined settings, except that the aperture was opened by one stop. The film was "pushed" to ASA 1600 during processing. Photographs were taken through the main window from either a low, profile perspective from ahead of the vertical plane of the model's helicopter hangar or from the rear port and starboard quarters. Due to problems associated with glare and the need for high intensity illumination of the helium bubbles, camera angles were restricted to a very

narrow band. Most of the aperture settings used were in the range f5.6 to f16 with an exposure time of two seconds.

Video recording was used in addition to still photography, mostly from the main window of the tunnel. More ambient lighting was used to help the camera, which used an automatic iris, to maintain the proper aperture. This additional lighting prevented the bubbles from being overexposed due to the iris being too far open.

B. SMOKE

Smoke provided a very accurate, though limited view of the flow. Several different configurations were tried, but it was found that a single smoke 3.175 mm (1/8") copper tube worked best for introducing the smoke into the area of interest. This prevented a large amount of smoke from accumulating over the flight deck and yielded the maximum contrast between the smoke patterns and the background.

To deal with the limited view that the single probe provided, an imaginary grid was used to divide the volume above the flight deck. This imaginary grid used the intersections of six vertical planes and three horizontal planes as positions for the smoke probe. These planes are shown in Figures 10 through 12. For the 0° and 30° yaw positions, the smoke tube was also placed on both sides of the hangar and on top of the hangar to the left and right of the model's helicopter tower. On average, thirty smoke tube locations were used for each ship yaw position.

Smoke used to visualize the flow immediately adjacent to the upstream deck edge was introduced through a straight tube that pointed vertically and was positioned just

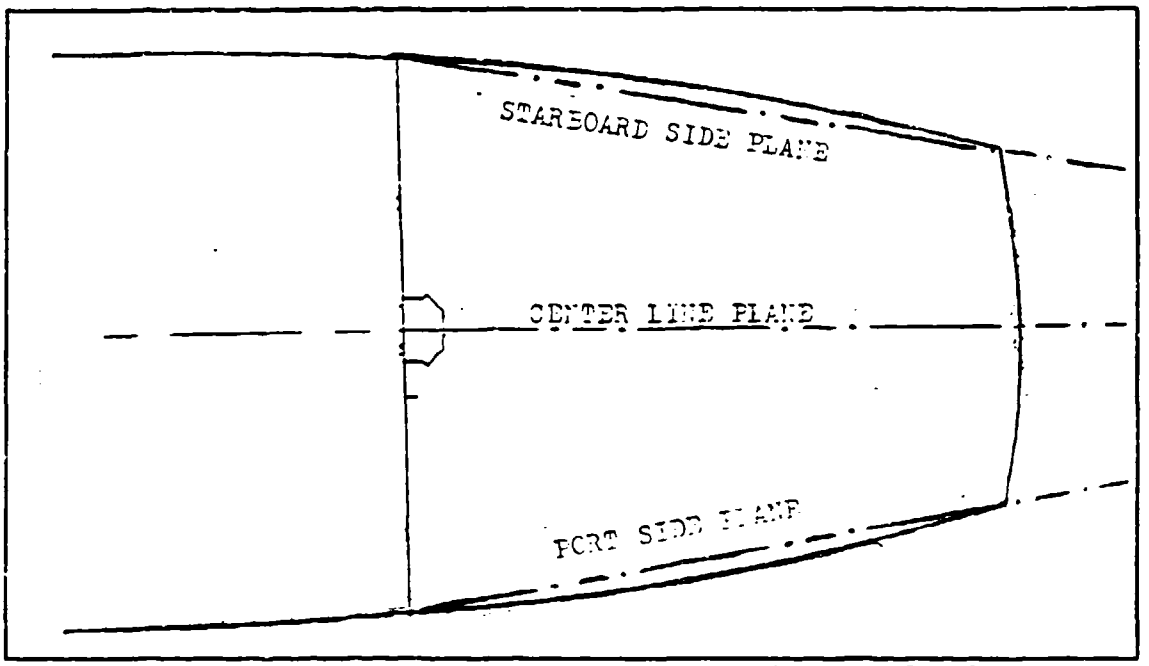

Figure 10. Illustration of Centerline, Port Side, and Starboard Side Planes.

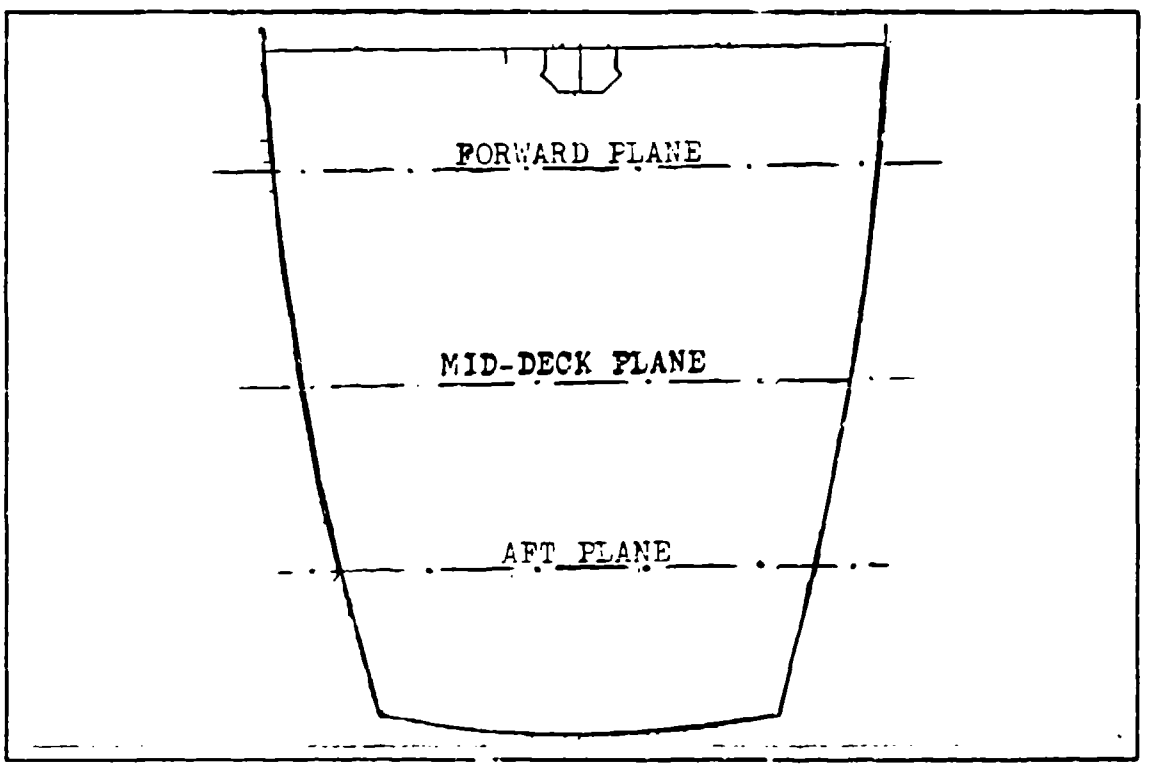

Figure 11. Illustration of Forward, Mid-deck, and Aft Planes.

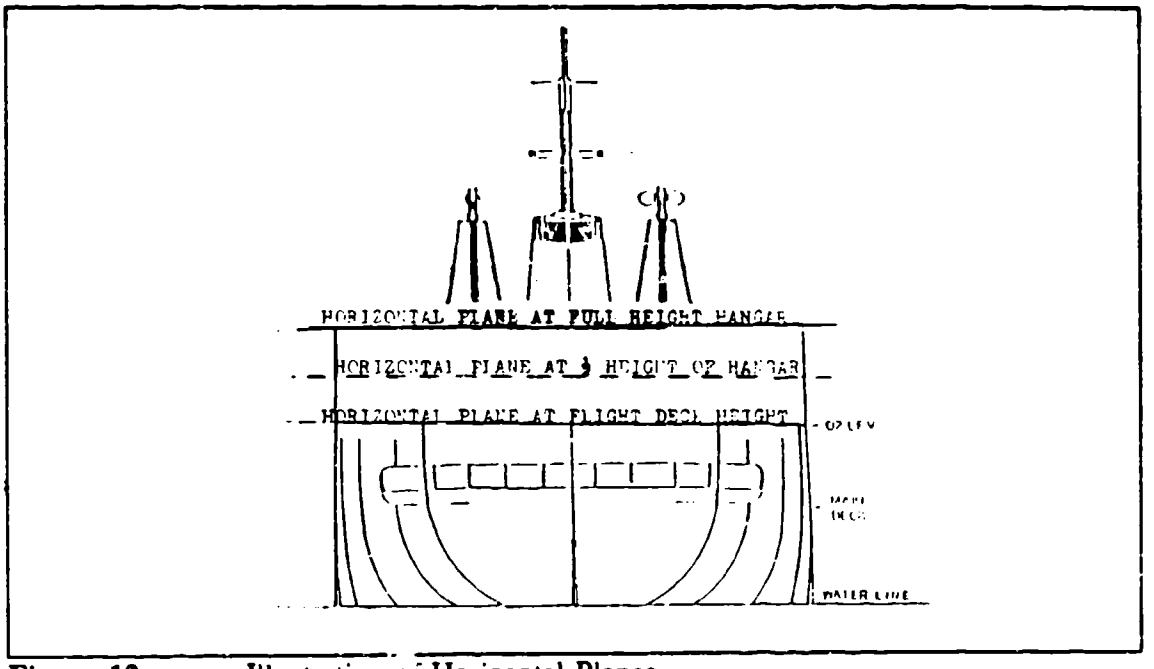

Figure 12. Illustration of Horizontal Planes.

below the deck edge. For the other positions, an elbow in the tube was used to introduce the smoke horizontally over the flight deck, from both the upstream and downstream. It is of interest to note that the aft rotor system of the H-46 is approximately 79% of the full-height of the hangar on an AOR ship. Variations in the smoke tube locations were necessary to completely illustrate the different phenomena found during each model yaw position.

Video recording was the only viable method to record the smoke streak lines. Still photography was not used as a result of the previous experience of Johns who stated:

> Attempts at still photography of the flow visualized by smoke proved fruitless. All the smoke areas blended into each other with no discernible flow direction depicted.

Video segments were taken from the same aspects as those used for the helium bubble research and were used extensively to make interpretative two-dimensional drawings.

C. HOT WIRE MEASUREMENTS

A number of measurements were taken over the model's flight deck, and at the location equivalent to the ship's anemometer, using the hot wire anemometry system for each of the yaw positions; see Figure 13. This was by no means an attempt to map out the flow but was used to get some quantitative data in the area. At the time of this study, no quantitative data of any kind exists for the AOR class ships. It is hoped that future studies that involve real ships, under real conditions, can compare their results with this

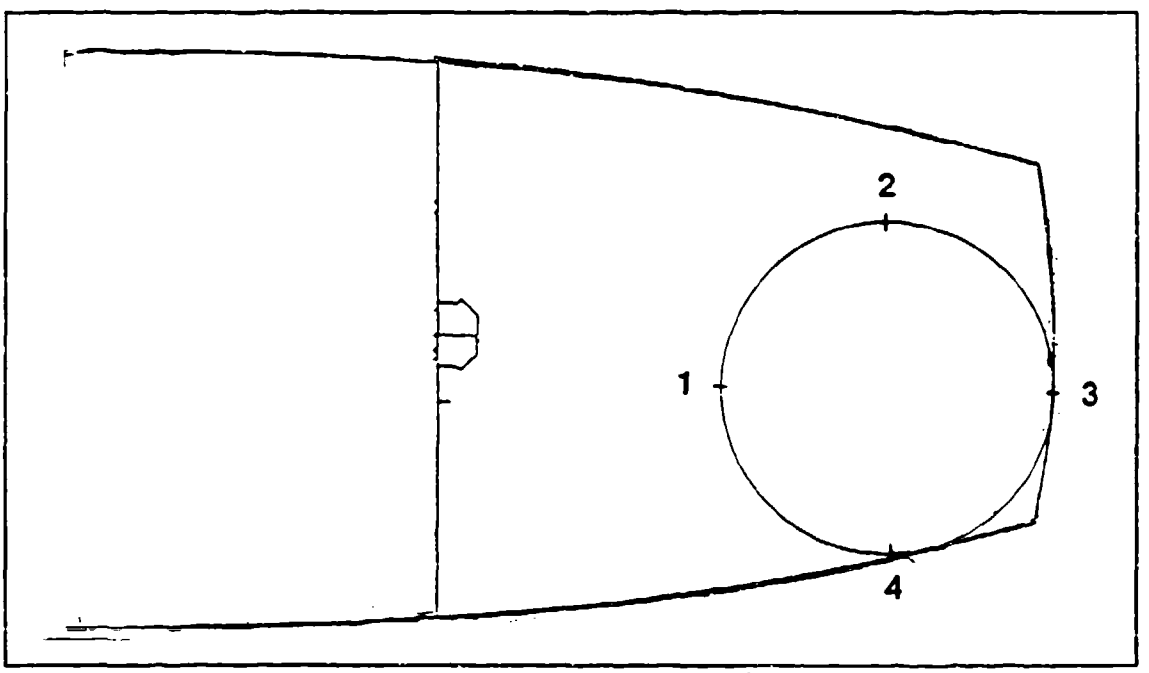

Figure 13. Velocity Measurement Locations on AOR Model

study to determine the validity of the modeling done at the Naval Postgraduate School. Moreover, these data can be used in preliminary analyses of the motion of a helicopter rotor in engagement/disengagement modes.

V. RESULTS

To illustrate the various flow patterns, photograph's showing the traces of helium bubbles and two-dimensional diagrams showing the mean streamlines are provided. The photographs are a representative set of a much larger set taken throughout this study. The mean streamlines are presented because the flow is very turbulent but does seem vary around certain mean directions.

While helium bubble traces can visualize a larger volume of flow than smoke, given turbulent conditions, it can be difficult to interpret the resulting photographs. It was found that very few bubbles entered recirculations which brought air from the leeward side of the ship over the flight deck. Smoke, on the other hand, provided a very accurate view of the flow patterns and video recordings were used to construct two-dimensional interpretative diagrams of the flow patterns observed from the smoke streaklines.

For the 000° and the 030° yaw positions, the diagrams illustrate the streamlines in the planes shown in Figure 14. For the other positions, the illustrated planes are shown in Figure 15. These planes were parallel to the aft hangar face and are located 31.75 mm (1.25"), 101.6 mm (4"), and 165.1 mm (6.5") aft of the hangar. It is important to note that the flight deck's width narrows as one move aft from the hangar face. This is shown in the rear view diagrams by contour lines, which indicate the shape of the hull in the three different planes just described.

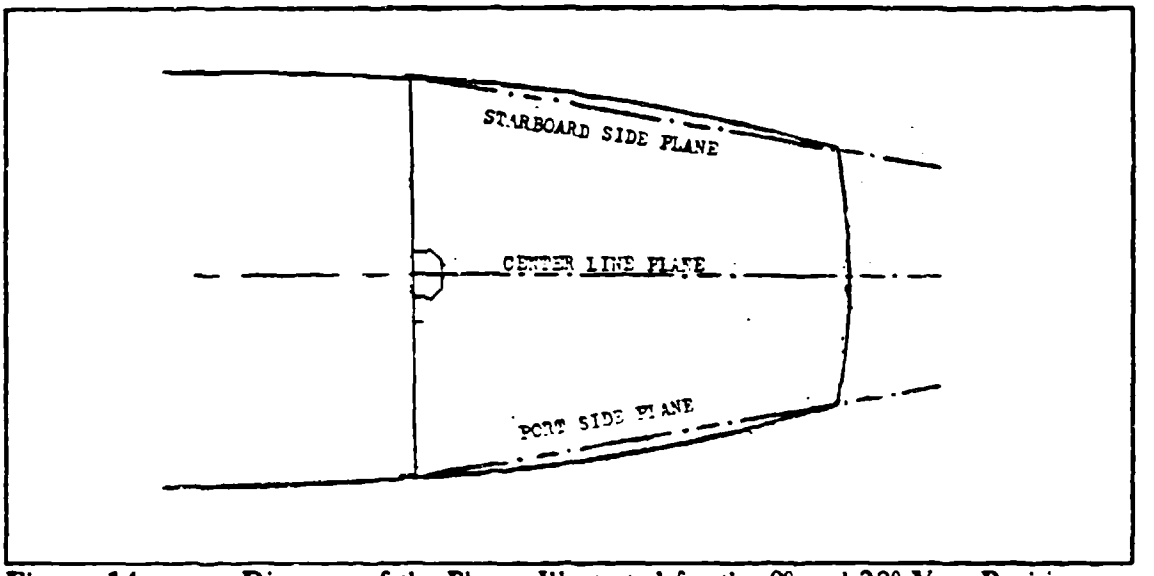

Figure 14. Diagram of the Planes Illustrated for the 0° and 30° Yaw Positions.

The top views illustrate a plane which was parallel to the flight deck's surface but was elevated from that surface by half the height of the hangar, approximately 15.87 mm.

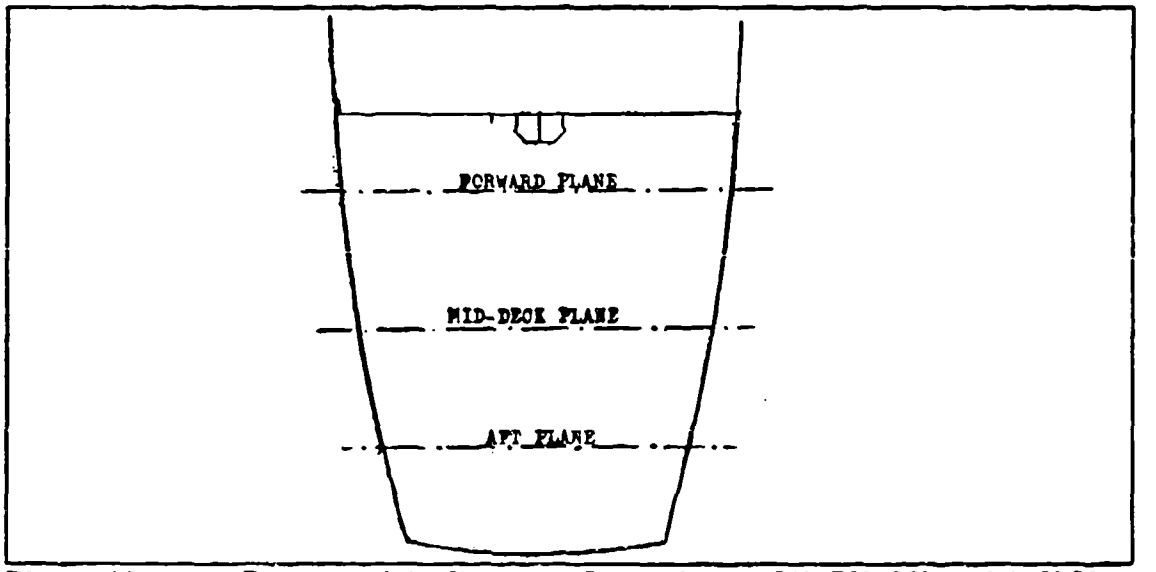

Figure 15. Diagram of the Illustrated Planes for the 50°, 70°, 90°, and 110° Yaw Positions

Generally, two distinct flow regions exist over the flight deck. One, shown as Region 1 in Figure 16, was outside the curved shear layer that was produced by the air flowing around the hangar. This region typically had a small recirculation just downwind of the windward deck edge but was otherwise smooth. The recirculation was bounded on the downwind side by a shear layer that attaches on the surface of the flight deck.

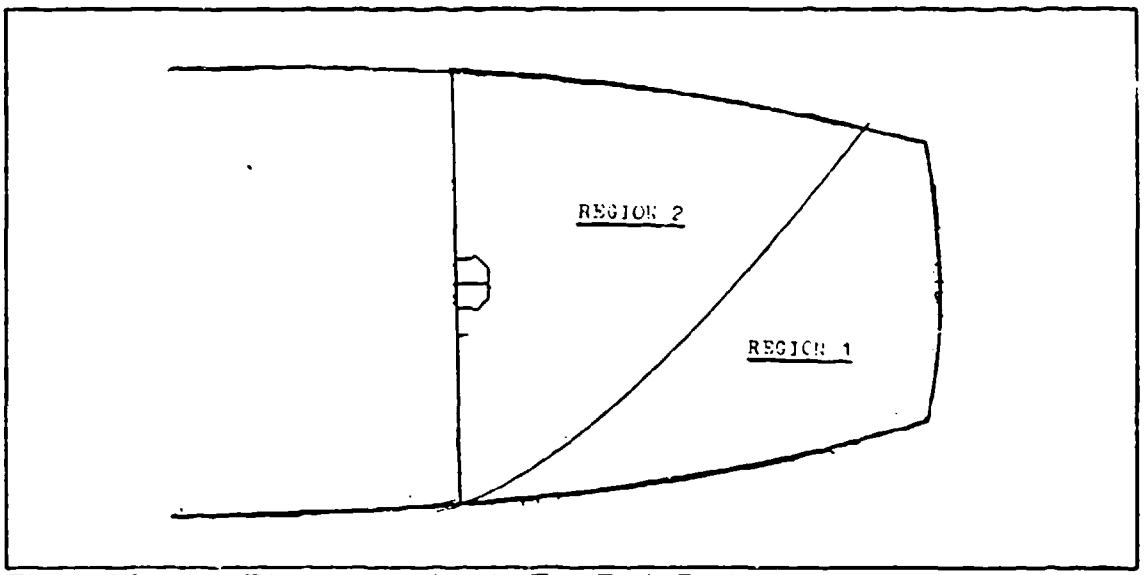

Figure 16. Diagram showing the Two Basic Regions

This attachment point moves rapidly port and starboard. The range of travel of this attachment is shown in the diagrams by a dashed double-headed arrow just under the line that represents the flight deck's upper surface.

The second, shown as Region 2 in Figure 16, was contained inside the curved shear layer. Here the flow was dominated by recirculations, which were very three-dimensional in nature. Everything about this region was unsteady, due to the extreme amount of turbulence. A typical vertical recirculation is shown in Figure 17. The streamlines

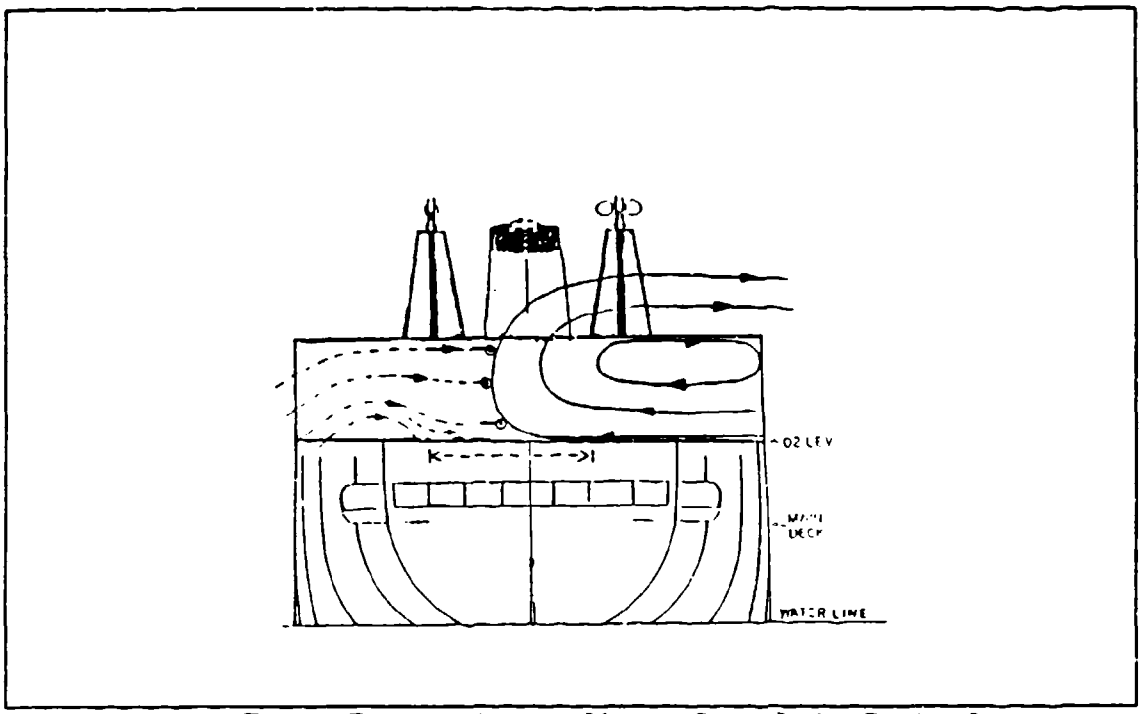

Figure 17. Typical Recirculation in a Vertical Plane Inside Region 2

ending at circles pass out of the plane of the paper towards the reader and proceed along the face of the recirculation.

Figure 18 shows a typical recirculation, when viewed from above, that was bounded on the downstream side by a shear layer that attaches on the aft hangar face. The point where this occurs moves port and starboard along the hangar face, with the range of travel being indicated in the figures by a dashed double-headed arrow parallel to the line representing the aft hangar face. During the study of some positions, it was found that the attachment point would move downwind, starboard, and separate from the hangar face. Where this separation occurred is indicated in the figures by an "X" on the downwind end of the dashed arrow in the top view diagrams. This looked somewhat similar to a bubble bursting on one side. After the separation, the shear layer would

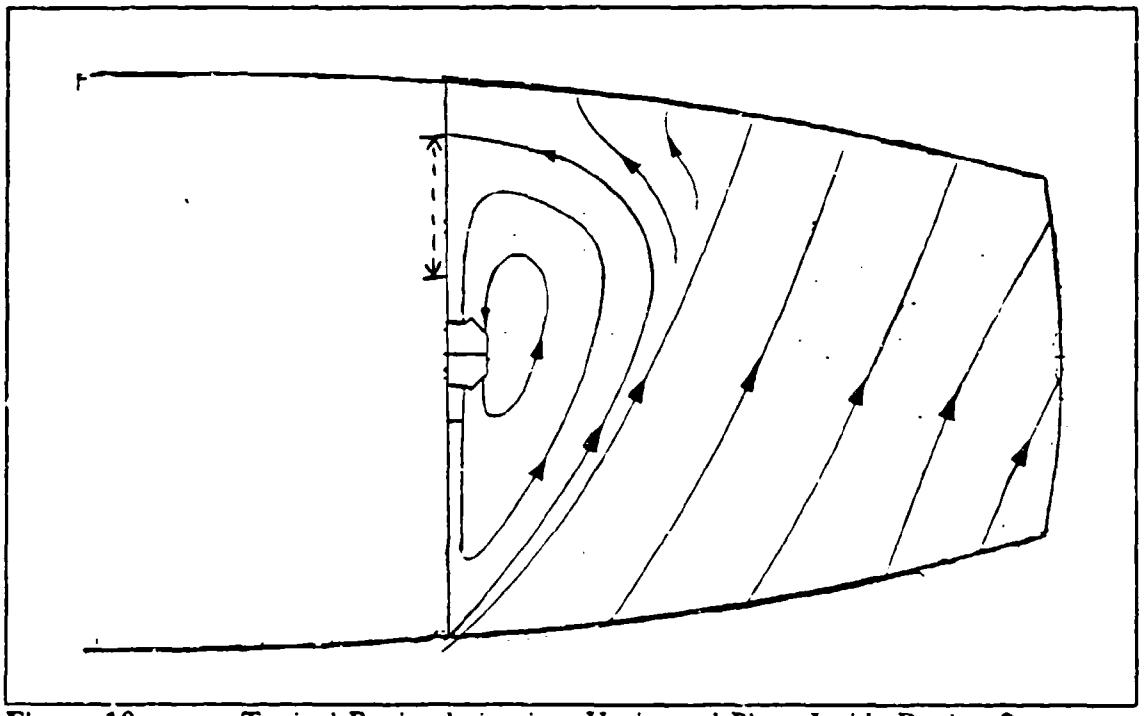

Figure 18. Typical Recirculation in a Horizontal Plane Inside Region 2.

swing out over the deck and a short section of this layer, very near to the upwind corner of the hangar, would bend in toward the hangar and reattach again to the hangar face forming a new recirculation which would repeat the process just described. This motion was repeated with a nearly periodic nature with a average period between 1/3 and 1/5 of a second.

A. 0° YAW POSITION

The AOR class ship is more symmetrical than most ships, having only one extra replenishment station on the port side which far forward of the flight deck. This led to very symmetrical flow patterns over the deck, as shown in Figure 19.

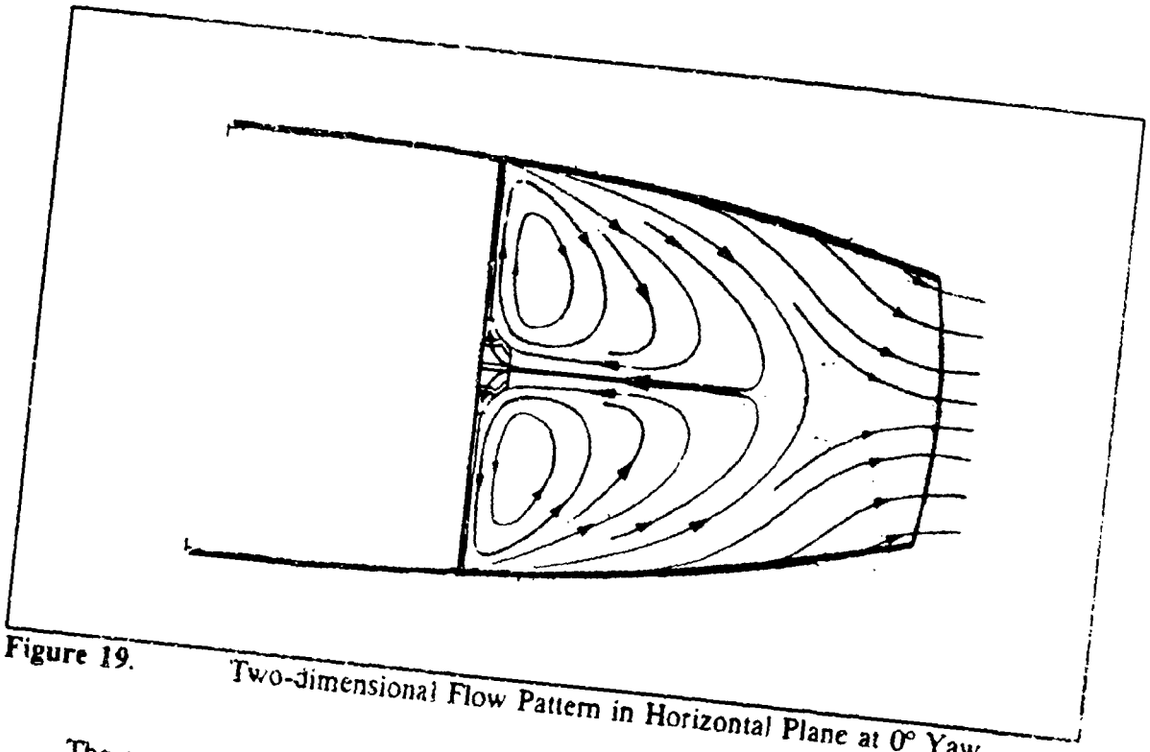

Figure 19. Two-dimensional Flow Pattern in Horizontal Plane at 0° Yaw.

The general flow patterns seen behind the aft hangar face are similar to those found behind the back side of a three-dimensional cube, as was illustrated earlier in Figure 3. There is a recirculation just behind the aft hangar that is bounded by a shear layer that attaches on the flight deck's surface. As shown in Figure 20, there is very little of the deck that is exempt from this recirculation, this is also evident from the helium bubble traces shown in Figure 21. The rotations of the flow in the vertical and horizontal planes are slower than those found in the other positions. The air flow that comes up and over the port and starboard deck edges is more or less smooth as shown in Figures 22 and 23.

B. 30° YAW POSITION

This position quickly showed the significant effects of yawing the ship on the flow patterns. Figures 24 through 26 show that the port aft corner of the flight was subject

Figure 20. Airwake over Flight Deck at 0° Yaw.

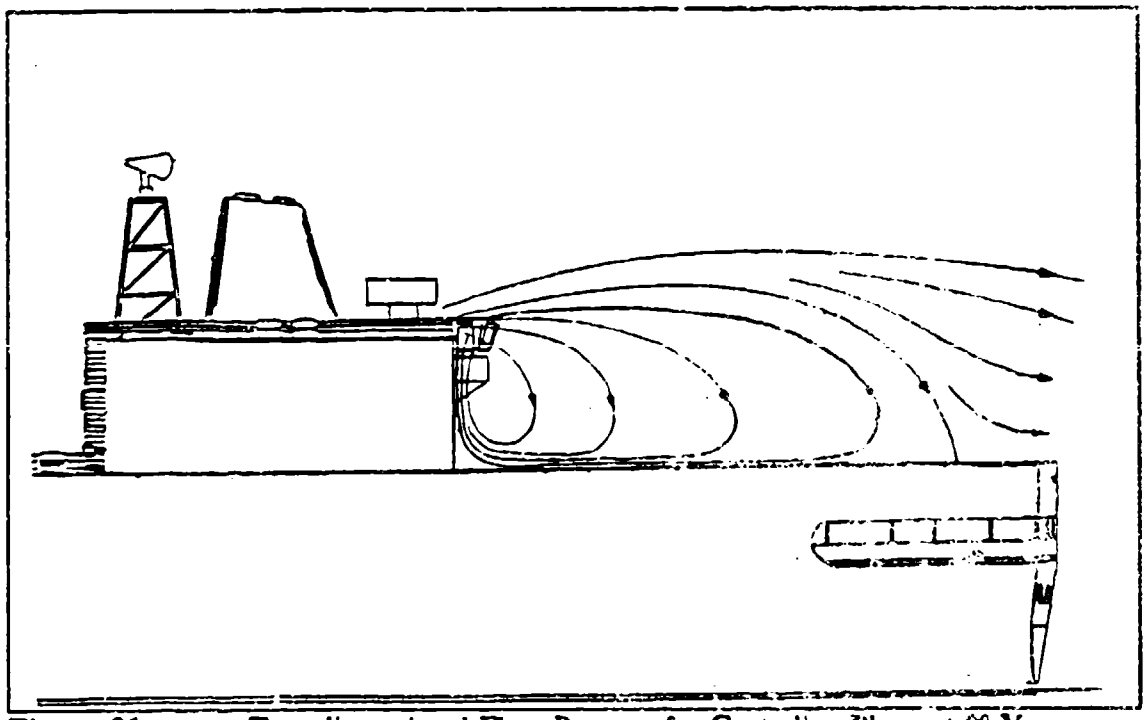

Figure 21. Two-dimensional Flow Patterns for Centerline Plane at 0° Yaw.

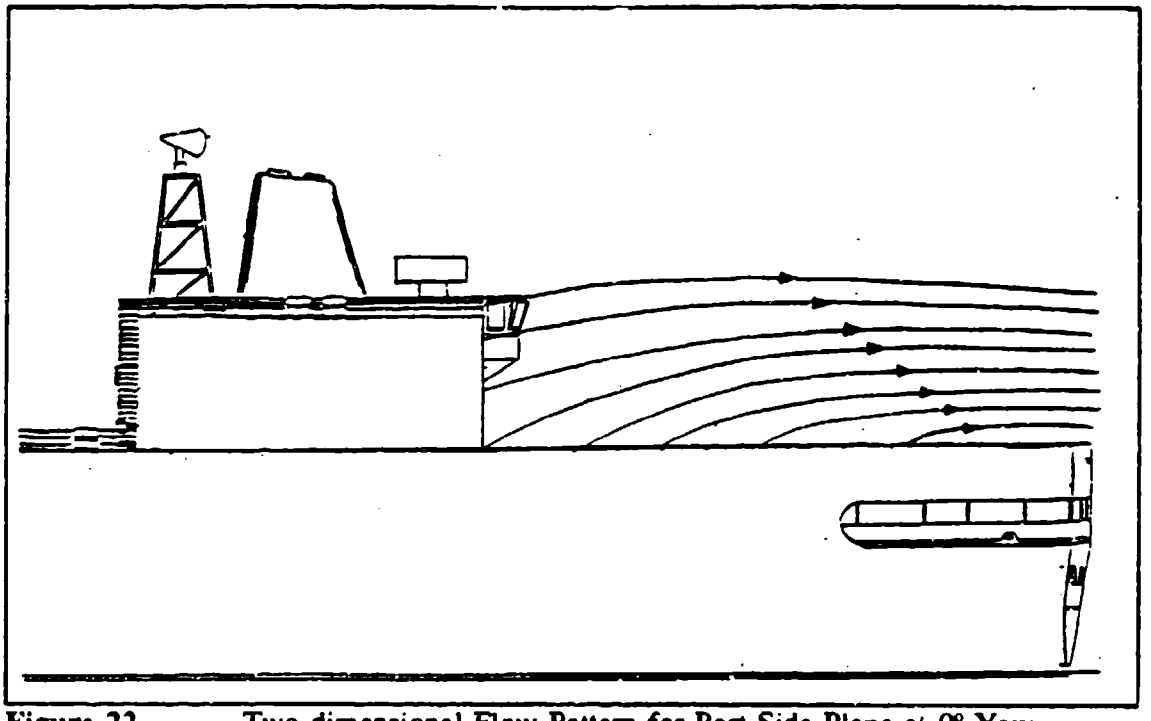

Figure 22. Two-dimensional Flow Pattern for Port Side Plane at 0° Yaw.

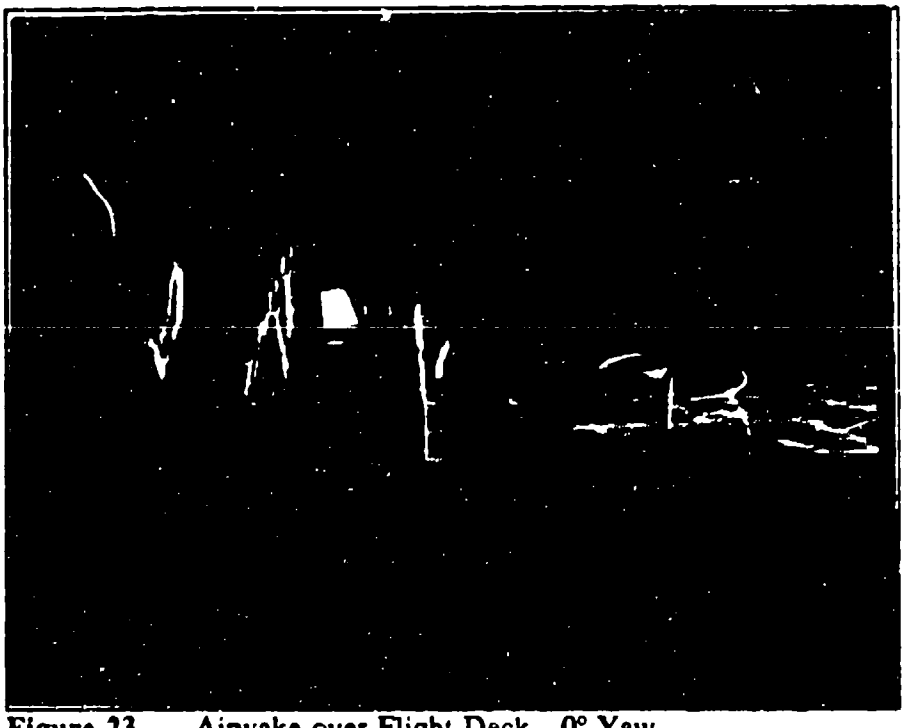

Figure 23. Airwake over Flight Deck - 0° Yaw.

to relatively smooth flow that had an upward component when it crossed the port deck edge. This was also confirmed by the smoke visualization, with the resulting interpretative diagram shown in Figure 27. The remaining area, approximately three-quarters of the flight deck area, was engulfed in the very turbulent region caused by the presence of the hangar in the flow. Figures 24 and 28 both illustrate that the flow patterns behind the hangar are somewhat similar to those found in the 000° position, with a large recirculation behind the aft hangar face. However, when viewed from above, some great differences appear. The flow is obviously skewed to starboard due to change in the direction of the relative wind, as shown in Figure 25. There was a significant flow coming from the leeward side of the ship, which is evident in Figure 26 by a solitary

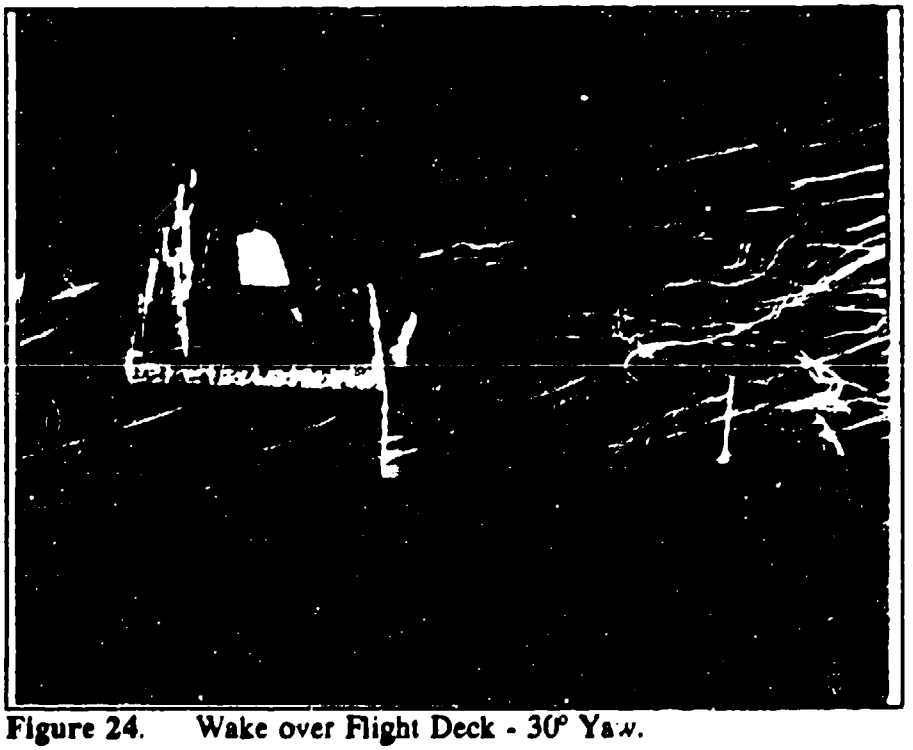

Figure 24. Wake over Flight Deck - 30° Yaw.

Figure 25. Wake over Flight Deck - 30° Yaw.

bubble trace that seems to travel almost the full span of the deck. Since this flow originated from the leeward side, and the helium bubbles were introduced on the windward side, very few bubbles entered this flow. More complete evidence was found using smoke, with the resulting flow patterns shown in Figure 29. Figure 30 shows that the flow coming around the aft starboard corner of the hangar rotates clockwise, that was the only identifiable pattern in the starboard side plane.

As one goes to higher elevations above the flight deck, approximately 125% of the hangar height, the flow rapidly changes to smooth flow in the direction of the free stream. This was very evident in the smoke visualization but is also evident in Figure 25 and Figure 26.

Figure 26. Wake over Flight Deck - 30° Yaw.

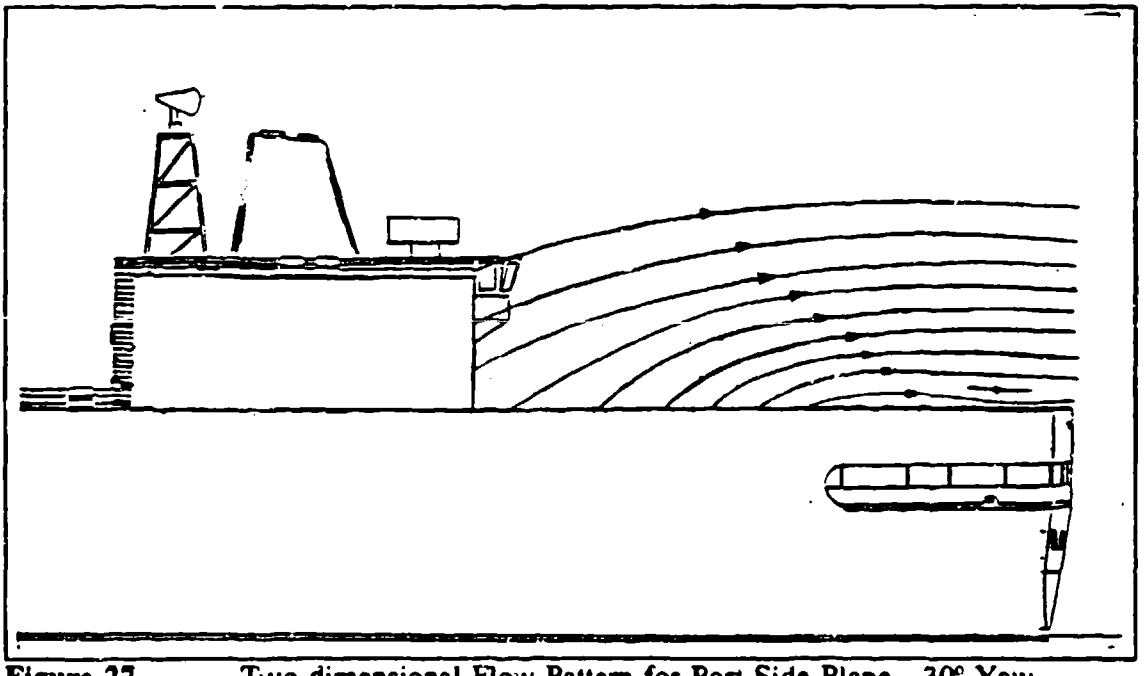

Figure 27. Two-dimensional Flow Pattern for Port Side Plane - 30° Yaw.

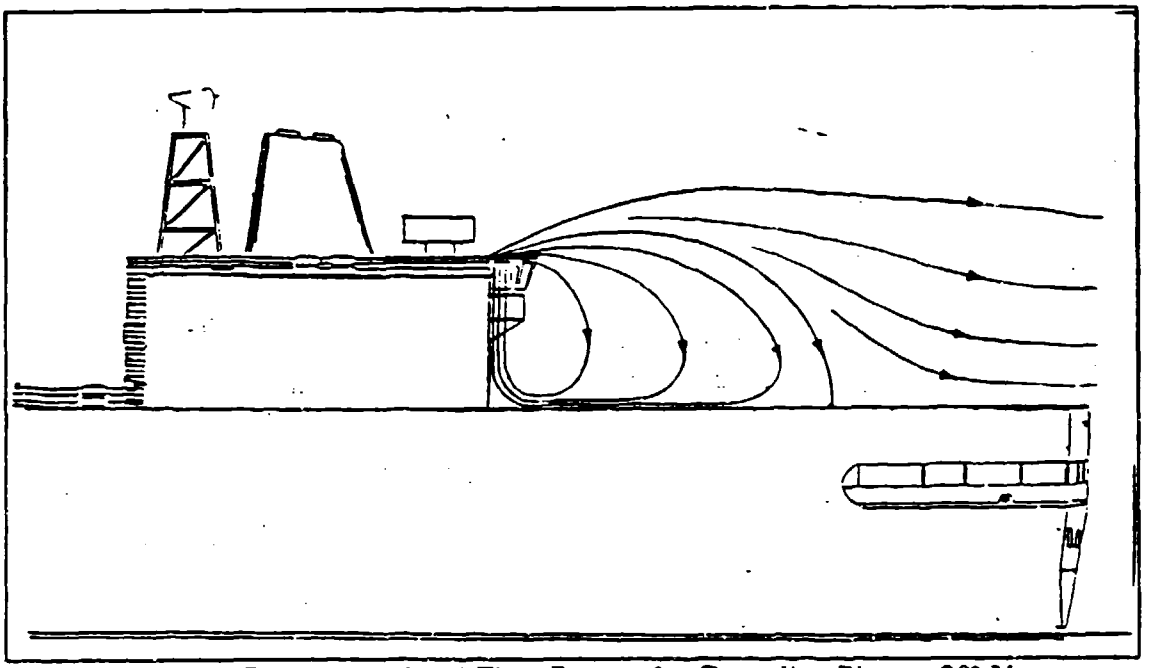

Figure 28. Two-dimensional Flow Pattern for Centerline Plane - 30° Yaw.

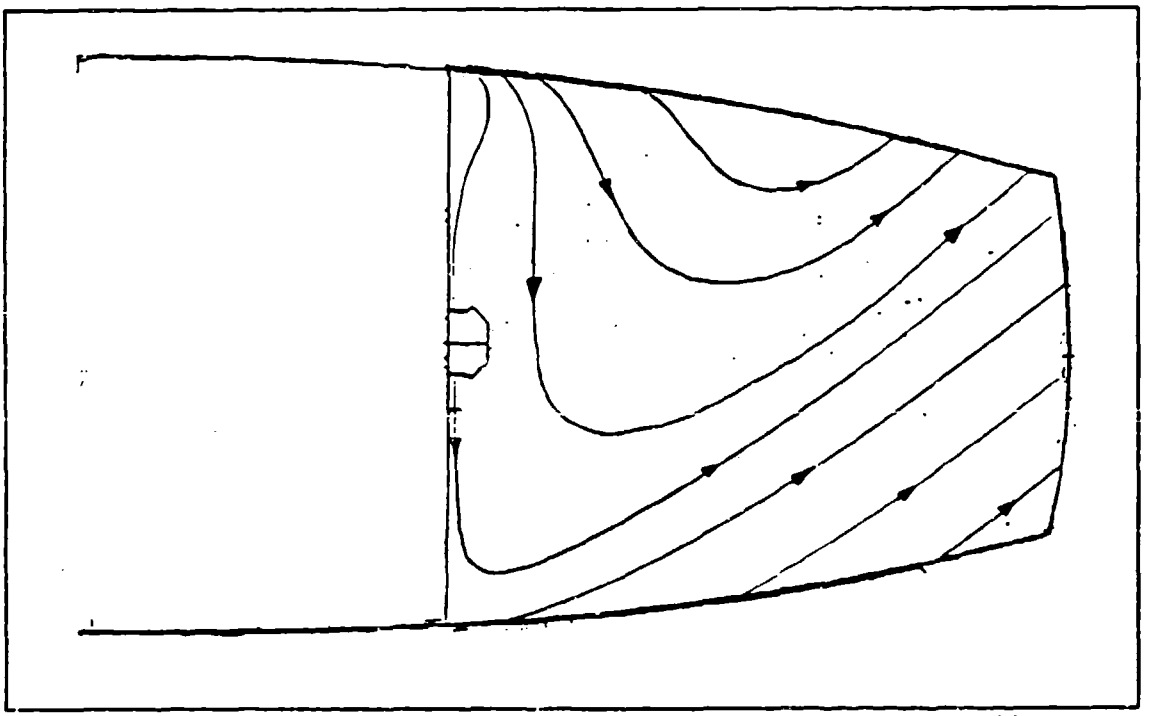

Figure 29. Two-dimensional Flow Patterns over Flight Deck when View from Above - 30° Yaw.

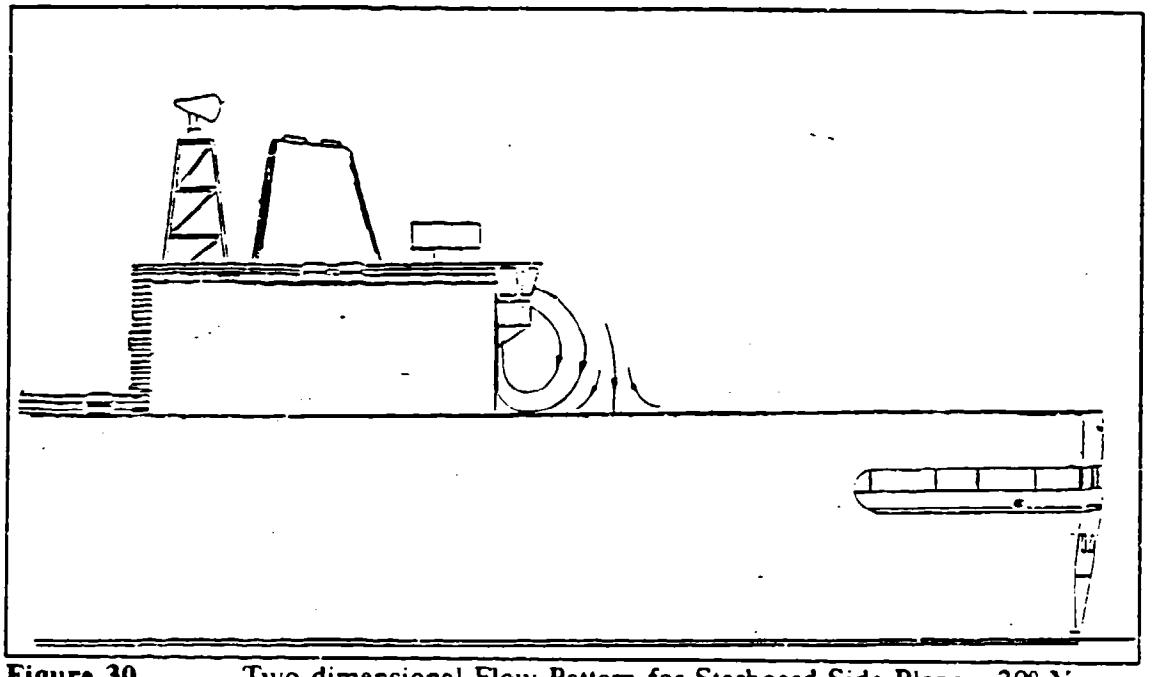

Figure 30. Two-dimensional Flow Pattern for Starboard Side Plane - 30° Yaw

C. 50° YAW POSITION

The 50° yaw position offered the unique opportunity to photograph the helium bubbles from two different camera angles, one from just ahead of the hangar face plane and the other from the ship's port quarter. Figure 31 very clearly illustrates the distinct separation of the Regions 1 and 2, described on page 39 of this paper. The helium bubble traces over the aft port corner are very smooth; unfortunately they are also very faint in the figure but are quite visible in the original photograph.

When visualizing the flow with smoke, a unique feature of this position became evident. It appeared that the aft port hangar corner was shedding vortices, when the ship model was viewed from above at normal video recording speeds. When the same recording was viewed in slow motion, it was found that the recirculation which formed near the aft port corner grew in size, and that the reattachment point moved starboard

Figure 31. Wake over the Flight Deck When Viewed from Ahead of Aft Hangar Face - 50° Yaw

towards a position where it would ultimately detach from the hangar face. This position is indicated by an "X" in Figure 32. When the shear layer detached, the rotation of the recirculation would continue but its center would move downstream at angle about 45° from the hangar face plane, as shown in Figure 33. This would happen very quickly, on the order of 1/6 to 4/15's of a second based upon a camera shutter speed of 1/30th of a second, and would repeat almost periodically. This caused the smoke streaklines to form puffs and appeared similar to shed vortices, see Figure 34.

The aft-view diagrams show how very large, approximately 150% of the hangar height, the recirculation region was in the vertical plane, and how very turbulent, as shown in Figures 35 and 36. This proved to be the largest region of all the yaw positions, see Figures 37 and 38. The windward tip of that recirculation would move port and starboard to some degree very quickly, the range of which is indicated in the

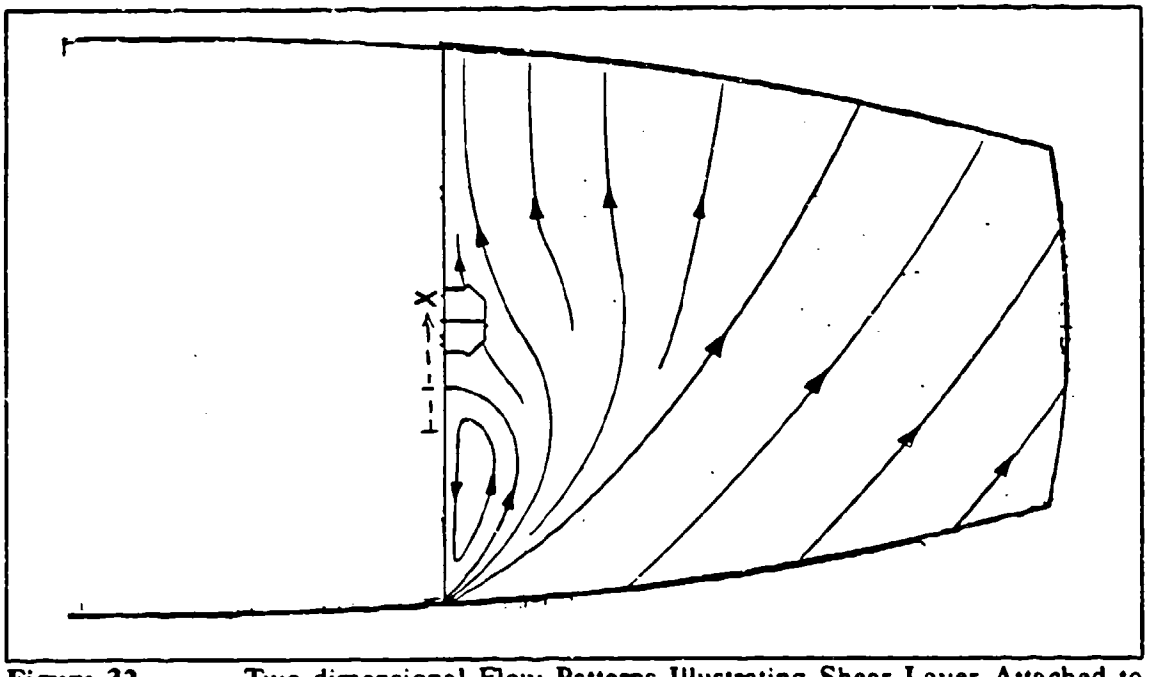

Figure 32. Two-dimensional Flow Patterns Illustrating Shear Layer Attached to Rear Hangar Face - 50° Yaw.

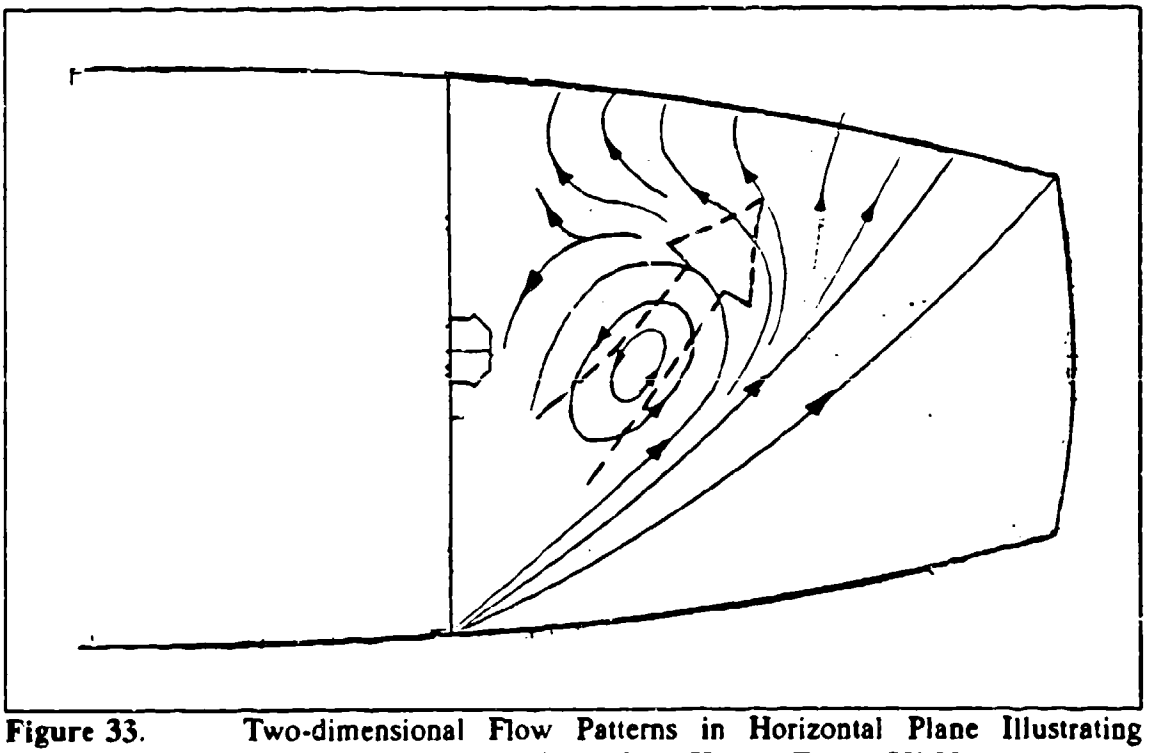

Figure 33. Two-dimensional Flow Patterns in Horizontal Plane Illustrating Recirculation Moving Away from Hangar Face - 50° Yaw

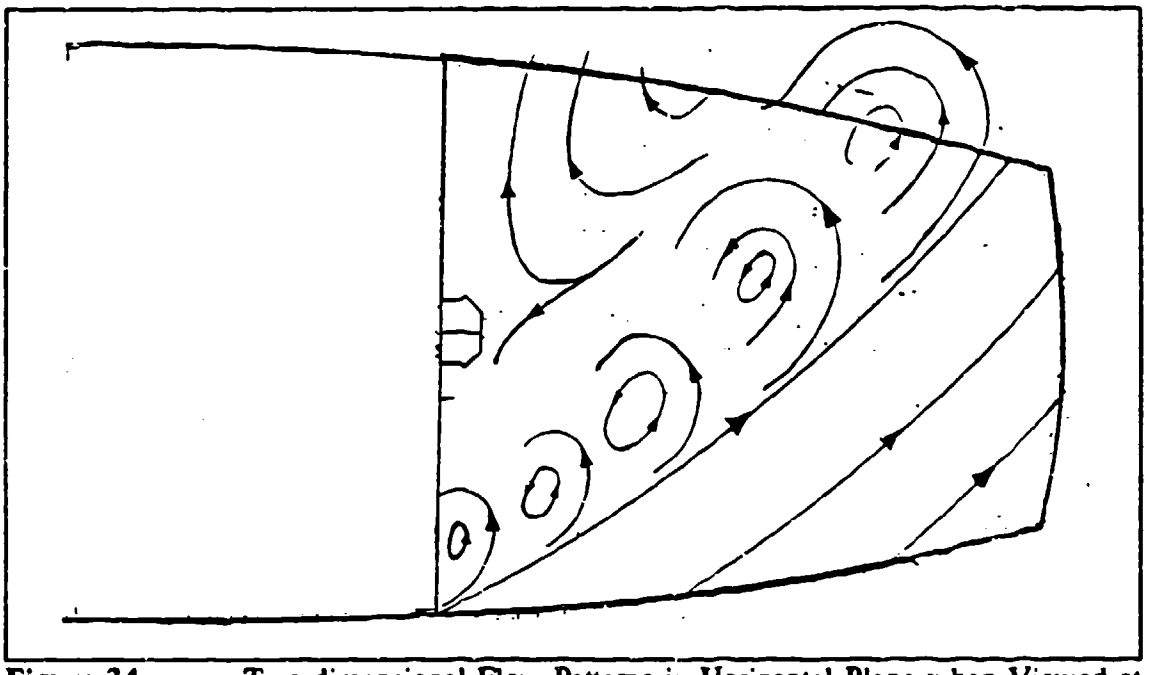

Figure 34. Two-dimensional Flow Patterns in Horizontal Plane when Viewed at Normal Video Playing Speed - 50 Yaw.

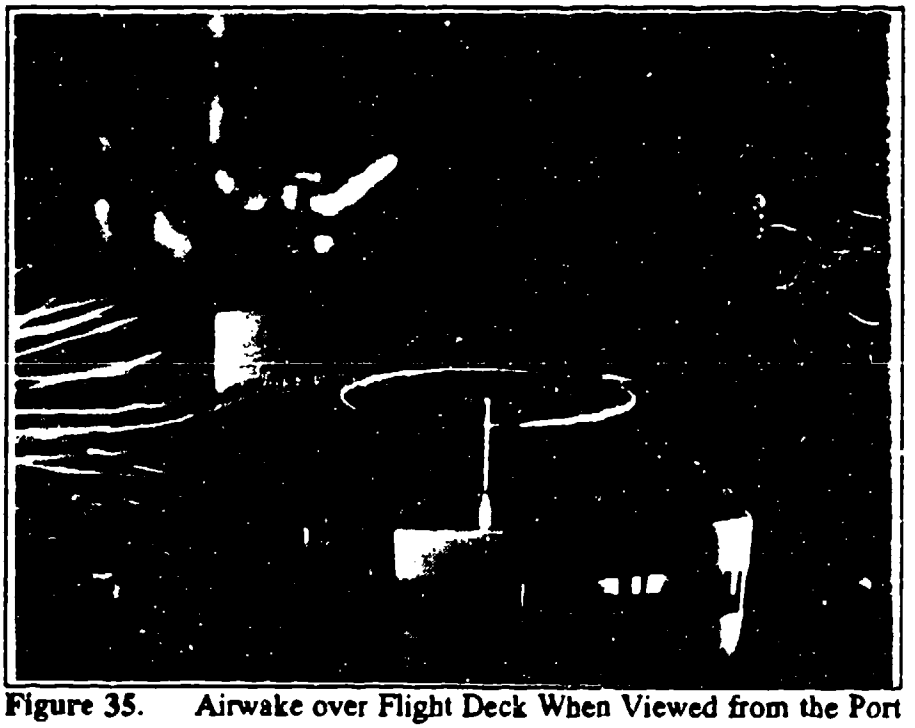

Figure 35. Airwake over Flight Deck When Viewed from the Port Quarter - 50° Yaw.

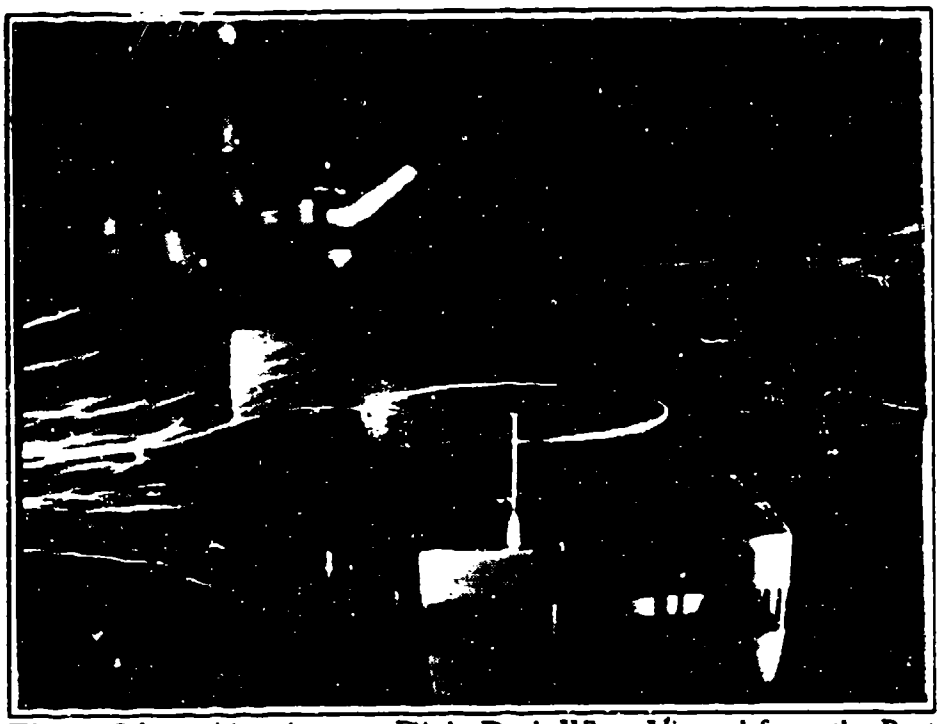

Figure 36. Airwake over Flight Deck When Viewed from the Port Quarter - 50° Yaw.

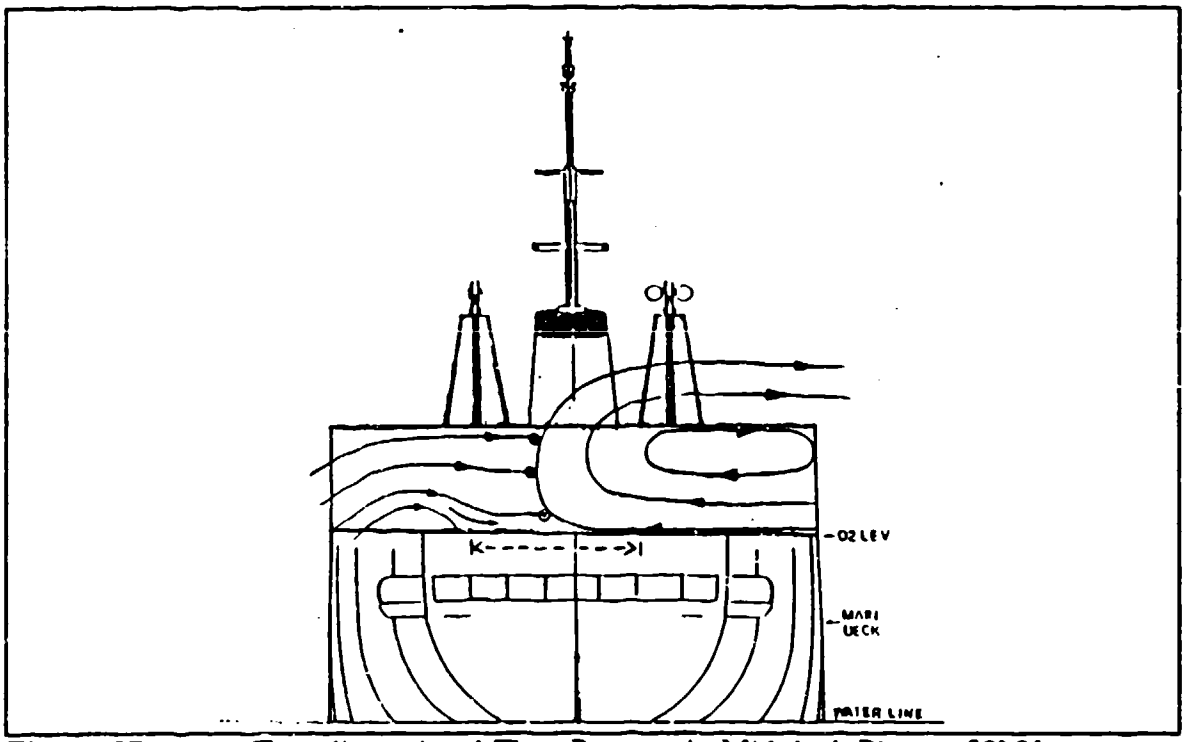

Figure 37. Two-dimensional Flow Patterns in Mid-deck Plane - 50° Yaw.

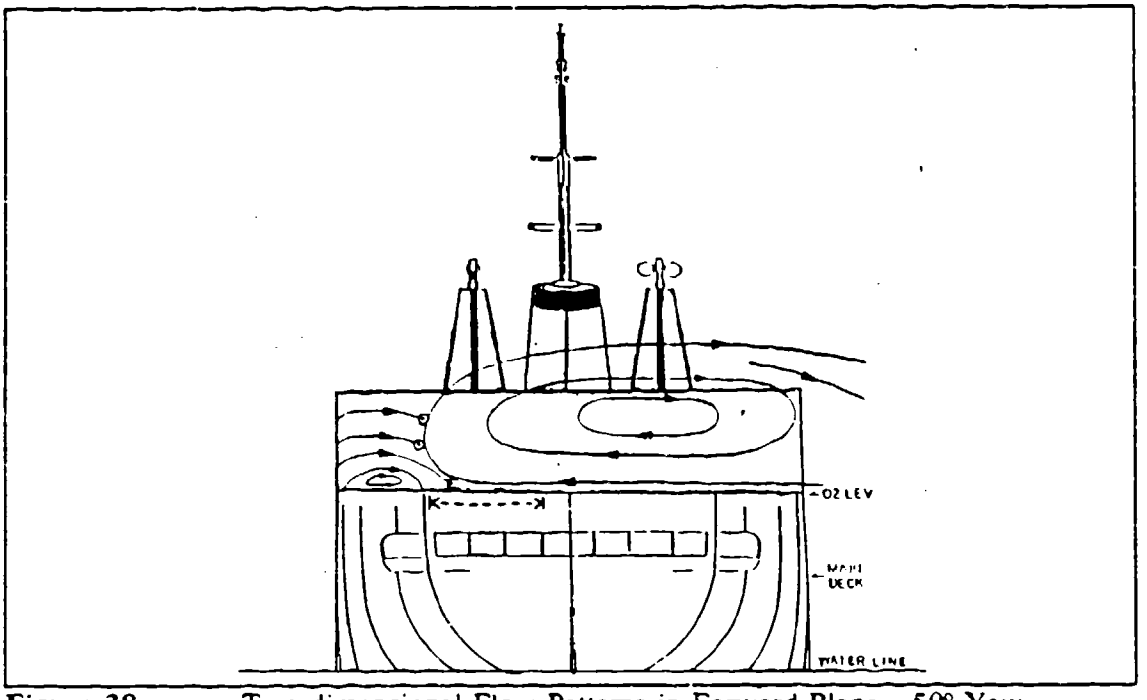

Figure 38. Two-dimensional Flow Patterns in Forward Plane - 50° Yaw.

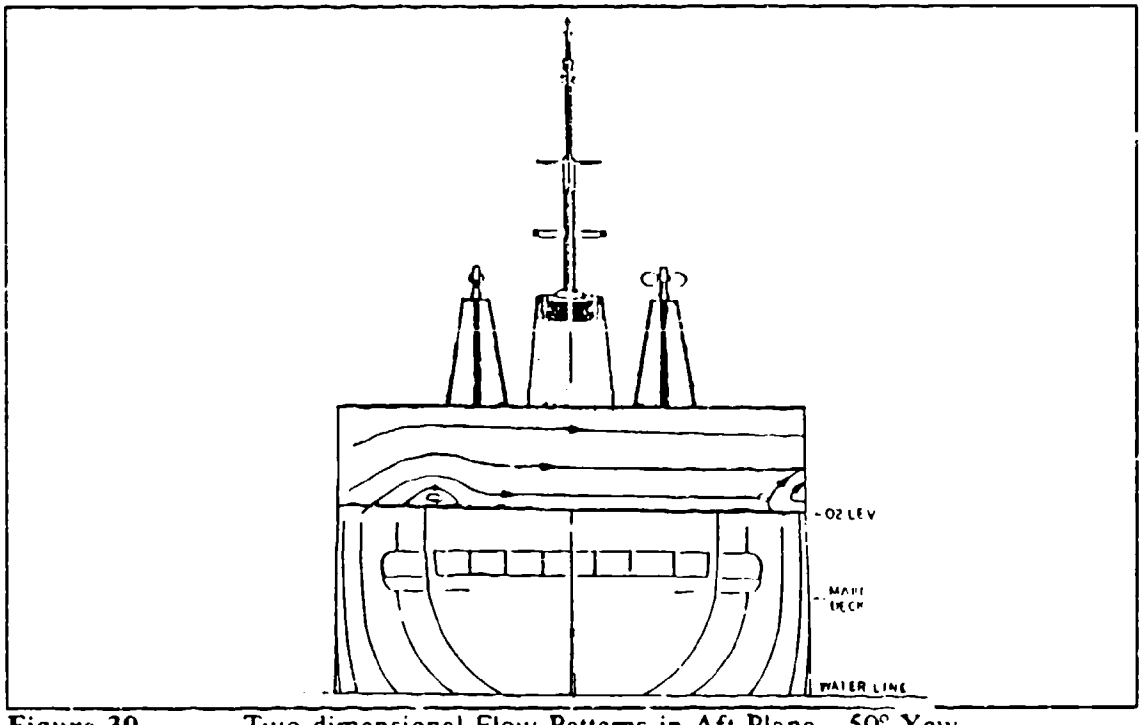

Figure 39. Two-dimensional Flow Patterns in Aft Plane - 50° Yaw.

figures by a dashed double-headed arrow just below the line representing the flight deck's surface. This movement is surely linked to the movement of the reattachment point on the rear hangar face described in the preceding paragraph.

D. 70° YAW POSITION

The 70° position yielded results somewhat similar to those found for the 50° position, but the recirculation area behind the hangar was not as large in the vertical direction. The flow in this region recirculated in an elliptical pattern which had a larger length-to-width ratio, than the 50° position. See Figures 40 and 41. This condition also leads to much smoother conditions over the flight deck, as evidenced by the straighter bubble traces shown in Figures 42 and 43.

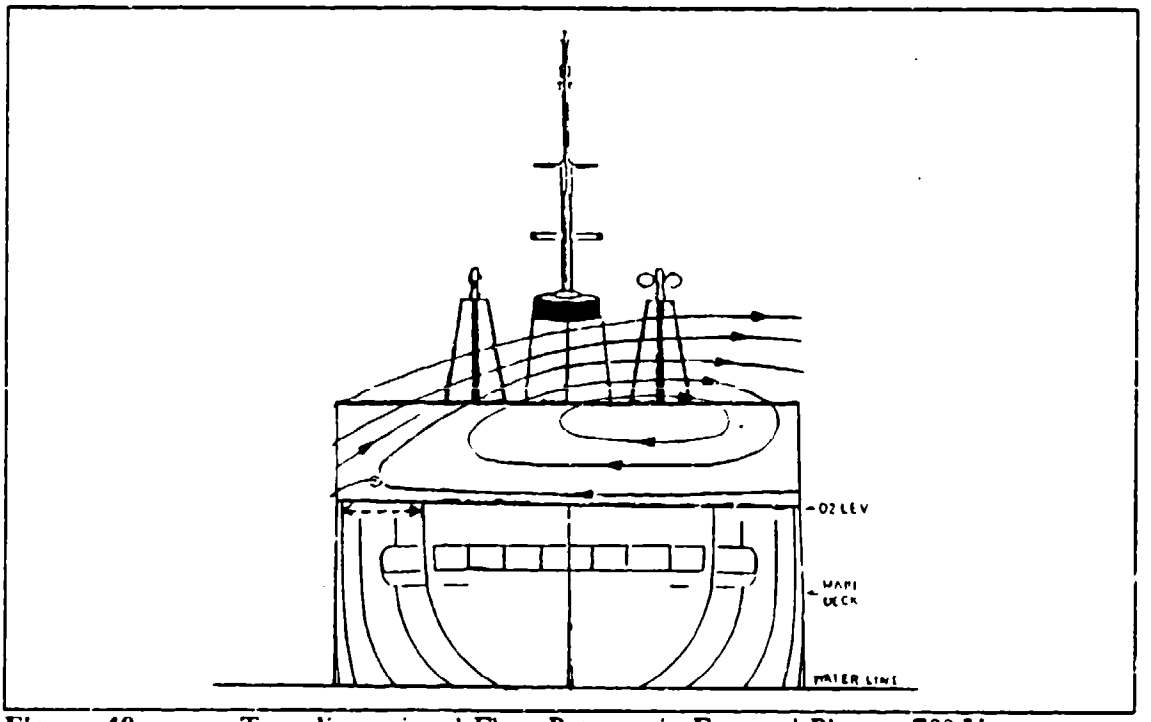

Figure 40. Two-dimensional Flow Patterns in Forward Plane - 70° Yaw.

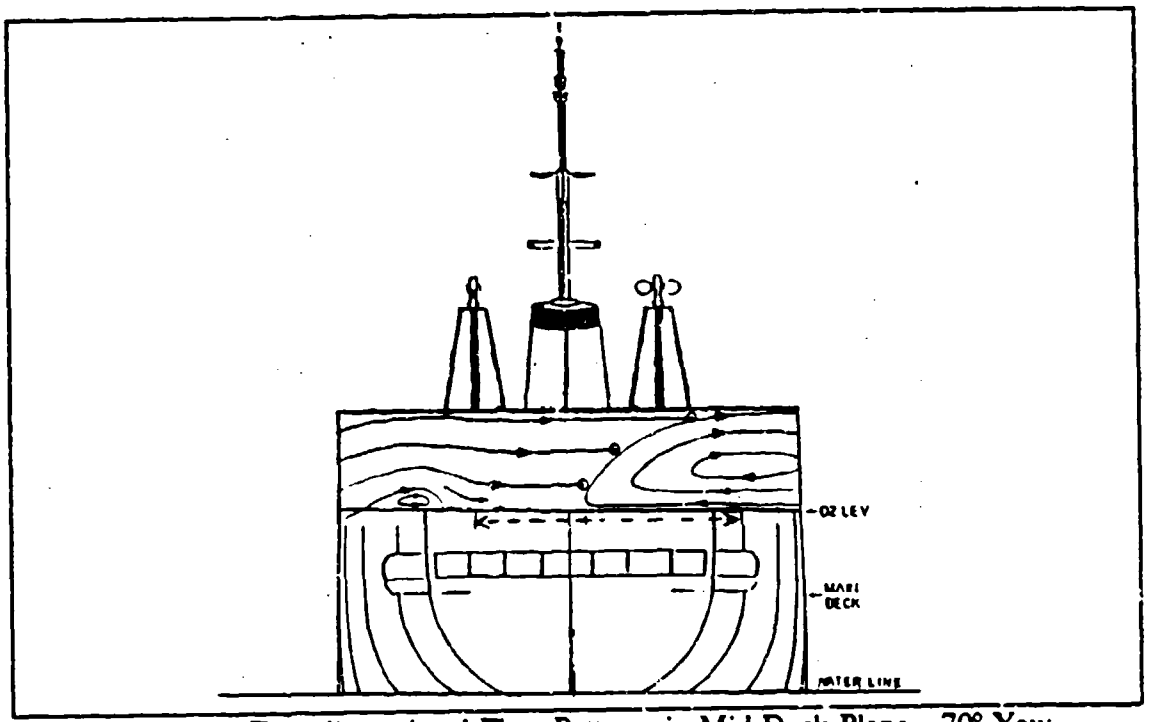

Figure 41. Two-dimensional Flow Patterns in Mid-Deck Plane - 70° Yaw.

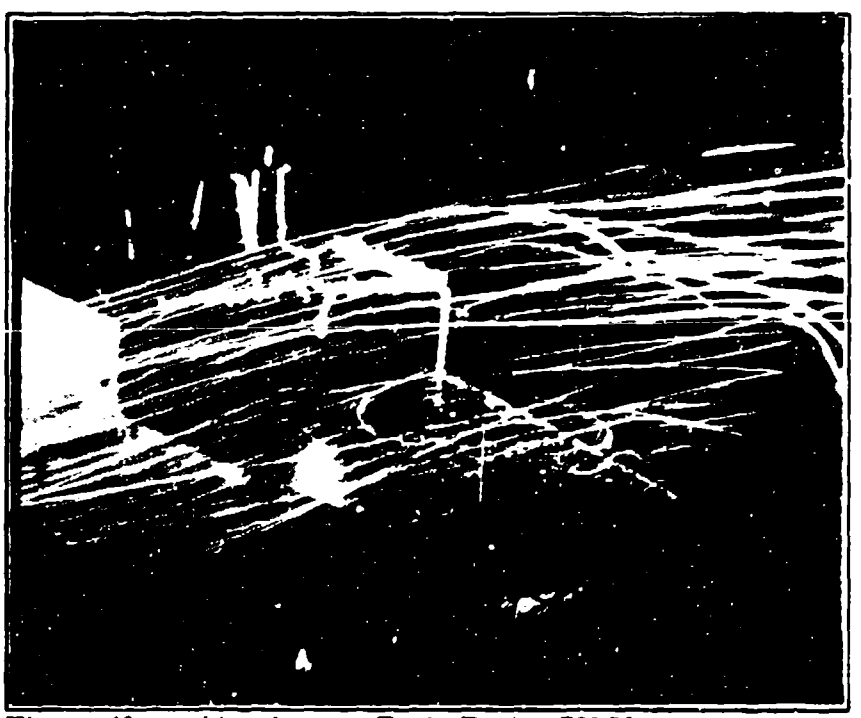

Figure 42. Airwake over Flight Deck - 70° Yaw.

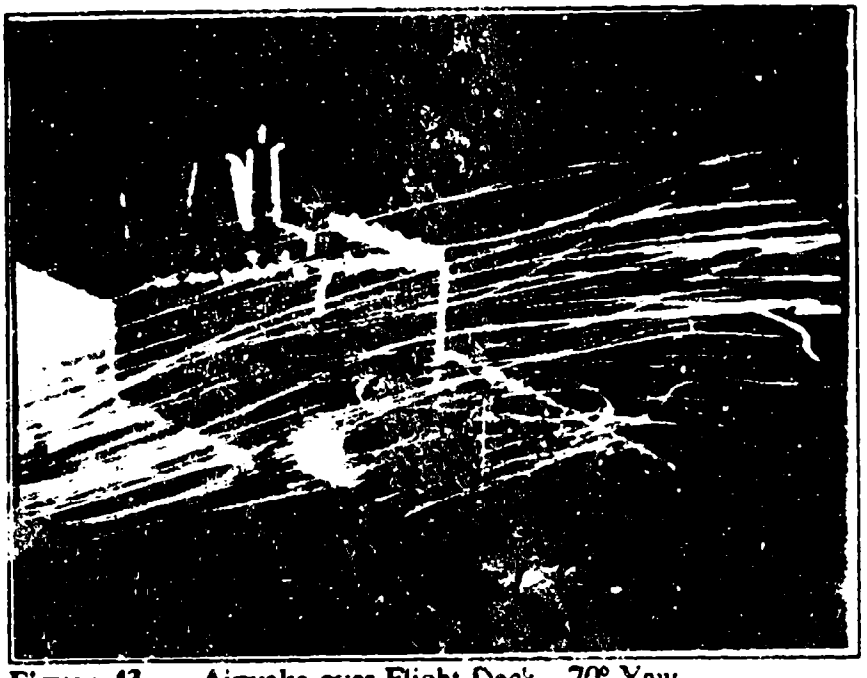

Figure 43. Airwake over Flight Deck - 70° Yaw.

Another notable difference was that the shear layer remained attached to rear hangar face with the reattachment point moving port and starboard. Figure 44 shows the flow patterns when the reattachment point is in its extreme port location, while Figure 45 illustrates the extreme starboard location. In both of these figures, one can see the larger area of smooth flow. However, the small recirculation that is located near the port deck edge is slightly larger than that found in the 50° case. This recirculation is illustrated in Figure 46.

E. 90° YAW POSITION

In the 90° yaw position the model ship experiences winds from 270° relative. The most obvious feature of the flow pattern was the upward flow over the port edge, as seen in Figures 47, 48, and 49. This upward flow made an angle of 15° to 20°

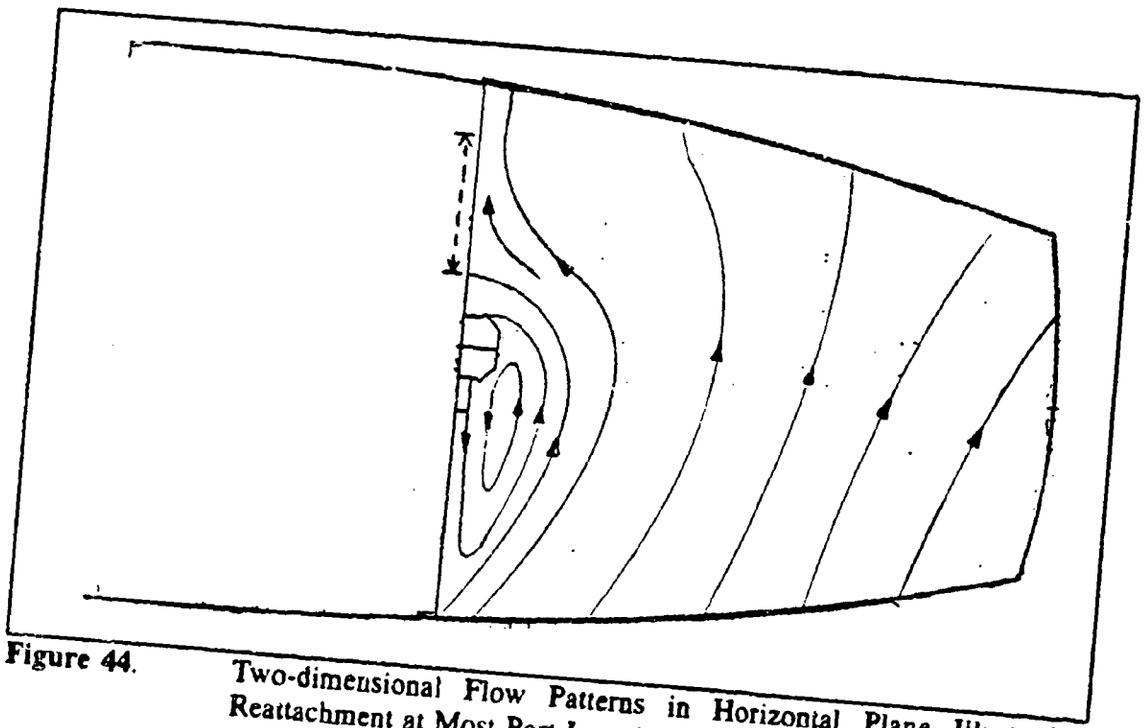

Figure 44. Two-dimensional Flow Patterns in Horizontal Plane Illustrating Reattachment at Most Port Location - 70° Yaw.

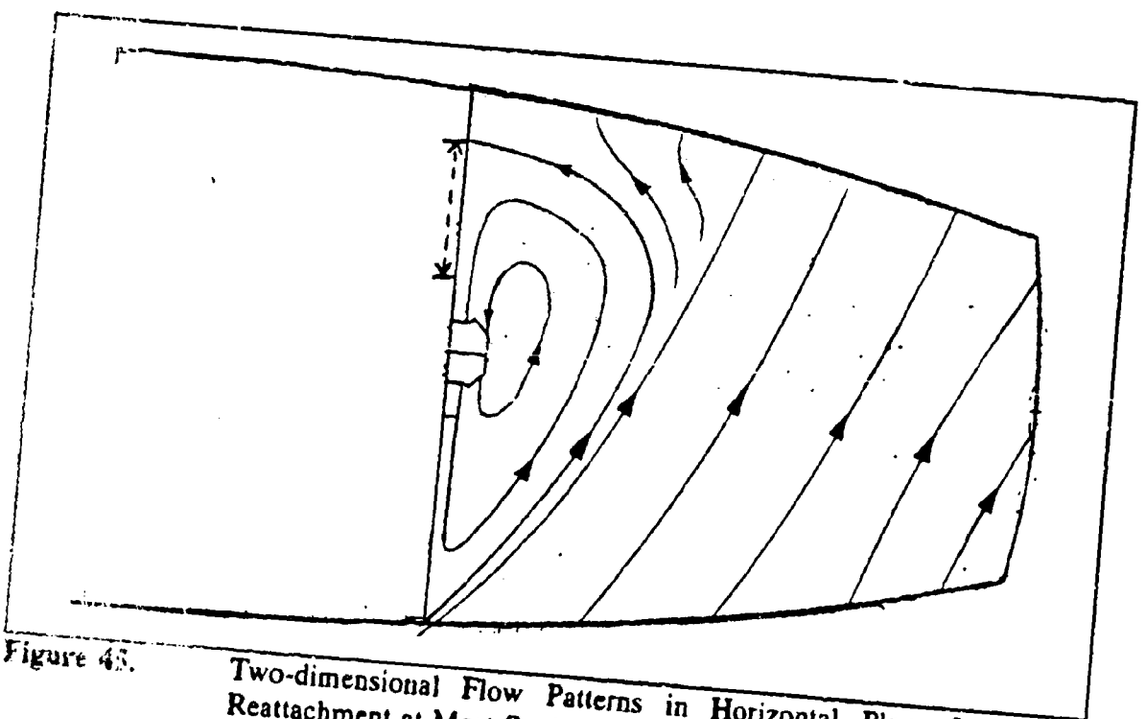

Figure 45. Two-dimensional Flow Patterns in Horizontal Plane Illustrating Reattachment at Most Starboard Location - 70° Yaw.

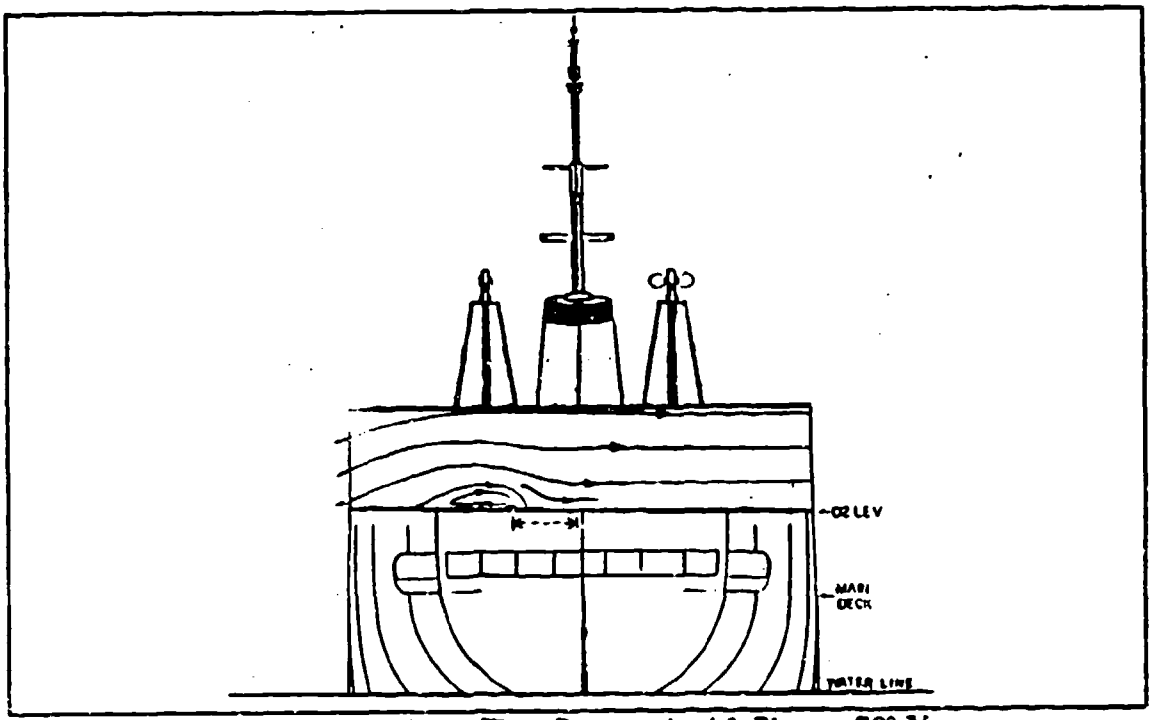

Figure 46. Two-dimensional Flow Patterns in Aft Plane - 70° Yaw.

Figure 47. Airwake over Flight Deck - 90° Yaw.

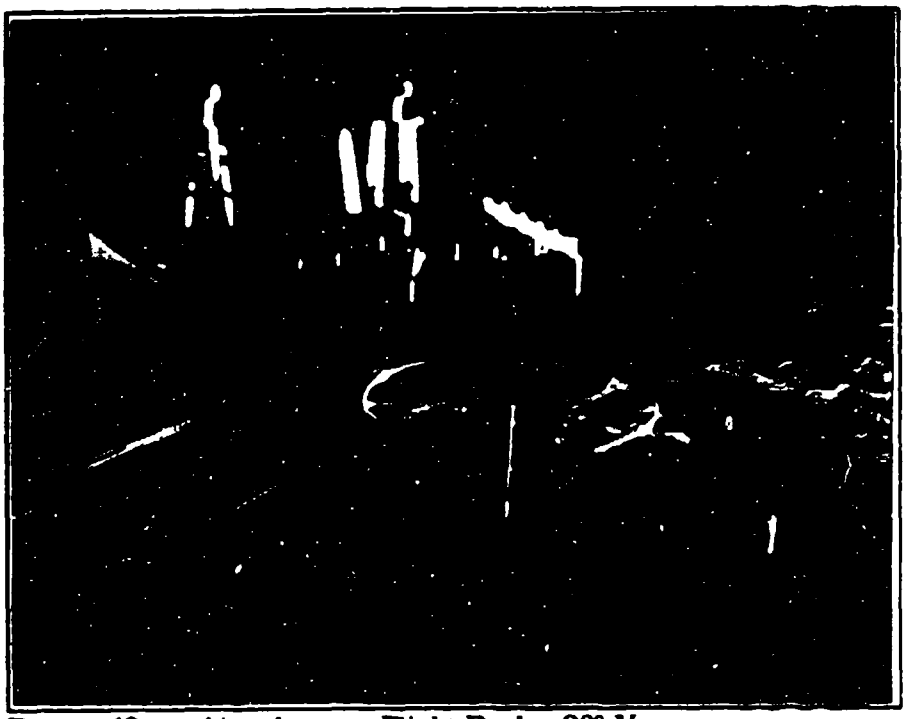

Figure 48. Airwake over Flight Deck - 90° Yaw.

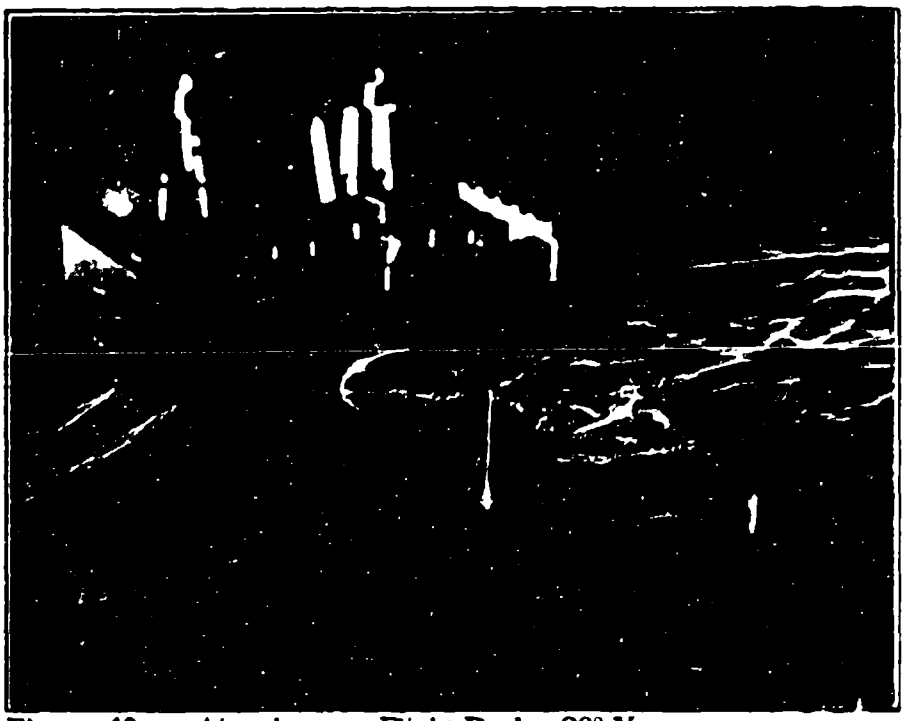

Figure 49. Airwake over Flight Deck - 90° Yaw.

with the horizontal and continued up and over the flight deck. Below this flow was a recirculation zone, as shown in Figure 50. This recirculation was bounded on the downwind side by a shear layer that reattaches to the flight deck. From the video recording of the smoke visualization, one could see that this point moved very rapidly back and forth over the span of the flight deck. However, the reattachment point usually remained in the area between 25% and 75% of the span of the deck.

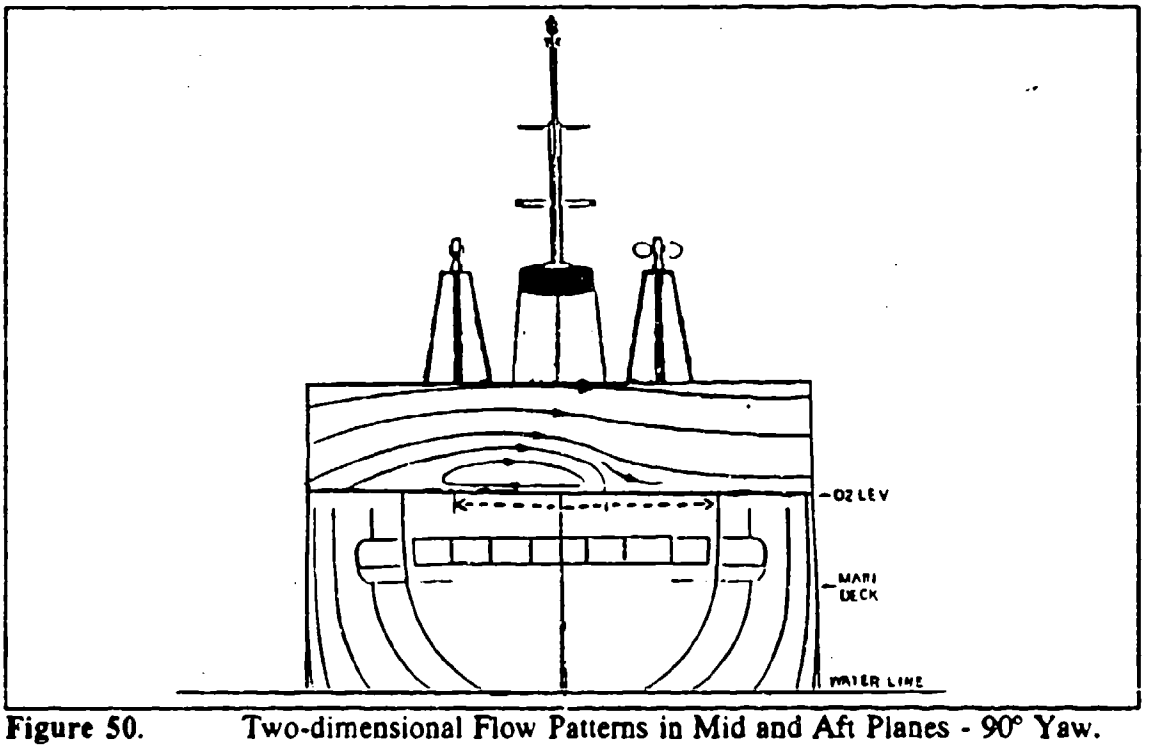

Figure 50. Two-dimensional Flow Patterns in Mid and Aft Planes - 90° Yaw.

An intuitive feeling about this yaw position might lead one to believe that the air would flow straight across the deck from the port side to the starboard. However, that was not the case. There was a very significant flow from around the port hangar face, which created a shear layer. Inside the shear layer, i.e. inside region 2, there was a

recirculation which was about the same size as found for the 70° position. However, this recirculation had a range of travel that was greater, as shown in Figure 51. As in previously discussed positions, this layer would reattach to the rear hangar face and move toward the starboard side of the ship, Figure 52 illustrates the flow patterns present when the attachment point is in its extreme port location. Unlike the previous cases, the shear layer would detach from the hangar when it reached the starboard side of the ship. The flow patterns for this condition are shown in Figure 53.

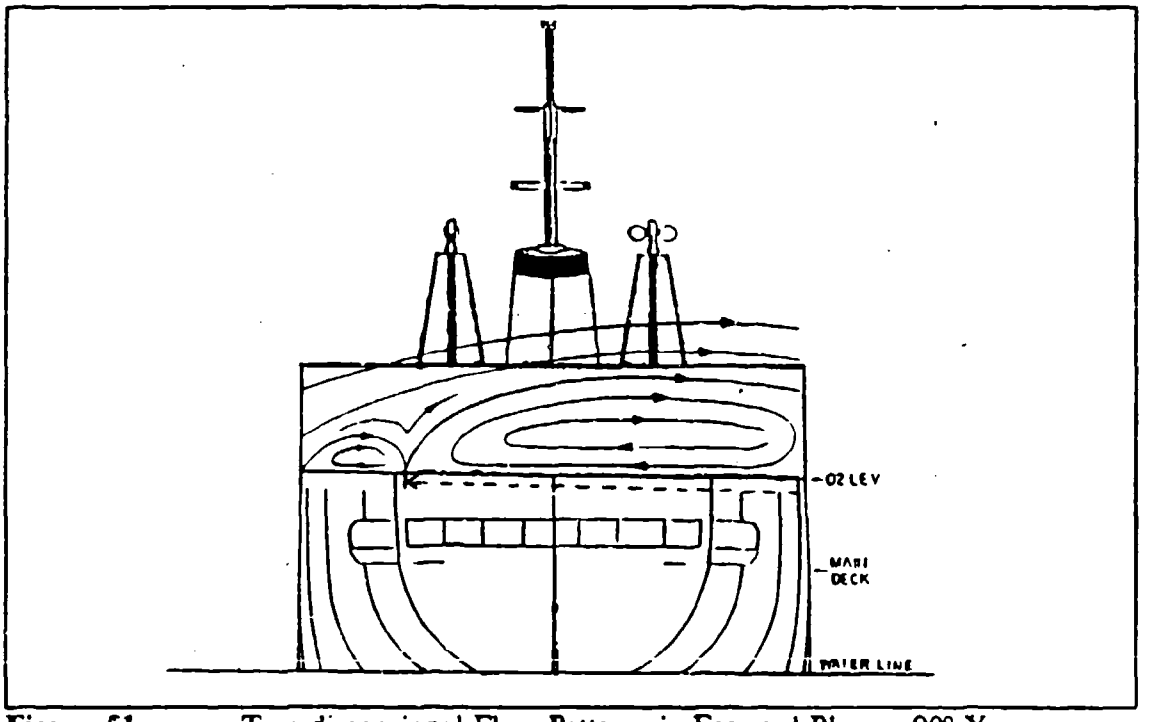

Figure 51. Two-dimensional Flow Patterns in Forward Plane - 90° Yaw.

F. 110° YAW POSITION

This position proved to have the greatest extent of smooth flow over the deck, which was largely due to the almost complete absence of recirculations caused by the

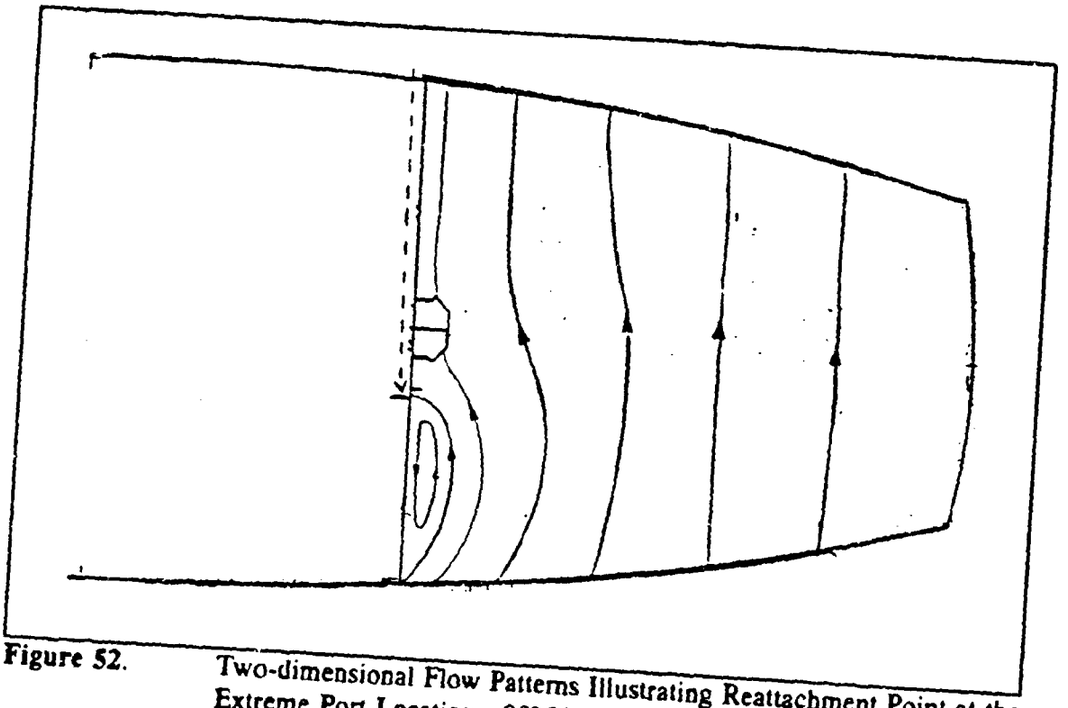

Figure 52. Two-dimensional Flow Patterns Illustrating Reattachment Point at the Extreme Port Location - 90° Yaw.

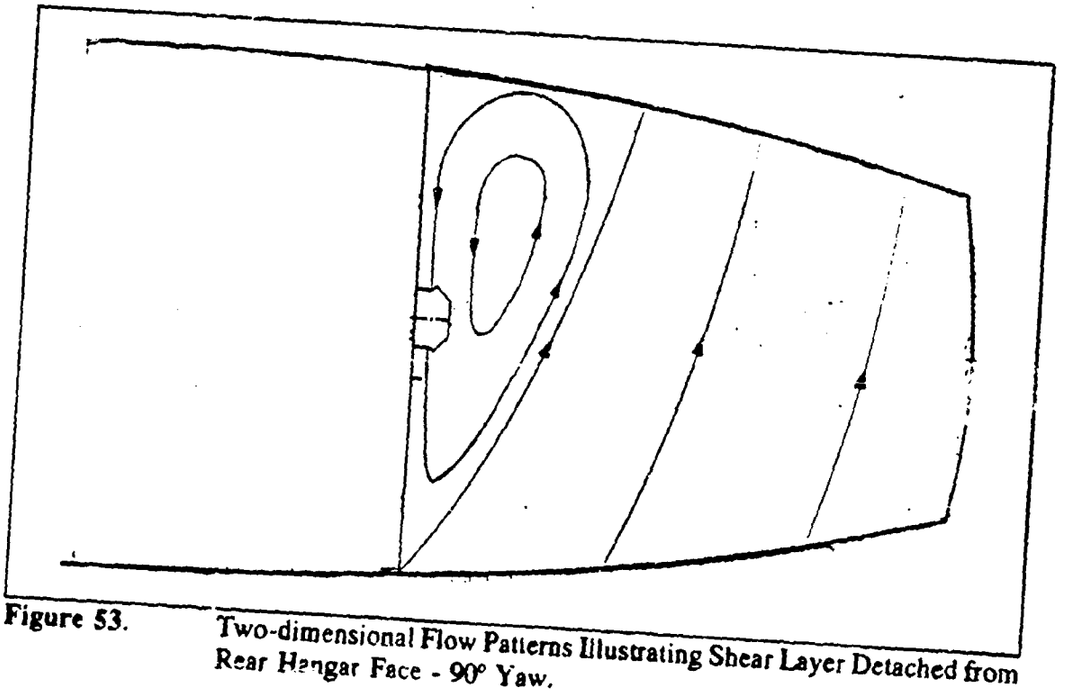

Figure 53. Two-dimensional Flow Patterns Illustrating Shear Layer Detached from Rear Hangar Face - 90° Yaw.

hangar, as shown in Figure 54. This smooth flow is strikingly evident in Figure 55 and Figure 56 by the almost perfectly straight bubble traces. The air coming over the port deck edge had a significant upward component and, like the 90° case, the angle was approximately 15° to 20° from the horizontal. This upward component is caused primarily by a significant recirculation that formed just starboard of the port deck edge, shown in Figure 57. The recirculation was smaller in the aft plane, as indicated by Figure 58. This was probably due to some of the air being able to flow around the fantail instead of having to cross over the flight deck.

There was still a very small recirculation immediately aft of the rear hangar face, as shown in Figure 59, but it was short in the vertical direction and very thin in the ship's longitudinal direction.

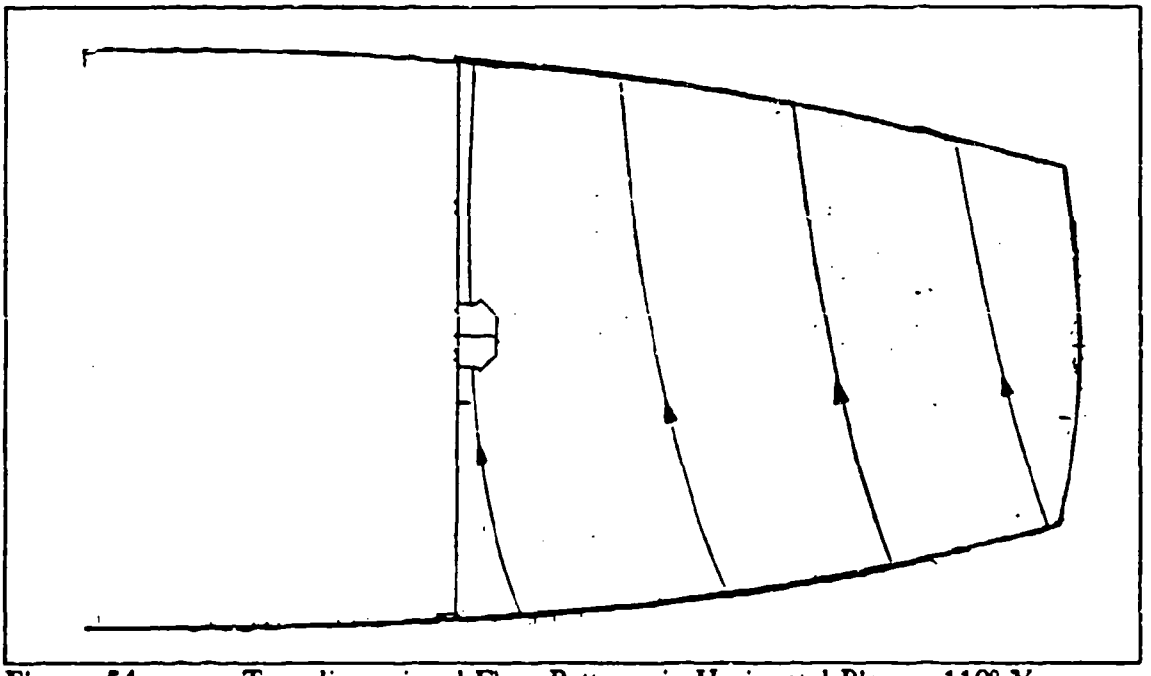

Figure 54. Two-dimensional Flow Patterns in Horizontal Plane - 110° Yaw.

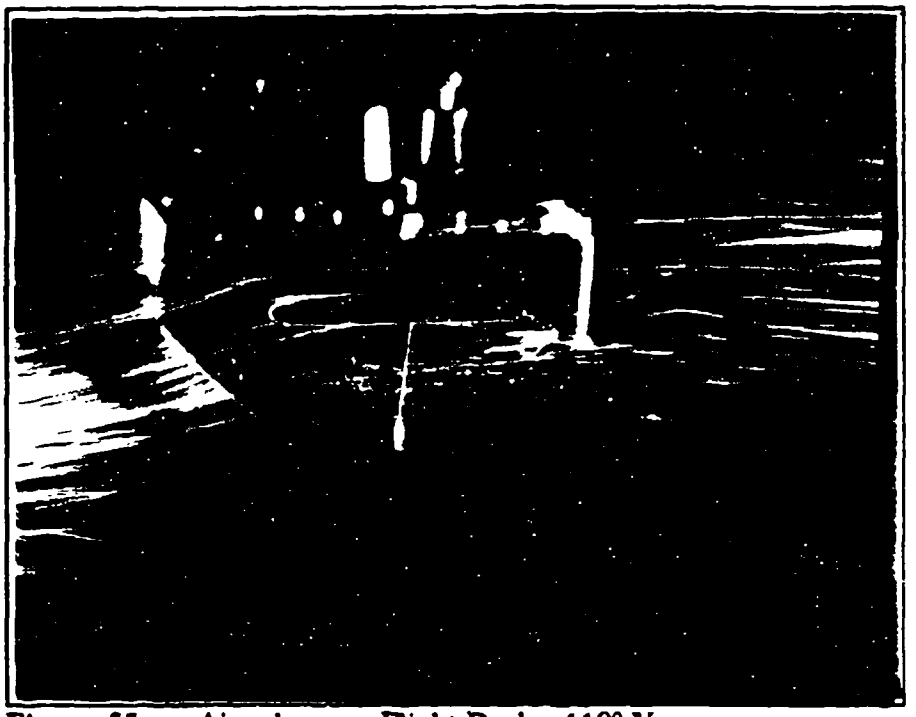

Figure 55. Airwake over Flight Deck - 110° Yaw.

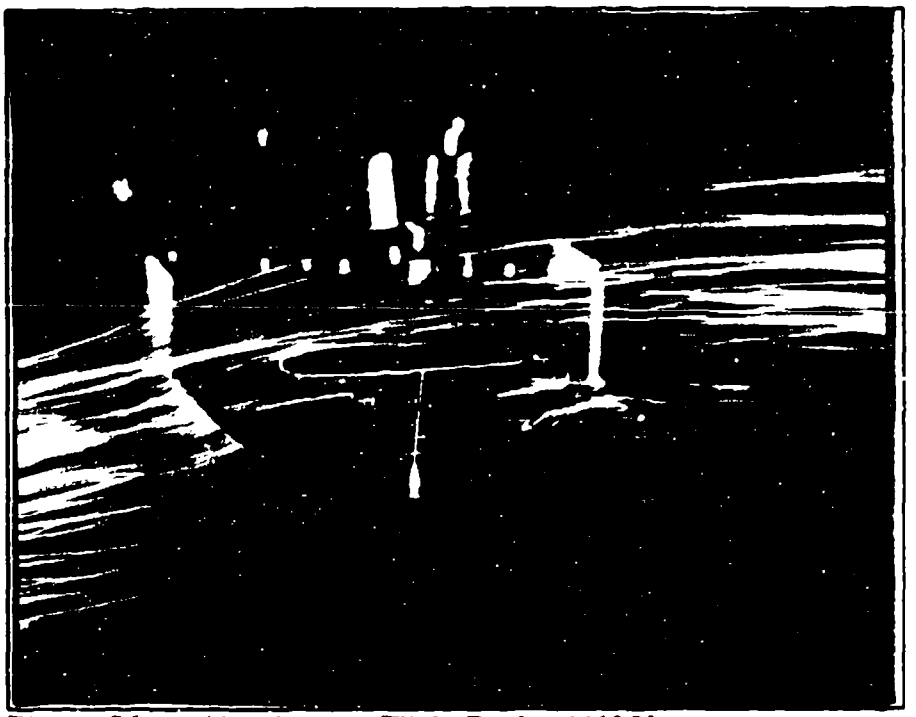

Figure 56. Airwake over Flight Deck - 110° Yaw.

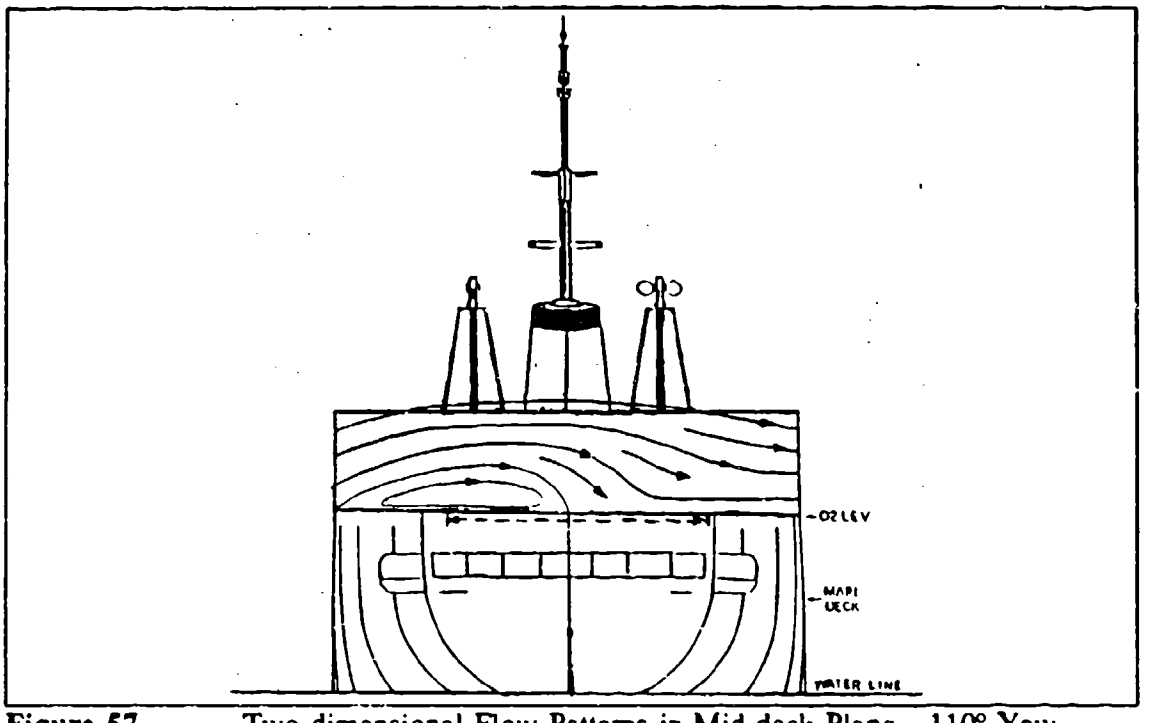

Figure 57. Two-dimensional Flow Patterns in Mid-deck Plane - 110° Yaw.

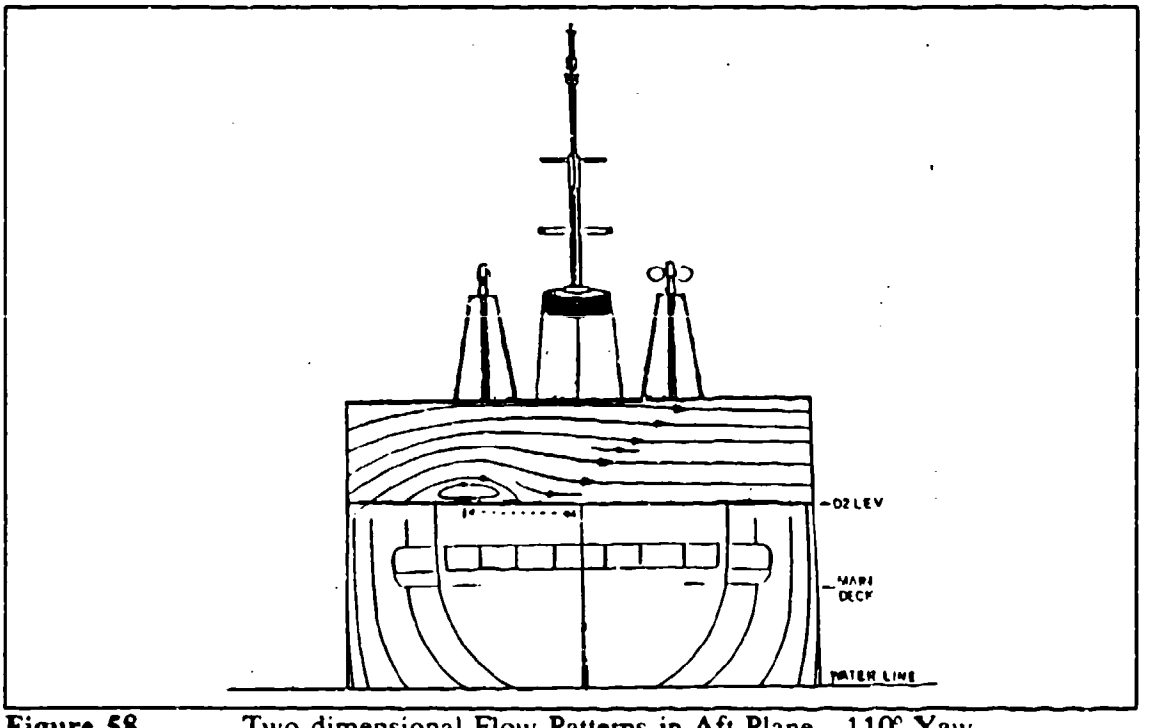

Figure 58. Two-dimensional Flow Patterns in Aft Plane - 110° Yaw.

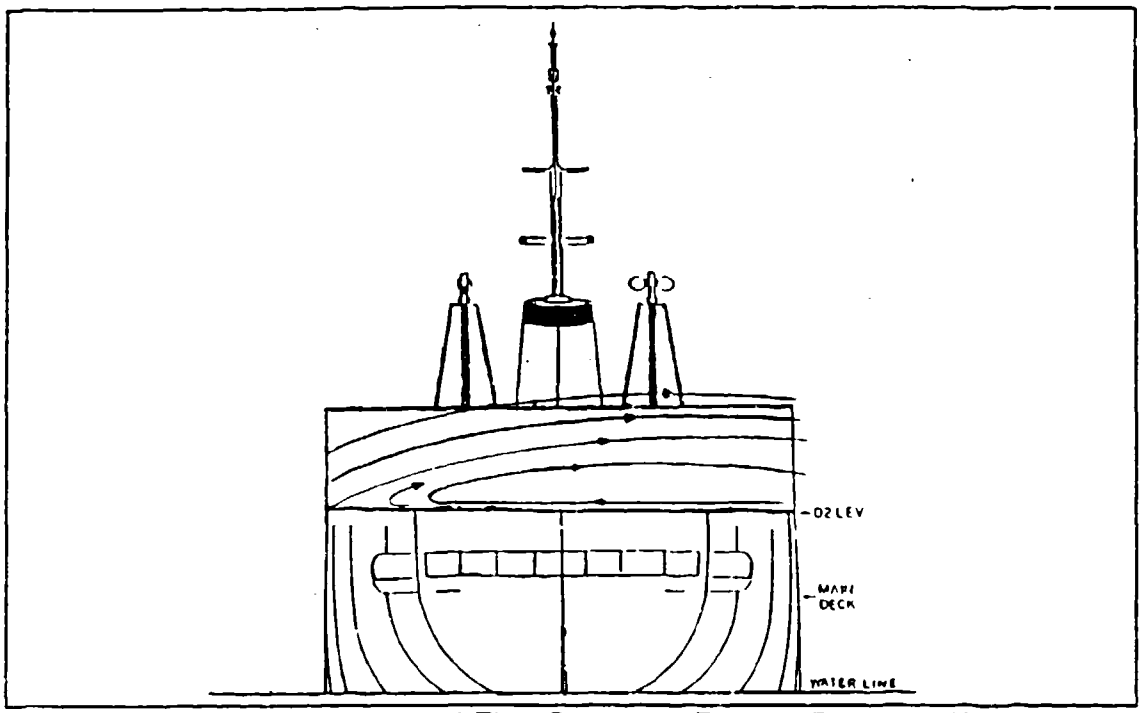

Figure 59. Two-dimensional Flow Patterns in Forward Plane - 110° Yaw.

G. 50° YAW WITH DEFLECTORS

In an attempt to eliminate some of the more unruly flow patterns, two curved deflectors were constructed and installed on the model ship. Both deflectors were made by cutting a 19 mm (3/4") diameter thin-walled tube longitudinally. The tube was cut in a manner such that one-quarter of the circumference was removed to act as the deflector, i.e. the resulting arc was 90°. One deflector, 203.2 mm (8") long, was installed horizontally over the port deck edge. The other, 31.75 mm (1.25") long, was installed vertically in an attempt to turn the flow around the aft port corner of the hangar. There was a 6.35 mm (0.25") gap between ship's surface and the deflector in both cases. Due to the limited amount of time, only the 50° position was investigated.

was a 6.35 mm (0.25") gap between ship's surface and the deflector in both cases. Due to the limited amount of time, only the 50° position was investigated.

The results of this attempt were mixed. The long, horizontal deflector seemed to effectively turn the flow passing by the port deck edge. This eliminated the recirculation that usually formed just starboard of that deck edge. See Figure 60.

The short deflector did not work very well, however. It appeared to turn the flow only a small amount but seemed to increase greatly the turbulence and the size of the recirculation that was behind the aft hangar face, as shown in Figure 61. This is not desirable, but does prove that the deflector can influence the flow field. The adverse

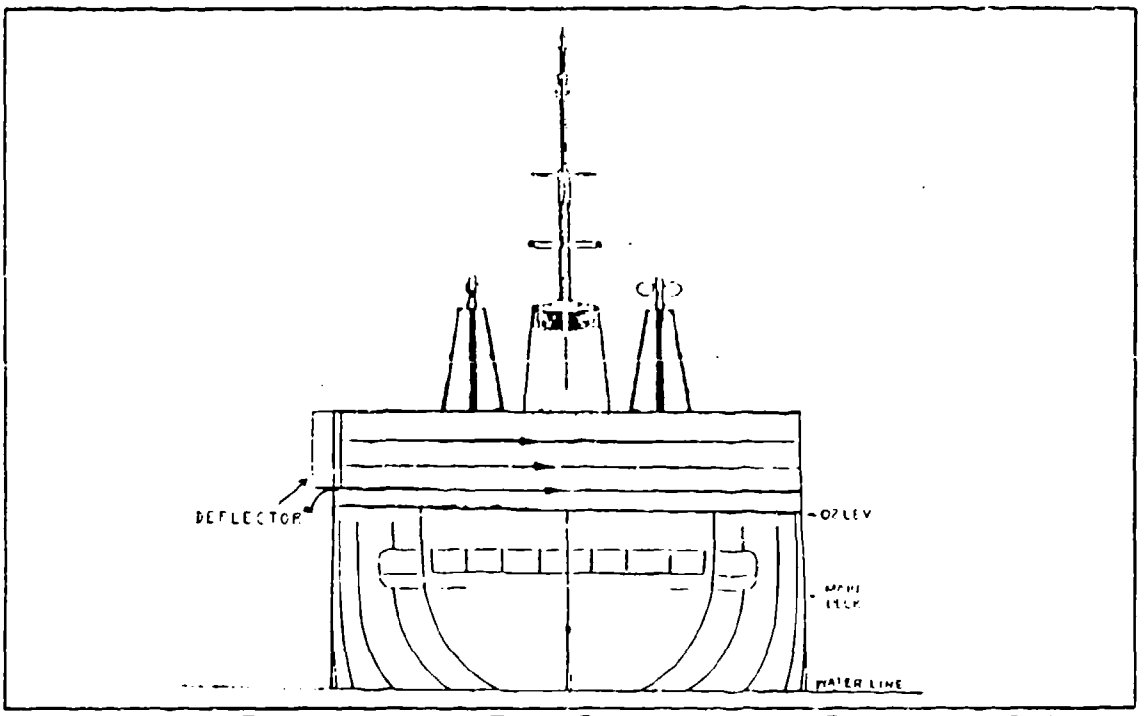

Figure 60. Two-dimensional Flow Patterns in Aft Plane with Deflectors Installed - 50° Yaw.

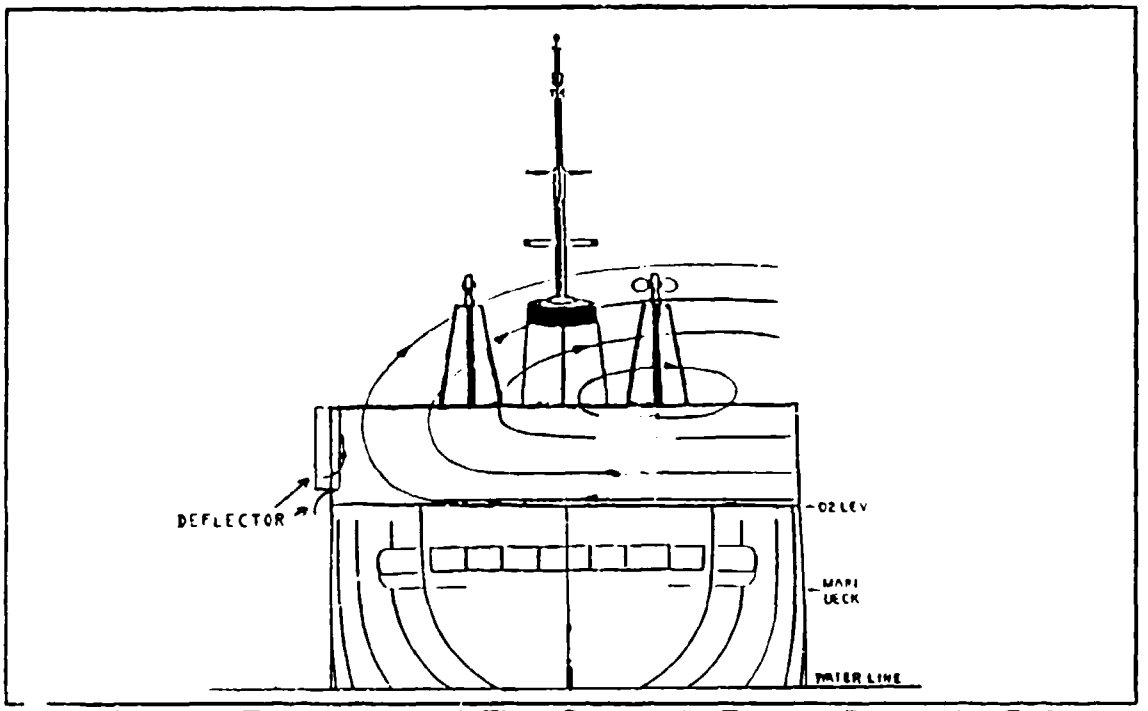

Figure 61. Two-dimensional Flow Patterns in Forward Plane with Deflectors Installed - 50° Yaw.

behavior could be a result of having an improper amount of space between the deflector and the surface of the ship. Due to the limited amount of time, this hypothesis could not be investigated further.

When the smoke streaklines were viewed from above, they revealed a very strong recirculation right behind the hangar. It was somewhat narrow in width but did oscillate angularly back and forth across the deck with the shear layer detaching and reattaching to the rear hangar face. The two extreme positions shown in Figure 62 and Figure 63.

H. VELOCITY MEASUREMENTS

As stated earlier, in the Experimental Procedure section, a number of velocity measurements were made. Five locations around the ship were investigated. Those

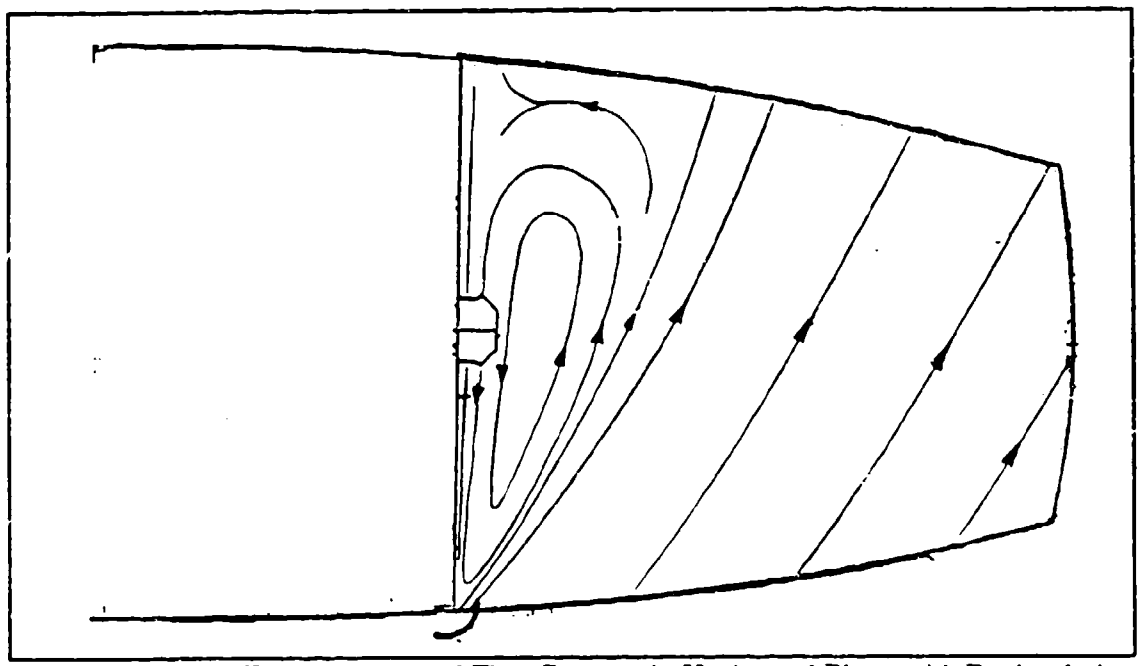

Figure 62. Two-dimensional Flow Patterns in Horizontal Plane with Recirculation Near Hangar Face - 50° Yaw.

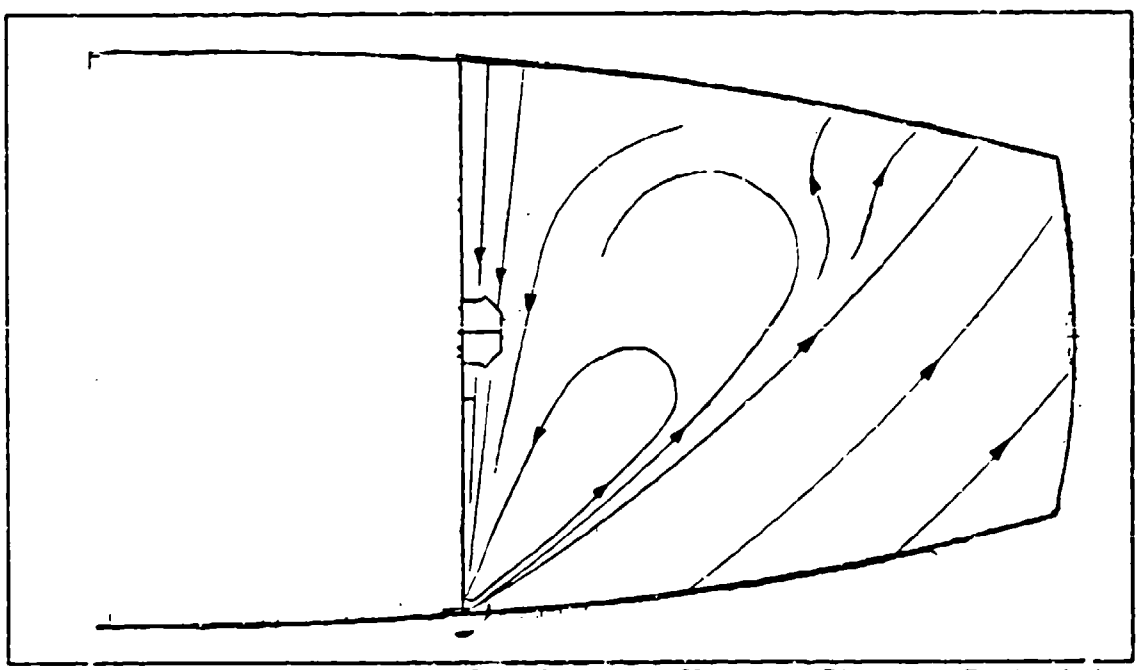

Figure 63. Two-dimensional Flow Patterns in Horizontal Plane with Recirculation Detached from Hangar - 50° Yaw.

were: the ship's anemometer position, and four positions around the equivalent rear rotor arc of the H-46, as shown in Figure 13.

A hot-wire anemometer, using a triple-wire probe, was used to take 65,536 velocity measurements, per channel, at a rate of 2 Khz for each of five locations per yaw position. This yielded a total sampling time of 32.768 seconds. These samples were processed using Dantec's "acqWIRE" software. The numerical results of these measurements are summarized in Table 5. The coordinate system used, considered the positive x-axis along the tunnel's longitudinal axis in the downstream direction, the positive y-axis extending out to the left, as one looks in the downstream direction, and the positive z-axis being vertical. This system was used because it kept the velocity vector inside of a 20° cone measured from the probe axis, which is required to make accurate measurements using this type of probe.

Unfortunately, because of software problems, there was insufficient time to do a detailed analysis of the results; instead the attention will be focused on a number of important positions. Only the 50° and the 90° yaw positions were examined in detail. For these yaw positions, two locations on the flight deck were considered; one inside the the recirculation zone, position 2 as shown in figure 13, and the other outside the zone, position 4.

An important factor in these measurements is turbulence intensity. The accuracy of the measurements of the velocity components are highly questionable whenever the turbulence intensity exceeds 30% for any component of velocity, as stated by Lomas [Ref. 17]. Nevertheless, Lomas only considered an x-wire configuration in basically a

TABLE 5. SUMMARY OF VELOCITY MEASUREMENT DATA

(All velocities - m/sec)

0° YAW

POSITION	MEAN U	RMS U	SKEW U	TURB U	MEAN V	RMS V	SKEW V	TURB V	MEAN W	RMS W	SKEW W	TURB W
AMEM	2.019	0.097	0.141	0.048	0.175	0.088	0.164	0.505	0.108	0.035	0.002	0.882
1	0.836	0.04	-20.969	0.047	-0.001	0.024	-2.756	-17.157	-0.007	0.042	-7.263	-5.994
2	0.841	0.043	-15.672	0.051	-0.003	0.037	-5.438	-11.484	-0.016	0.062	-4.679	-3.962
3	0.846	0.053	-7.016	0.062	-0.005	0.047	-3.766	-9.396	-0.02	0.07	-3.865	-3.537
4	0.858	0.069	-0.999	0.08	-0.031	0.095	-3.055	-3.085	-0.005	0.068	-1.865	-14.934

30° YAW

POSITION	MEAN U	RMS U	SKEW U	TURB U	MEAN V	RMS V	SKEW V	TURB V	MEAN W	RMS W	SKEW W	TURB W
AMEM	1.842	0.107	-0.291	0.058	-0.089	0.097	-0.018	-1.08	0.266	0.105	-0.076	0.395
1	0.858	0.08	0.924	0.094	-0.025	0.109	-2.871	-4.295	0.001	0.073	-0.64	58.584
2	0.845	0.059	-4.267	0.069	-0.002	0.051	-4.571	-20.756	-0.022	0.087	-3.514	-3.859
3	1.36	0.321	0.095	0.236	-0.158	0.257	0.034	-1.631	0.099	0.216	0.017	2.187
4	1.729	0.19	0.118	0.11	-0.094	0.163	0.261	-1.723	0.278	0.125	0.084	0.449

50° YAW

POSITION	MEAN U	RMS U	SKEW U	TURB U	MEAN V	RMS V	SKEW V	TURB V	MEAN W	RMS W	SKEW W	TURB W
AMEM	1.933	0.108	-0.241	0.056	-0.109	0.1	-0.015	-0.917	0.3	0.097	0.013	0.323
1	1.755	0.323	-0.266	0.184	0.166	0.257	0.145	1.55	0.077	0.254	-0.168	3.282
2	1.33	0.372	0.365	0.28	-0.053	0.261	-0.225	-4.893	-0.06	0.271	0.017	-4.556
3	1.79	0.221	-0.556	0.123	-0.133	0.2	0.631	-1.51	0.165	0.164	0.392	0.998
4	1.824	0.174	-0.174	0.096	0.112	0.163	0.325	1.458	0.353	0.129	0.162	0.366

70° YAW

POSITION	MEAN U	RMS U	SKEW U	TURB U	MEAN V	RMS V	SKEW V	TURB V	MEAN W	RMS W	SKEW W	TURB W
AMEM	2.241	0.109	-0.317	0.048	0.167	0.113	0.028	0.674	0.351	0.104	-0.014	0.295
1	2.525	0.268	-0.384	0.106	0.262	0.272	0.172	1.04	0.065	0.207	0.632	3.196
2	2.188	0.297	-0.578	0.136	0.109	0.286	-0.04	2.617	-0.129	0.218	0.135	-1.697
3	2.232	0.241	-0.52	0.108	0.197	0.226	0.176	1.149	0.288	0.208	0.276	0.72
4	2.135	0.207	-0.262	0.097	0.398	0.2	0.081	0.503	0.546	0.178	0.224	0.326

90° YAW

POSITION	MEAN U	RMS U	SKEW U	TURB U	MEAN V	RMS V	SKEW V	TURB V	MEAN W	RMS W	SKEW W	TURB W
AMEM	2.327	0.12	-0.279	0.051	0.062	0.122	0.067	1.978	0.37	0.109	0.074	0.294
1	2.05	0.251	0.411	0.123	-0.221	0.368	0.936	-1.664	0.938	0.196	-0.904	0.208
2	1.606	0.362	-0.015	0.226	-0.016	0.385	0.291	-23.678	0.527	0.309	-0.825	0.586
3	1.803	0.154	-0.209	0.086	0.087	0.356	-0.014	4.092	0.843	0.126	-2.368	0.15
4	1.828	0.137	-0.113	0.075	0.098	0.331	-0.019	3.372	0.871	0.107	-0.45	0.122

110° YAW

POSITION	MEAN U	RMS U	SKEW U	TURB U	MEAN V	RMS V	SKEW V	TURB V	MEAN W	RMS W	SKEW W	TURB W
AMEM	1.709	0.144	0.407	0.084	-0.395	0.116	1.298	-0.292	0.803	0.107	-0.434	0.133
1	1.905	0.247	0.555	0.129	0.371	0.364	-0.845	0.981	0.773	0.218	-1.217	0.281
2	1.771	0.161	-0.683	0.091	0.053	0.328	-0.054	6.184	0.78	0.117	-1.633	0.15
3	1.789	0.123	-0.407	0.069	0.049	0.313	-0.022	6.364	0.863	0.084	-0.475	0.097
4	1.819	0.123	-0.179	0.067	0.145	0.296	-0.235	2.044	0.865	0.101	-0.659	0.117

one-dimensional flow. Under that condition, any fluctuations in the transverse component of velocity would yield an infinite turbulence intensity. He did not consider the current case where there are small but significant transverse and vertical velocities. Surprisingly enough, there is little or no coverage of three-dimensional hot-wire measurements of turbulent flows in the most of the available literature.

Another indicator of the validity of these data is the histograms of the velocity measurements. The velocity distributions found from the free-stream flow are very close to Guassian bell shape. Histograms which show very non-Gaussian shapes, such as for position 2 shown in Appendix B, cast serious doubt on the accuracy of the data.

Of the two yaw positions chosen, there was only one point that came close to meeting the criteria of having turbulence intensities less than 30% and the resulting histogram had a Guassian bell shape, and that was for the 90° yaw at location number 4. To provide more complete information for the 90° position, the spectrum functions of the three velocity components as well as the longitudinal auto-correlation for location number 4 are provided in Appendix B. The three spectra, not surprisingly, show an almost complete lack of an inertial sublayer, usually indicated by a -2/3 slope on the graph, and a relatively uniform energy distribution up to about 100 Hz. In the absence of any other information on the longitudinal length scale, a crude approximation involving Taylor's from turbulence hypothesis, yields the value 137.25 mm which scales up to 22.61 m for the full scale ship.

Not considering the velocity components that had turbulence intensities above 30%, some conclusions can still be derived. There is a significant drop in the longitudinal

component of velocity in the 0° position due to the presence of the hangar, this is confirmed by the earlier flow visualization. The measurements also confirm the presence of the upward flow over the port deck edge in the 90° and 110° yaw positions. The actual flow angles were estimated earlier as being between 15° and 20° which closely match the 22° to 25° found by the measurements. No conclusions can be drawn about the flow inside the recirculation zones due to high levels of turbulence from these data.

Perry [Ref. 18] stresses the need for linearized circuitry when measuring turbulent flows by hot-wire anemometry, hence it would have been desirable to take the measurements with electronic linearizers in the hot-wire circuits. These units were available and an attempt was made to set them up, but lack of time and technician support forced the abandonment of the idea.

VI. CONCLUSIONS AND RECOMMENDATIONS

The flow over an AOR class ship has two distinct regions: one that is extremely turbulent and dominated by recirculations and the other with relatively smooth flow. The relative sizes of the two regions is very dependent on the approach angle of the wind.

The turbulence levels, and the size of the recirculation zones over the deck, were found to increase as the ship was yawed and maximized at the 50° position, whereupon the turbulence levels began to decrease until they were relatively small for the 110° position.

Due to high levels of turbulence, all of the velocity measurements had turbulence intensities in excess of the accepted 30% limit for at least one of the velocity components. This casts serious doubt on the accuracy of the measurements that were made.

The most detrimental aerodynamic features of the AOR class ship were determined to be the large square cornered hangar and the high flight deck. The hangar caused massive recirculations over the flight deck in every case except the 110° position, this lends credibility to the suggestion of putting helicopter flight decks forward of the ship's superstructure.

The high flight deck caused a significant blockage to the air flow coming from the side of the ship. This air was forced to rise over the flight deck this caused a recirculation to form just starboard of the port deck edge. This led to a significant upward component of flow as the air passed over that edge. If the deck was low to the

water, the air would not have to rise so drastically and would form a much smaller recirculation thus eliminating most, if not all, of the upward velocity in the flow.

The high levels of turbulence, rapid movement of the recirculation zones, and the significant upward velocity of the air passing over the port deck edge must be significant contributors to the current blade strike problem on AOR class ships in the presence of port-side winds. In an effort to identify local airflows that would be likely to cause the strikes, the Naval Air Test Center was requested to provide information about the blade motion immediately preceding the strike. The hope was, that the cause could be attributed to the upflow near the edge of the deck or to the strong turbulent eddies in the recirculation zone, and that appropriate measures could then be taken to control that particular flow. Unfortunately, the NATC was unable to provide an answer, as of the time of finishing this thesis. The only hope of alleviating the blade strike problem is to tailor the flow to eliminate some of the more unruly flow patterns with deflectors.

To aid in that endeavor, it is recommended to continue investigating airwake aerodynamics with heavy emphasis on flow tailoring. This can be done both numerically, using computational fluid dynamics, and experimentally.

Some other recommendations are:

1. Make further measurements over the flight deck area of the AOR model ship using a pulsed-wire or flying-wire anemometer or laser-doppler-velocimeter, due to the high level of turbulence.

2. Investigate further the effects of the helicopter's fuselage on the flow field.

3. Compare the information derived from this study to that found from computational fluid dynamics programs test the validity of their results.

4. Apply the information found in this study to future ship designs to avoid repeating the poor aerodynamic qualities of the AOR class ship.

5. Provide badly needed technician support for the large amount of equipment used for airwake studies.

6. Introduce a better method of producing half-tones or their equivalent, due to the substantial losses in detail when half-tones are produced from clear, sharp pictures. This loss of detail is compounded when the thesis is copied for further distribution.

APPENDIX A

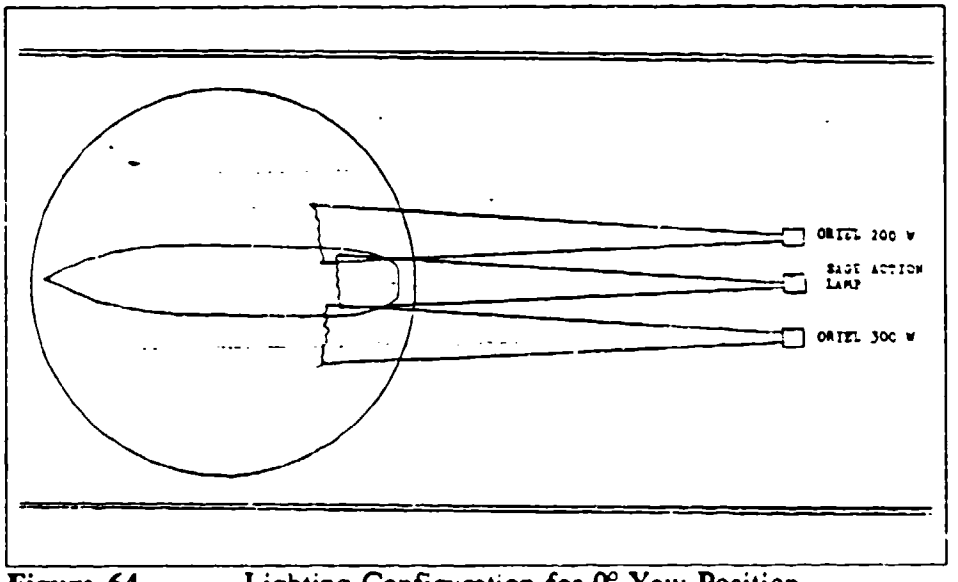

Figure 64. Lighting Configuration for 0° Yaw Position.

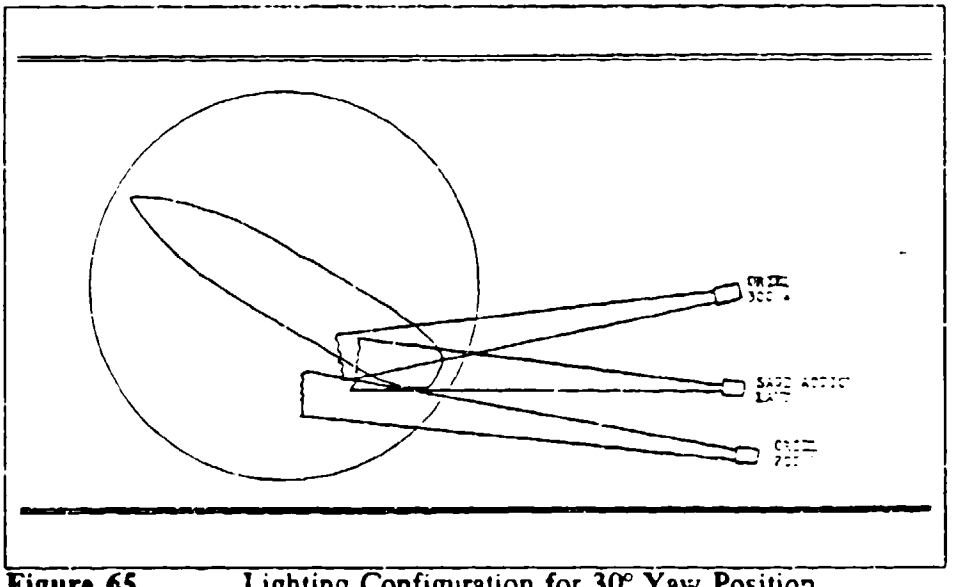

Figure 65. Lighting Configuration for 30° Yaw Position.

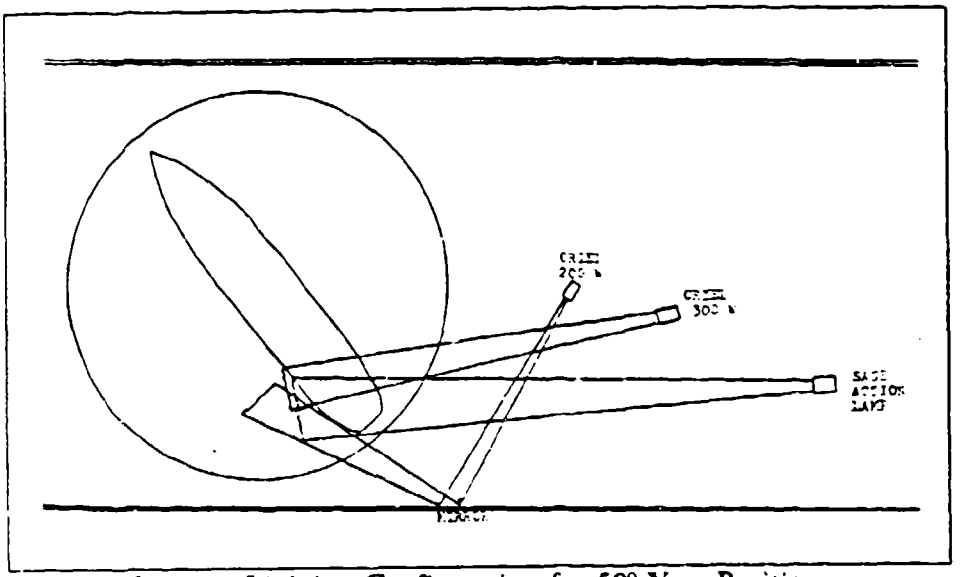

Figure 66. Lighting Configuration for 50° Yaw Position.

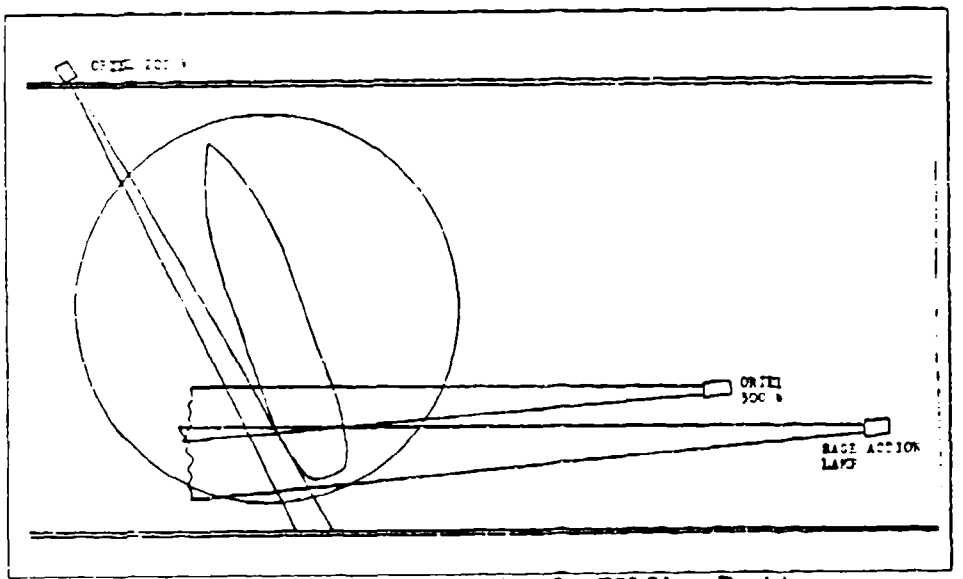

Figure 67. Lighting Configuration for 70° Yaw Position.

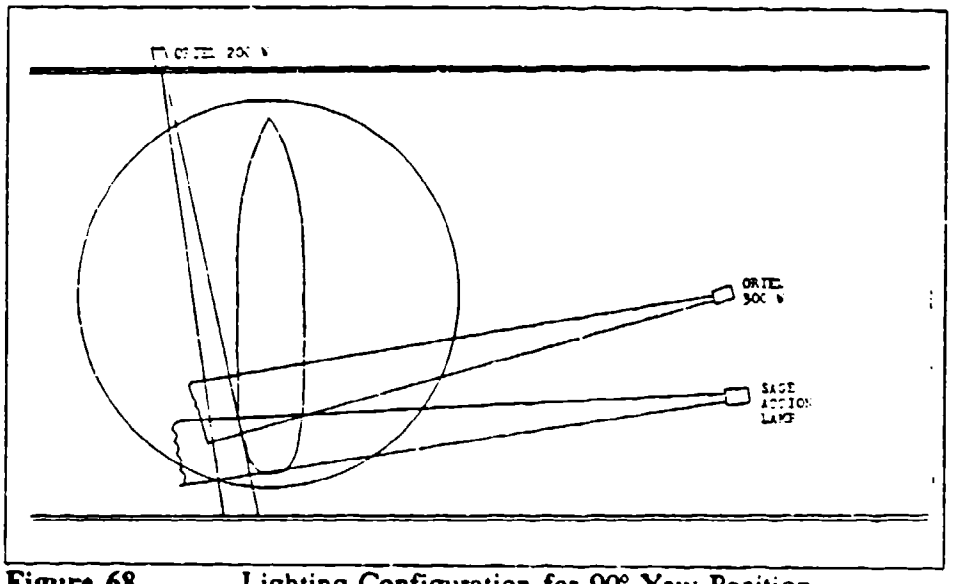

Figure 68. Lighting Configuration for 90° Yaw Position.

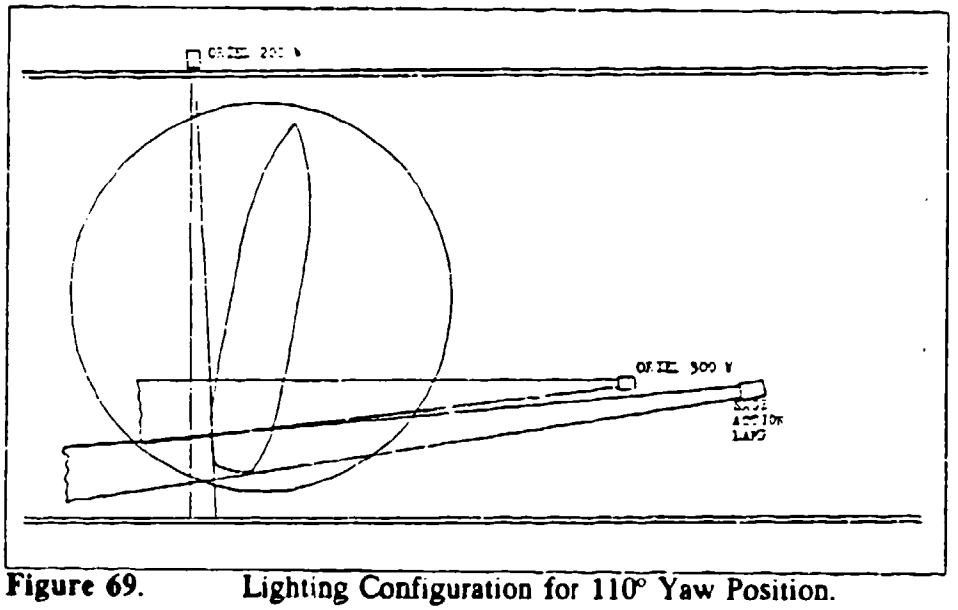

Figure 69. Lighting Configuration for 110° Yaw Position.

APPENDIX B

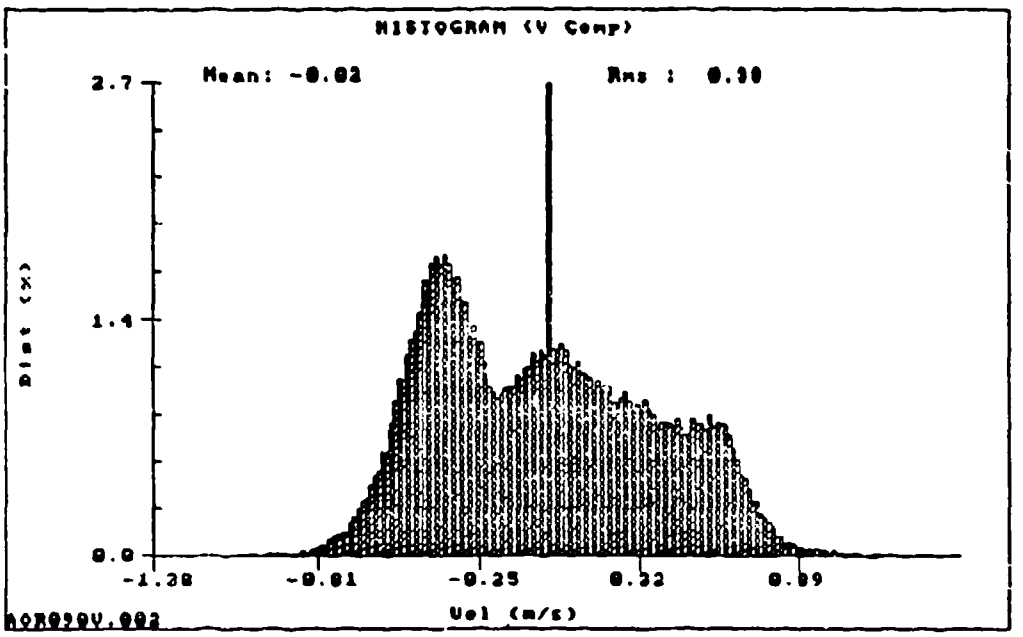

Figure 70. Velocity Histogram - 90° Yaw - Location 2

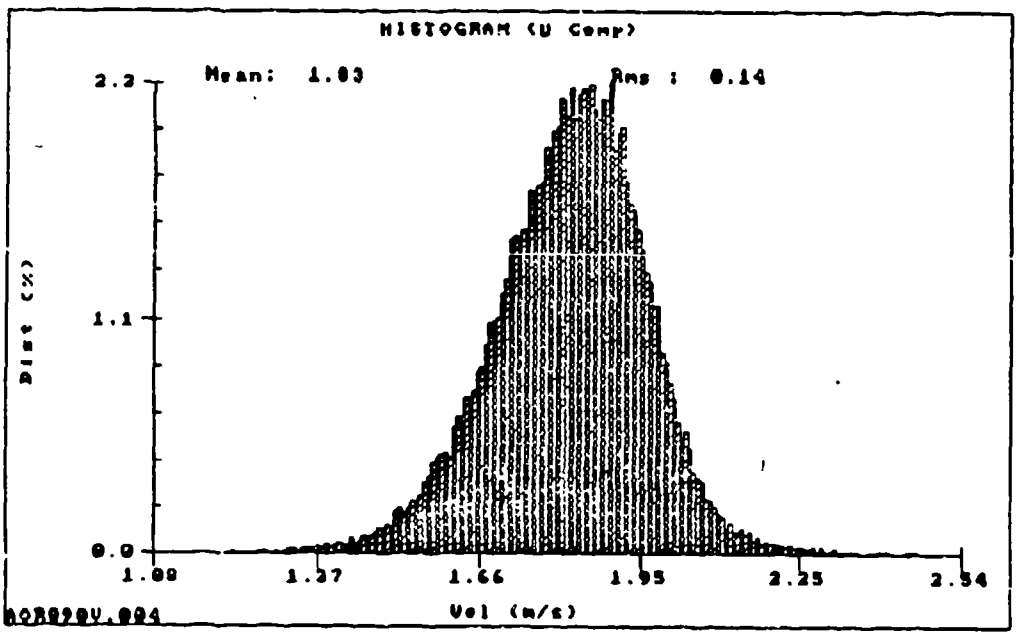

Figure 71. Velocity Histogram of U Component - 90° Yaw - Location 4

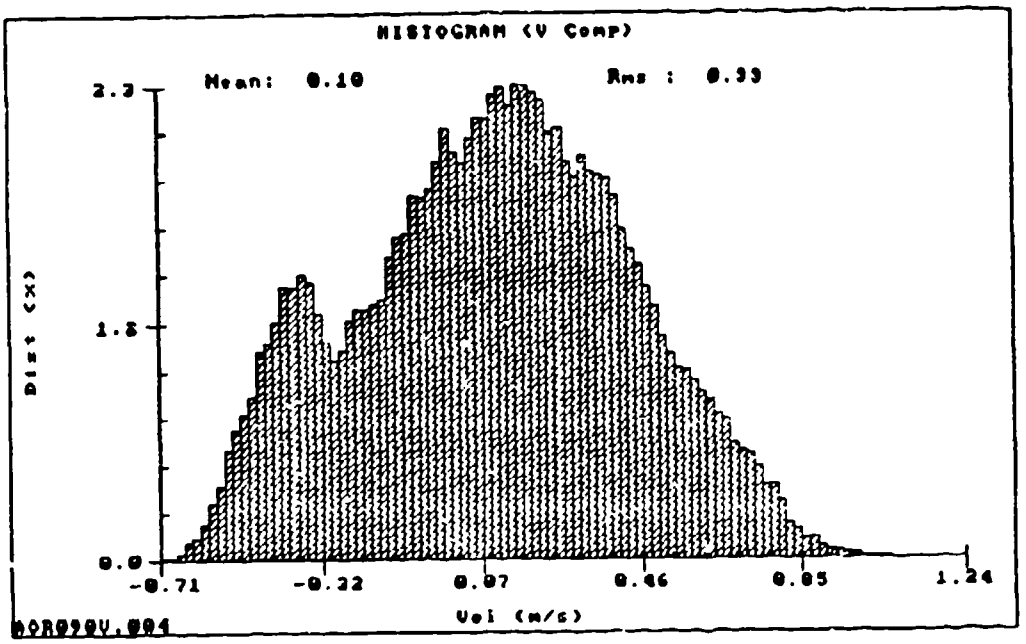

Figure 72. Velocity Histogram of V Component - 90° Yaw - Location 4

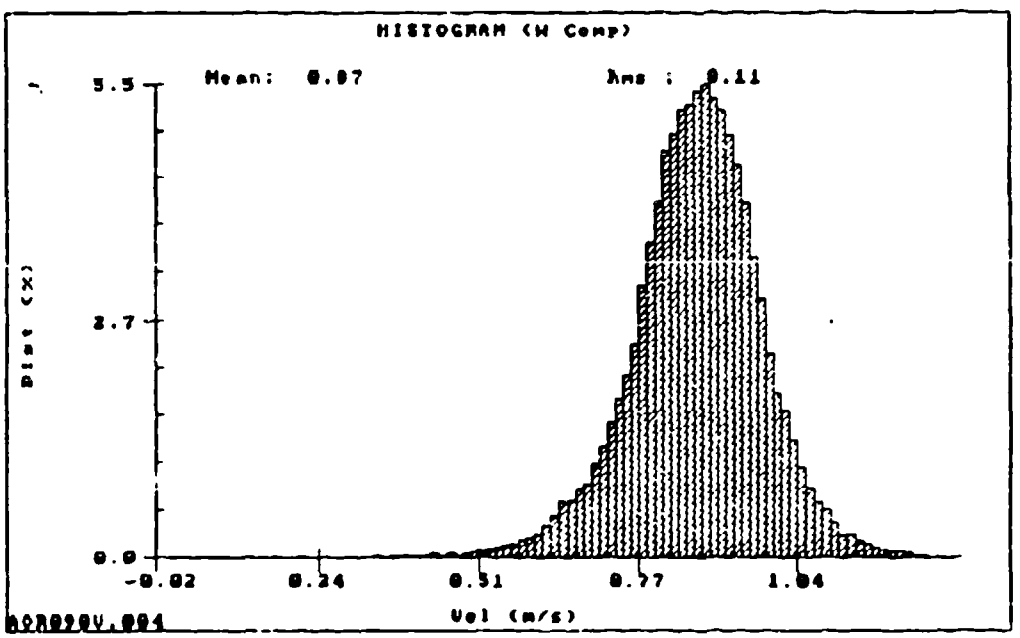

Figure 73. Velocity Histogram of W Component - 90° Yaw - Location 4

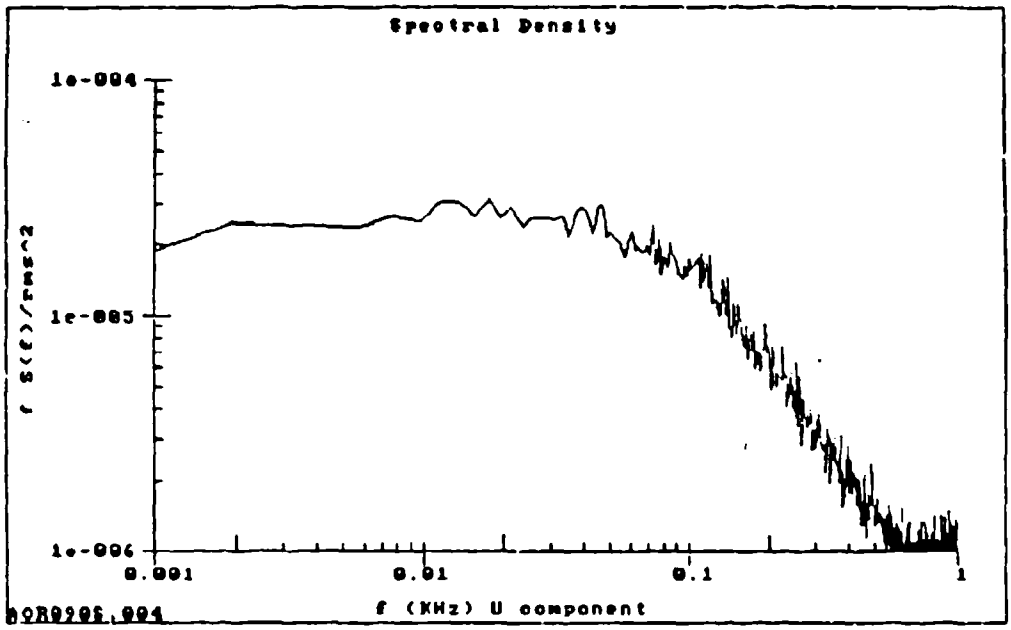

Figure 74. Spectrum Function of U Component - 90° Yaw - Location 4

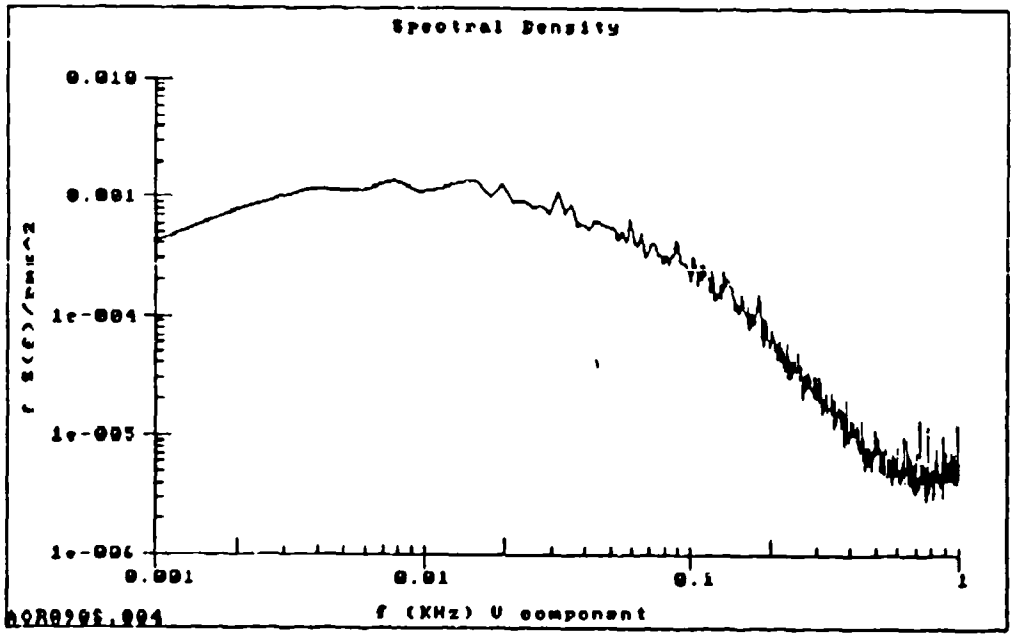

Figure 75. Spectrum Function of V Component - 90° Yaw - Location 4

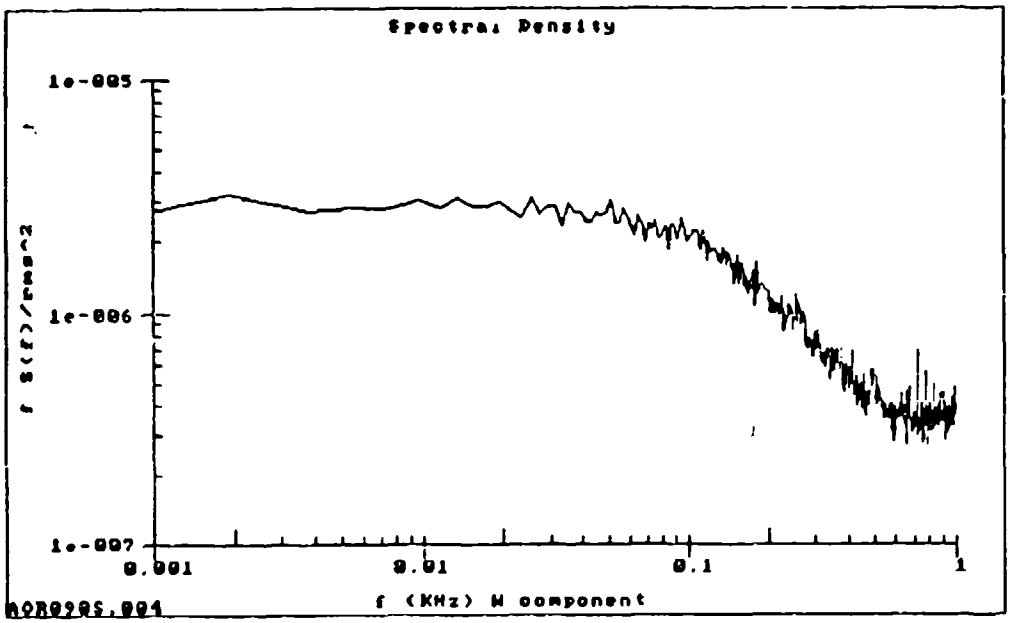

Figure 76. Spectrum Function of W Component - 90° Yaw - Location 4

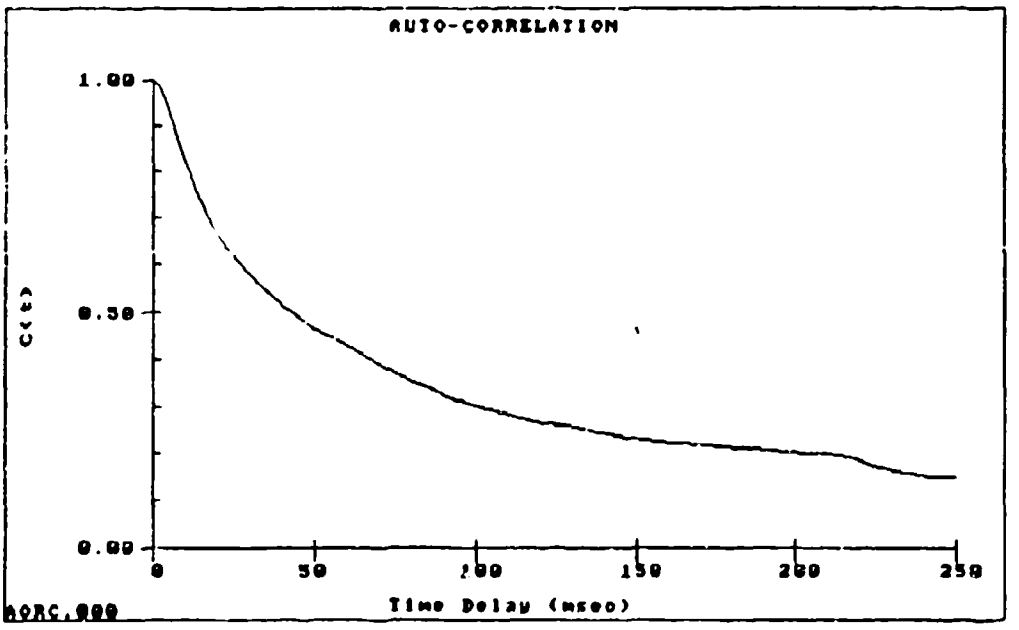

Figure 77. Longitudinal Auto-Correlation -90° Yaw - Location 4

LIST OF REFERENCES

1. Naval Warfare Publication (NWP-42 Rev. H), *Shipboard Helicopter Operating Procedures*, pp. 1-1, Washington D.C., Department of the Navy, December 1988.

2. Telephone conversation between CDR. Ivan A. Needles, Commanding Officer Helsuppron Eleven and the author, 2 March 1990.

3. Helsuppron Eight, VA Naval Message, Subject: Final General Use Naval Aircraft Mishap Report Helsuppron Eight Det Two Class B FM, 01-88, 5 Nov 88, UH-46D, 153408, Report Symbol 3750-20, DTG 201700Z Dec 88.

4. Interview between D. J. Rafetto, Captain, USN, Executive Director of the Group Operations Systems and Engineering Group at Naval Air Systems Command, J. V. Healey, Associate Professor, Naval Postgraduate School and the author, 28 February 1990.

5. Healey, J. Val., *The Prospects for Simulating the Helicopter/Ship Interface*, Naval Engineer's Journal, Vol. 99, No. 2, pp. 45-63, March 1987.

6. Hunt, J.C.R., C.J. Abell, J.A. Peterka and H. Woo, *Kinematic Studies of the Flows around Free or Surface-Mounted Obstacles; applying Topology to Flow Visualization*, pp. 179, 200, Journal of Fluid Mechanics, Vol. 86, 1978.

7. Beranek, W.J., *General Rules for Determination of Wind Environment*, pp. 225, 234, in Proceedings of the 5th. International Conference on Wind Engineering, Fort Collins, Colorado, July 1979.

8. Sinha, S.N., and Gupta, A.K., *Laminar Separating Flow over Backsteps and Cavities*, pp. 370-375, American Institute of Aeronautics and Astronautics, Vol. 20, 1982.

9. Goldstein, R. J., *Fluid Mechanics Measurements*, pp. 311, Hemisphere Publishing Corporation, 1983.

10. Anderson, G. A., *Mapping the Airwake of a Model DD-963 Along Specific Helicopter Flight Paths*, Naval Postgraduate School, Monterey, California, December 1989.

11. E.S.D.U. Data Items 74030, 74031, Engineering Sciences Data Unit International, Suite 200, Chain Bridge Road, McLean, Virginia, 22101.

12. Plate, E. J., *Engineering Meteorology*, pp 573-636, Elsevier Scientific Publishing Company, 1982.

13. Healey, J. V., *Establishing a Database for Flight in the Wakes of Structures*, to be published, September 1990.

14. Biskaduros, J. L., *Flow Visualization of the Airwake of an Oscillating Generic Ship Model*, Master's Thesis, Naval Postgraduate School, Monterey, California, December 1987.

15. Johns, M. K., *Flow Visualization of the Airwake Around a Model of a DD-963 Class Destroyer in a Simulated Atmospheric Boundary Layer*, Master's Thesis, Naval Postgraduate School, Monterey, California, September 1988.

16. Frota, M. N., and Moffat, R. J., *Effect of Combined Roll and Pitch Angles on Triple Hot-Wire Measurements of Mean and Turbulence Structure*, pp. 18, DISA Information, No. 28, February 1983.

17. Lomas, C. G., *Fundamentals of Hot Wire Anemometry*, pp. 140, Cambridge University Press, 1986.

18. Perry, A. E., *Hot-wire Anemometry*, Chapter 8, Oxford University Press, 1982.

INITIAL DISTRIBUTION LIST

1.	Defense Technical Information Center Cameron Station Alexandria, Virginia 22304-6145	2
2.	Library, Code 52 Naval Postgraduate School Monterey, California 93943-5002	2
3.	Department Chairman, Code AA/Wo Department of Aeronautics and Astronautics Naval Postgraduate School Monterey, California 93943-5000	1
4.	Commander Naval Air Systems Command Air Vehicle Division Attn: Mr. Jonah Ottensoser, Code Air 53011C Jefferson Plaza 2, Rm. 904 Washington, D. C., 20361	1
5.	Mr. Bernard Ferrier CANDAIR LTD 1800 Laurentieu Blvd. Saint Laurent Quebec, Canada H4R1KZ	1
6.	Naval Air Test Center Attn: Dean Carrico, Code RW40A Patuxent River, Maryland 20670	1
7.	Dr. J. Val Healey, Code AA/He Department of Aeronautics and Astronautics Naval Postgraduate School Monterey, California 93943-5000	4

8. Mr. Neil Gilbert 1
Aeronautical Division
Aeronautical Research Laboratories
506 Lorimer Street
Fisherman's Bend
Box 4331 P. O.
Melbourne, Victoria 3001
Australia

9. Lt. Mark M. Rhoades 2
10979 Creekbridge Place
San Diego, California 92128